Using functionalized nonlinear optical chromophores to prepare NLO-active polycarbonate films

M. González-Lainez[a], M.T. Jiménez-Ruiz [a], N. Martínez de Baroja [a], J. Garín [a], J. Orduna[a*], B. Villacampa[b*], M.J. Blesa[a*]

Abstract

Novel functionalized second order nonlinear optical (NLO) chromophores have been prepared with functionalized aniline as electron donor, thiophene or isophorone as a π-spacer and 1,3-diethyl-2-thiobarbituric acid as electron acceptor. The films prepared from dyes with alkylsilyl bulky groups gave better performance than the corresponding non functionalized chromophores due to the reduction of the intermolecular electrostatic interactions. The incorporation of chromophores **4** and **10** in a polycarbonate matrix allowed the preparation of good optical-quality films. Nonlinear coefficients d_{33} and d_{31} as high as 17 and 5.6 pm V^{-1}, respectively, were obtained. Moreover, the temporal stability of these host-guest films was confirmed up to eight months (>80%).

Keywords: chromophore, multichromophore, nonlinear optical materials, temporal stability, poled films

Using functionalized nonlinear optical chromophores to prepare NLO-active polycarbonate films

1. Introduction

During the last decades, organic materials have been proposed as promising candidates for a variety of nonlinear optical (NLO) applications, such as frequency doublers, optical storage devices, and electro-optic (EO) switches and modulators [1]. High NLO susceptibility, fast response time, low dielectric constant, small dispersion in refractive index, structural flexibility, and ease of material processing have brought organic materials to the forefront of NLO research. To achieve good device functionality, the NLO chromophore must simultaneously possess high microscopic molecular hyperpolarizability (β), good thermal and photostability, low optical absorption, high solubility in polymer hosts and weak intermolecular electrostatic interactions in a given host matrix [2].However, a relevant obstacle to the development of organic materials is the difficulty of translating the high hyperpolarizability of chromophores into an adequate macroscopic property. At high chromophore density, dipole-dipole interactions between the chromophores favor centrosymmetric arrangements and therefore the polar order of the material is difficult. Modification of chromophore shape with bulky substituents would make them more spherical and hence limits intermolecular electrostatic interaction. Thus, the resulting material will be easier to be polarized. Polymers provide systems with high synthetic versatility and easy processability. Strategies for the design second order nonlinear polymers not only imply the incorporation of dipolar, highly polarizable electron donor-π-acceptor molecules (normally used as NLO-phores) into a macromolecular structure but also a noncentrosymmetric organization. The experimental technique used for this purpose is

based on the electric field poling; after the poling NLO chromophores show a preferential orientation along the field direction, defining an optical axis perpendicular to the film surface (C∞υ symmetry)[3, 4].

Polar chromophores with a common structural characteristic of flat highly conjugated system have high $\mu\beta$ values. However, the resulting dipole moment makes the chromophores aggregate. Several studies have been carried out to solve this problem, for example, by attaching side chains to polymers, by incorporating the chromophore inside a dendrimer structure separating the chromophores with bulky peripheral chains [5, 6] and by modifying tricyanovinyldihydrofuran type electron acceptors with different substituents to reach a three dimensional shape chromophore [7]. Having this in mind, we suggest to simply functionalize hydroxyl chromophores with *tert*-butyldimethylsilyl group (TBDMS) with the aim to inhibit electrostatic interactions among "high $\mu\beta$" chromophores.

In this paper, we report the synthesis and the optical properties of hydroxyl functionalized push-pull systems bearing an aniline ring as an electron donor [8-12], a conjugated tiophene bridge systems [13, 14] or a isophorone ring [15] in the spacer group and one strong electron acceptor, the 1,3-diethyl-2-thiobarbituric acid. The choice of an aniline ring results in the possibility of having more planar rigid structures due to the intramolecular interactions between the thiophene and the aniline rings which can affect the electronic properties and hence the nonlinear response of the chromophores. In a similar way we have studied the effect of silylation of the hydroxyl group in the nonlinear optical behavior of these derivatives and finally silylated chromophores have been incorporated to a polycarbonate host matrix to evaluate their macroscopic NLO response.

2. Results and discussion

2.1. Synthesis

The detailed synthetic procedure of chromophores **1-11** is presented in **Schemes 1** and **2**.

The protection of the hydroxyl group of **Ald 1** gave **Ald 2** following the method describe in the literature [16, 17].

The compound **1** was prepared by Knovenagel condensation of the 4-((2-hydroxyethyl)(methyl)amino)benzaldehyde (**Ald 1**) with 1,3-diethy1-2-thiobarbituric acid (**T**). The compound **3** was synthesized in successive steps. Firstly, the electron acceptor 1,3- diethyl-5-(3,5,5-trimethyl-2-cyclohexen-l-ylidene)-2-thiobarbituric acid (**IT**) was prepared by the method described by Brooker [18, 19]. Secondly, the electron acceptor **IT** was reacted with **Ald 1** in the presence of piperidine to give chromophore **3.** The conditions used to prepare this compound were analogous to that described in the literature [15, 20, 21]. Analogous reactions were carried out with 4-((2-(((1,1-dimethylethyl)dimethylsilyl)oxy)ethyl)methylamino)-benzaldehyde (**Ald 2**) to produce chromophores **2** and **4** (**Scheme 1**).

The chromophore was synthesized by esterification of **3** with **acetic acid**. This reaction was carried out following the experimental procedure described by Hudhomme [22] in the presence of dicyclohexylcarbodiimide (DCC), 4-(dimethylamino)- pyridine (DMAP), and 1-hydroxybenzotriazole (HOBT). This esterification afforded the corresponding compound **5**.

The synthesis of chromophores **8**, **9**, **10** and **11** was depicted in **Scheme 2**. To begin with the synthesis of **9**, aldehyde **Ald 4** is used. The previously unreported aldehyde

Ald 4 was prepared by a convergent method described in the literature [23-25]. On one hand, 2-bromomethylthiophene was prepared by the bromination of 2-methylthiophene with *N*-bromosuccinimide. Next, diethyl 2-thiophenylmethylphosphonate was prepared by the Arbuzov reaction of 2-bromomethylthiophene with triethylphosphite [26-28]; on the other hand, 2-(methylphenylamino)ethanol was protected using benzoyl chloride to give 2-(methyl(phenyl)amino)ethylbenzoate and then was formilated by the Vilsmeier reaction to produce the previously unreported **Ald 3**. Then, the 4-(*N*-ethyl-*N*-((benzoyl-oxy)ethyl)amino)benzaldehyde (**Ald 3**) reacted with the described phosphonate derivative through the Horner-Emmons reaction [29] to give the compound (*E*)-2-methyl(4-(2-thiophen-2-yl)vinyl)phenyl)amino)ethyl benzoate (**6**) and the corresponding alcohol due to a partial hydrolysis caused by the formed NaOH. The Vilsmeier-Haack formylation [30] of the benzoate gave the aldehyde **Ald 4.** In a similar way, a lithiation was carried out starting from the corresponding aniline protected by the *tert*-butyl dimethyl silyl group (**7**) and using LDA followed by the addition of DMF. This aniline was selectively formylated at *p*-position and **Ald 5** was obtained [32].It should be notice that both aldehydes, **Ald 4** and **Ald 5**, were obtained as a mixture *E* and *Z*. Finally, chromophores **8** and **10** were isolated as an all *E* isomer after a Knoevenagel reaction between the electron acceptor 1,3-diethy1-2-thiobarbituric acid **(T)** and the aldehydes **Ald 4** and **Ald 5**, respectively. At the end, compound **8** was hydrolyzed to produce chromophore **9**. Finally, the electron acceptor **IT** was reacted with **Ald 5** in the presence of piperidine to give chromophore **11** in low yield. The characterization of compound **11** was not complete due to its instability in solution.

2.2.Linear optical properties

The linear optical properties of chromophores dissolved in organic solvents were studied by Ultraviolet-visible (UV/Vis) spectroscopy. The UV/Vis absorption data of the studied compounds are collected in **Table 1**.

Inspection of the spectra reveals some common trend; all compounds show strong intramolecular charge-transfer transitions in the visible region and in every series the λ_{max} values increase on lengthening the spacer.

Solvatochromic effect is related with the molecular nonlinearity of NLO chromophores [33].The comparison between the D-π-A compounds with a hydroxyl group (**1**, **3**, **9**) and functionalized compounds with a *tert*butyldimethylsilyl group (**2**, **4**, **10**) depicts a red shift in dichloromethane and a slight blue shift in dimethylformamide (DMF). The compounds **1-5** and **8, 9** present a positive solvatochromic effect on passing from dichloromethane to dimethylformamide. This positive solvatochromic shift serves as an indicator of the increased dipole moment upon excitation [34]; thus confirming the CT character of these transitions [35] and indicating positive hyperpolarizability.

However, compounds **10** and **11** present no shift when the solvent is changed from dichloromethane to dimethylformamide. Thus, the UV spectrum of chromophore **10** was carried out in hydrogen bond acceptor (HBA) solvents such as 1,4-dioxane, ethyl acetate and dimethylsulfoxide (DMSO) and in both hydrogen bond acceptor (HBA) and donor (HBD) solvents such as acetonitrile and ethanol (**Table 2**).

A positive solvatochromic shift is observed on passing from 1,4-dioxane to ethyl acetate or DMSO and also on passing from acetonitrile to ethanol. Thus, the chromophore **10** confirms the batochromic behaviour.

In order to obtain further information about the ground state structure of chromophore **10**, the transition energy plot as a function of solvent polarity was studied. The scales Z-scale, E^N_T, p* and ET(30) have been evaluated [35, 36]. It has been established linear correlations of transition energy with the typical solvent parameter (Z-scale (R^2=0.97), E^N_T (R^2=0.98), p* (R^2=0.97) or ET(30) (R^2=0.98)). Therefore, the transition energy plot as a function of solvent polarity decreases linearly with increasing the solvent polarity. (See S-37, S-38, S-39, S-40. *Supporting Information*).The declining transition energy with increasing solvent polarity is indicative of an increase of the dipole moment upon excitation ($\mu_g<\mu_e$), suggesting the predominance of the neutral form in the ground state structure.

*2.2.1. pH dependence on the absorption of chromophore **9***

Among the compounds studied, chromophore **9** showed an absorption spectrum strongly dependent on pH. The titration of HCl with a blue solution of chromophore **9** in EtOH (2 10^{-5} M, pH= 4.68) gives a relevant change of solution color turning yellowish in acidic medium. The corresponding absorption spectra are gathered in **Figure 1**. In this figure, a clear isosbestic point is observed at 515 nm, the specific wavelength at which the two chemical species (acid and basic) have the same molar absorptivity (ε).

The equivalence point, or stoichiometric point, corresponds to the mixing of stoichiometrically equivalent amounts of acid and base. As an indication of the sharpness of color change, it should be mentioned that the solution at pH= 2.85 is green and clearly different from both solutions at pH=3.04 (light blue) and at pH=2.72 (yellow). Thus, this chromophore solution has a potential use as pH-indicator in the range 2.72-3.04. On the other hand, the titration of KOH with the same solution of

compound **9** in EtOH (2 10^{-5} M) was also carried out and the blue color disappeared when the pH was changed from 10 to 11 value (See S-43. *Supporting Information*). This behavior is reversible.

2.3. Electrochemistry

The redox properties of the target compounds were measured by cyclic voltammetry (CV) in CH_2Cl_2 (**Table 3)**. Chromophores **1-5**, **8-11** show one oxidation and one reduction waves corresponding to the electron processes of oxidation of the electron donor unit and reduction of the electron acceptor fragment, respectively. Oxidation process is reversible or quasi-reversible.

The lengthening of the π-spacer gives rise to a decrease of the $E_{1/2}$ and $E_{p,c}$ values. On chain lengthening, the smaller the interaction between the electron donor and electron acceptor end groups, the easier both oxidation and reduction processes. In particular, as an oxidation process is concerned, this process is favored when either an isophorone (**3**, **4**) or a thiophene (**9**, **10**) ring are introduced on the π-spacer to get a better delocalization of the charge. Thus, the easiest oxidation was obtained with the compound with both isophorone and thiophene ring (**11**).

These observed trends in $E_{1/2}$($E_{p,c}$) are confirmed by theoretical calculations (PCM, CH_2Cl_2), which show that the E_{HOMO} (E_{LUMO}) values increase (decrease) with the length of the spacer. The variation of the $E_{1/2}$ values is more noticeable than that of $E_{p,c}$, in agreement with the trends shown by the energy levels of the frontier orbitals.

The comparison between the D-π-A compounds with a hydroxyl group and the ones functionalized with a silicon group show no important variation on the redox behavior.

2.4. Nonlinear optical properties

The second-order NLO properties of the prepared compounds have been measured by electric-field-induced second harmonic generation (EFISH) technique in CH_2Cl_2 at *1907 nm*. The measured $\mu\beta$ values, together with the corresponding static $\mu\beta_0$ values calculated using the two-level model (TLM), [37, 38] are gathered in **Table 4** (for the sake of comparison and as a reference,$\mu\beta_0$ = 480. 10^{-48} esu has been obtained for *Disperse Red 1*under the same experimental conditions). TLM is widely used to estimate zero-frequency $\mu\beta_0$ values from single-frequency measurements, in particular when one-dimensional systems, in which one excited state dominates the nonlinearity, are involved. The $\mu\beta_0$ values calculated using coupled perturbed Hartree-Fock (CPHF) theory (gas phase) [39] are also collected in **Table 4.**

The experimental values show that the lengthening of the spacer using isophorone or thiophene heterocycles gives rise to the increase of the NLO response in the series **1**<**3**<**9**. An analogous behavior is observed for the corresponding compounds bearing the alkylsilyl group **2**<**4**<**10**.The electron-donor character of alkylsilyl groups causes a higher NLO response of silylated compounds compared to their hydroxyl analogous with the exception of compound **2**.

When the chromophores **10** and **11** are compared, the extra isophorone ring does not enhance the NLO response of the chromophore and, regarding their UV/Vis spectra, both compounds show the band maxima at the same wavelength in CH_2Cl_2 and DMF. Although the π-spacer length is increased by the introduction of the isophorone ring, these results could be explained by both the distortion of the planarity of the chromophore and the difficulties to align the μ and β vectors. Similar effects of an analogous structural modification have been previously reported and explained for the

compounds reported in ref.[40]. The better stability of compound **10** compared with compound **11** makes compound **10** more adequate chromophore for further applications.

Moreover, when compounds **3** and **9**are compared with the analogous with alkoxysilyl group, an improvement of the molecular NLO response is observed (compounds **4** and **10**). As the λ_{max} is scarcely modified, the presence of the silicon group improves the transparence-efficiency trade-off.

The calculations correctly reproduce the $\mu\beta$ increasing tendency associated with the lengthening of the π-spacer and the effect of the incorporation of the silyl group in chromophores **3** and **9**. However, the predicted increase of $\mu\beta_0$ for **2** compared to **1** has not be observed experimentally.

2.5.Thermal Stability.

The thermal stabilities of the chromophores were studied by thermogravimetric analysis (TGA) under nitrogen at a heating rate of 10 °C/min. The decomposition temperature (Td) was estimated as the temperature at the intercept of the leading edge of the weight loss with the baseline of the TGA scans.

The results [Td (°C): **1**, 220; **3**, 266; **9**, 224;**2**, 258; **4**, 296;**10**, 246; **11**, 284] show that the compounds have acceptable thermal stabilities for the high temperature poling processes carried out to induce macroscopic NLO response [41, 42].

In every case it can be observed that thermal stability improves with both the presence of the silicon group and the isophorone ring [43-46] in the NLO chromophore.

2.6.Electric field poling and macroscopic nonlinear properties

In order to undertake a further study, the two chromophores with the best NLO molecular response studied in this work were incorporated into a polymeric matrix. Both chromophores, **4** and **10,** contain bulky silicon groups and the presence of bulky groups is expected to minimize the electrostatic interactions. Moreover, their thermal stabilities, discussed above, make them suitable for high temperature poling in order to examine their macroscopic NLO response.

The optical properties of thin films of the chromophores **4** and **10** have been studied. These chromophores have been embedded in polybisphenol A carbonate (**PC**) (Mw = 6400, Tg = 150ºC) and thin films, with different chromophore content, from 4% up to 20%wt, were prepared by *spin coating* [47-49]. The UV/Vis spectra exhibited a strong absorption in the visible region as it is shown in **Figure 2** for **PC_10** films. The measurements of the different films have been scaled by the thickness. Very similar band shape was observed when the results for different chromophore concentration were compared. A slight increase of the bandwidth is observed with the chromophore content which could indicate some molecular aggregation; however, it does not seem to be very important. Moreover, the maximum absorption values scale essentially as 4:8:12:20, which indicates that the amount of the chromophore in the matrix corresponds with the nominal content.

Following with the optical characterization of thin films, refractive index measurements (mode coupling method) were performed at *1306 nm*. In addition to providing information on the initial state of the films (chromophore content, optical anisotropy...), refractive index evolution reflects the changes of molecular orientation, as the ones associated with the electric field poling processes [50].

The refractive indices of the doped polymer films are gathered in **Table 5**. The thickness of the films was in the range *1.5-2 μm*. On the one hand, it is observed the expected increase of the index values with the chromophore content, due to the optical absorption contribution. On the other hand, the measurements revealed that the index value measured with light polarization parallel to the film plane (n_o) is somewhat higher than that corresponding to light polarization perpendicular to the plane (n_e). This initial anisotropy, which indicates a preferential in-plane order, can be attributed to the film preparation conditions.

The **PC_4** and **PC_10** films were poled by using electric field "*corona"* poling process (*see Supporting Information*).The UV/Vis spectra taken at normal incidence showed a decrease of the absorption of the poled films as compared with the "*as prepared*" ones. In order to estimate the degree of the induced orientation, an order parameter, defined as ϕ=1-($ABS_{poled}/ABS_{unpoled}$), is usually given [51, 52]. In the present work, ϕ values about 0.16 and 0.14 have been obtained for compounds **4** and **10**, respectively. In accordance with that, index measurements revealed that the sign of the anisotropy is reversed upon the poling, and a positive birefringence (between 0.01 and 0.02) has been obtained.

The nonlinear optical properties of the poled films were evaluated by SHG measurements at *1907 nm*. Two different polarizations (*s* and *p*) of the excitation light were used in order to obtain the d_{31} and d_{33} coefficients. **Table 6** depicts the mentioned coefficients, calculated from the fitting of the harmonic signal measurements (Maker fringes) performed 24 hours after the poling process. It can be seen that d_{33}/ d_{31} ratios near to 3 have been obtained, which is in accordance with an essentially isotropic host matrix arrangement and the assumption of low poling electric field. [53].

On the other hand, the comparison of d_{ij} values of the three **PC_10** films, allows assuming a similar polar order degree, regardless of the chromophore content. Thus,

macroscopic nonlinear coefficients increase almost linearly with the chromophore content and, in accordance with UV/Vis results, saturation of the response has not been observed up to 20 % for **PC_10** films (expected, for example, if aggregation were relevant).

As the molecular relaxation tends to gradually reduce the polar ordering in poled guest-host polymeric systems, the NLO response of films was characterized after different intervals of time once the poling process was finished. After a week, a reduction of about 5-8 % respect to the coefficients shown in the **Table 6** has been observed for the films. The NLO signal (as well as the optical anisotropy) of the films with the highest chromophore content was monitored over longer times. Measurements performed up to eight months after the poling showed that the polar order was maintained in a fairly high degree, obtaining d_{ij} values over 80% of that measured just after the poling.

3. Conclusions

A new series of aniline electron donor-based chromophores with a thiophene or an isophorone ring in the π-spacer group have been synthesized and show a combined high/moderate nonlinear optical activities (NLO) with good transparency. Both experimental and theoretical results show the improvement of $\mu\beta_0$ values when the silicon substituent is placed on the electron donor moiety. The alkylsilyl group has improved the NLO response as well as the thermal stability. This functionalization contributes to increase the solubility of these compounds, key factor in order to further macroscopic studies.

The incorporation of chromophores **4** and **10** in a polycarbonate matrix allowed the preparation of good optical-quality films by spin coating. UV/Vis studies showed no evidence of aggregation for the different concentrations explored, from 4% up to 20%. Corona poling processes were undertaken and quite efficient polar order was achieved. Nonlinear coefficients as high as 17 and 5.6 pm.V^{-1} (d_{33} and d_{31}, respectively) were obtained for films with 20% wt content of chromophore **10**. Concerning the stability of the polar order, it should be noted that 8 months after the poling d_{ij} values over 80% of those measured just after the poling were obtained.

4. Experimental

Detailed Synthetic Procedures:

1,3-diethyl-5-(4-((2-hydroxyethyl)(methyl)amino)benzylidene)-2-thiobarbituric acid (1)

A solution of 1,3-diethyl-2-thiobarbituric acid, **T** (400 mg, 2.00 mmol) and 4-((2-hydroxyethyl)(methyl)amino)benzaldehyde, **Ald 1**, (358 mg, 2.00 mmol) was prepared in 30 mL ethanol. The mixture was refluxed under argon atmosphere with exclusion of light for 1 hour. After cooling, the residue was filtered and washed with cold ethanol. A red solid was obtained (642 mg, 89%). Molecular weight (g/mol): 361.46.

m.p. (ºC) at 760 mmHg: 209. **IR** (KBr)(cm^{-1}): 1685 (C=O), 3453 (O-H).**^{1}H NMR** (400 MHz, $CDCl_3$) δ: 1.29-1.34 (m, 6H), 3.21 (s, 3H), 3.69 (t, *J* = 5.5 Hz, 2H), 3.91 (t, *J* = 5.5 Hz, 2H), 4.55-4.62 (m, 4H), 6.77 (d, *J* = 9.26 Hz, 2H), 8.39-8.41 (m, 3H).**^{13}C NMR** (100 MHz, $CDCl_3$) δ: 12.4, 12.5, 39.5, 43.4, 44.0, 54.2, 60.2, 110.7, 111.3, 121.9, 139.9, 154.3, 159.7, 162.2. **HRMS (ESI^{+})** m/z 362.1521 $[M+H]^{+}$; $[C_{18}H_{24}N_3O_3S]^{+}$ requires 362.1533. **Uv-Vis data** $\lambda_{max}(CH_2Cl_2)$ (nm): 493, molar extinction coefficient $\varepsilon_{max}(ml^{-1}dm^3cm^{-1})$: 76. **Elemental analysis** found C 59.52; H 6.61; N 11.49; S 8.90 %; molecular formula $C_{18}H_{23}N_3O_3S$ requires C 59.81; H 6.41; N 11.63; S 8.87 %.

5-(4-((2-*terc*-butyldimethylsilyl)oxi)etil)(methyl)amino)benziliden)-1,3-diethyl-2-tioxodihydropyrimidine-4,6(1H,5H)-dione (2)

A solution of 1,3-diethyl-2-thiobarbituric acid, **T** (100.13 mg, 0.5 mmol) and **Ald 2** (146 mg, 0.5 mmol) were solved in ethanol (9 mL). The reaction mixture was stirred at 80 °C during 75 min with exclusion of light. The precipitated was filtered and 232.8 mg (0.4893 mmol) of a red solid was obtained with a yield of 98%. Molecular weight (g/mol): 475.72.

m.p. (^{o}C) at 760 mmHg: 151. **IR** (Nujol)(cm^{-1}): 820 (Si-$(CH_3)_2$), 1653 (C=O). **^{1}H NMR** (400 MHz, $CDCl_3$) δ:0.00 (s, 6H), 0.86 (s, 9H), 1.29-1.34 (m, 6H), 3.19 (s, 3H), 3.64 (t, *J*= 5.6 Hz, 2H), 3.84 (t, *J*= 5.6 Hz, 2H), 4.55-4.62 (m, 4H), 6.74 (d, *J*=8.8 Hz, 2H), 8.41-8.42 (t, *J*= 8.8 Hz, 3H). **^{13}C NMR** (100 MHz, $CDCl_3$) δ: -5.5, 12.4, 12.5, 18.1, 25.8, 39.8, 43.4, 43.9, 54.7, 60.5, 110.4, 111.4, 121.8, 139.9, 154.2, 159.6, 162.2, 178.8. **HRMS (HR-ESI^{+})** m/z 476.2401 $[M+H]^{+}$;$[C_{24}H_{38}N_3O_3SSi]^{+}$ requires 476.2398. **Uv-Vis data** $\lambda_{max}(CH_2Cl_2)$ (nm): 496, molar extinction coefficient ε_{max}($ml^{-1}dm^3cm^{-1}$): 78. **Elemental analysis** found C 60.32, H 7.85, N 8.99, S 6.53 %; molecular formula$C_{24}H_{37}N_3O_3SSi$ requires C 60.59, H 7.84, N 8.83, S 6.74 %

(*E*)-1,3-diethyl-5-(3-(4-((2-hydroxyethyl)(methyl)amino)estyryl)-5,5-dimethyl-2-cyclohex-2-en-1-yliden)-2-thiobarbituric acid (3)

To a solution of 4-((2-hydroxyethyl)(methyl)amino)benzaldehyde, **Ald 1**, (90 mg, 0.50 mmol)) and the acceptor **IT** (160 mg, 0.50 mmol) in dry acetonitrile (7.5 mL) piperidine (0.05 mL, 0.5 mmol) was added. The mixture was refluxed under argon atmosphere with exclusion of light for 7 hours (TLC monitoring). After cooling, acetonitrile was distilled, and CH_2Cl_2 was added (200 mL). The organic layer was washed with HCl 0.1 M (2×70 mL) and water (2×70 mL), dried ($MgSO_4$) and the solvent evaporated. The

crude product was purified by flash chromatography on silica gel (40-60 μm) with hexane: ethyl acetate (1:1) as eluent and a dark blue solid was obtained (170 mg, 70%). Molecular weight (g/mol): 481.65.

m.p. (ºC) at 760 mmHg: 90. **IR** (Nujol)(cm^{-1}): 1657 (C=O), 3434 (OH). **^{1}H NMR** (400 MHz, $CDCl_3$) δ: 1.06 (s, 6H), 1.27-1.34 (m, 6H), 1.58 (s, 1H), 2.46 (s, 2H), 3.08 (s, 3H), 3.10 (s, 2H), 3.58 (t, *J* = 5.6 Hz, 2H), 3.86 (t, *J* = 5.6 Hz, 2H), 4.50-4.58 (m, 4H), 6.78 (d, *J* = 7.3 Hz, 2H), 7.03 (c, *J* = 16.1 Hz, 2H), 7.43 (d, *J* = 8.8 Hz, 2H), 8.39 (s, 1H).**^{13}C NMR** (100 MHz, $CDCl_3$) δ: 12.6, 28.6, 31.9, 39.0, 43.6, 43.7, 44.9, 54.9, 60.1, 111.5, 112.3, 127.2, 127.5, 129.6, 137.5, 160.8, 161.2, 171.1, 178.0. **HRMS (ESI^+)** m/z 482.2481 $[M+H]^+$; $[C_{27}H_{36}N_3O_3S]^+$ requires 482.2472. **Uv-Vis data** $\lambda_{max}(CH_2Cl_2)$ (nm): 564, molar extinction coefficient $\varepsilon_{max}(ml^{-1}dm^3cm^{-1})$: 26. **Elemental analysis** found C 67.45, H 7.50, N 8.55, S 6.75 %; molecular formula$C_{27}H_{35}N_3O_3S$ requires C 67.33, H 7.32, N 8.72, S 6.66 %.

***(E)*-5-(3-(4-((2-((*terc*-butyldimethylsilyl)oxi)etil)(methyl)amino)styryl)-5,5-dimethylcyclohex-2-en-1-yliden)-1,3,diethyl-2-tioxodihydropyrimidine-4,6(1H,5H)-dione (4)**

To a stirred solution of **Ald 2** (586.95 mg, 2 mmol) in dry acetonitrile (8 mL) piperidine (0.1975 ml, 2 mmol) was added. After 15 min, **IT** (640.9 mg, 2 mmol) was also added. The mixture was refluxed during 1h. The solvent was removed and the residue was solved in dichloromethane (200mL) and washed with H_2O-HCl (9:1) (2x70 mL) and twice with water and dried. After concentration under reduced pressure, the residue was

purified by column chromatography hexane-ethyl acetate (1:0,1) on silica gel (40-60 μm) and the desired product was isolated as a dark blue solid 0.280 g with a yield of 24%. Molecular weight (g/mol): 595.33.

m.p. (^{o}C) at 760 mmHg: 76. **IR** (KBr)(cm^{-1}): 861 (Si-$(CH_3)_2$), 1180 (C=S), 1657 (C=O). ^{1}**H NMR** (400 MHz, $CDCl_3$) δ:0.02 (s, 6H), 0.87 (s, 9H), 1.07 (s, 6H), 1.28-1.35 (t, 6H), 2.46 (s, 2H), 3.11 (s, 2H), 3.13 (s, 3H), 3.55 (t, 2H), 3.87 (t, 2H), 4.47-4.60 (m, 4H), 6.95-7.10 (m, 4H), 7.48 (d, *J*=8.8 Hz, 2H), 8.39 (s, 1H). **^{13}C NMR** (100 MHz, $CDCl_3$) δ: -5.5, 12.6, 18.2, 25.8, 28.6, 31.9, 39.1, 43.6, 43.7, 44.8, 60.1, 129.5, 172.2, 173.9, 174.2, 177.5, 178.9, 179.9. **HRMS (ESI^{+})** m/z 596.3342 $[M+H]^{+}$; $[C_{33}H_{50}N_3O_3SSi]^{+}$ requires 596.3337. **Uv-Vis data** $\lambda_{max}(CH_2Cl_2)$ (nm): 579, molar extinction coefficient ε_{max}($ml^{-1}dm^3cm^{-1}$): 46. **Elemental analysis** found C 66.70, H 8.52, N 6.84, S 5.24 %; molecular formula$C_{33}H_{49}N_3O_3SSi$ requires C 66.51, H 8.29, N 7.05, S 5.38 %.

(*E*)-2-((4-(2-(3-(1,3-diethylthiobarbituric)-5,5-dimethyl-1-cyclohexen-1-yl)vinyl)phenyl)(methyl)amino)ethyl acetate (5)

To a solution of **acetic acid** (0.012 mL, 0.21 mmol) in dry dichloromethane (30 mL), 1-hydroxybenzotriazole (**HOBT**), (28 mg, 0.21 mmol), 4-dimethylaminopyridine (**DMAP**) (51 mg, 0.42 mmol) and 1,3-dicyclohexylcarbodiimide (**DCC**) (86 mg, 0.42 mmol) were added successively under nitrogen atmosphere and after 15 minutes compound **3** (100 mg, 0.21 mmol) was also added. The reaction mixture was stirred at

room temperature during 4 days with exclusion of light. The mixture was filtered and dichloromethane (200 mL) was added. The organic phase was washed several times with both NH_4Cl and water and it was dried with $MgSO_4$. After concentration under reduced pressure, the residue was purified by column chromatography (CH_2Cl_2) on silica gel (40-60 μm) and the ester was isolated as a dark blue solid (40 mg, 36%). Molecular weight (g/mol): 523.68.

m.p. (ºC) at 760 mmHg: 135. **IR** (Nujol)(cm^{-1}): 1271 (C-O), 1651 (C=O), 1739 (C=O).**^{1}H NMR** (400 MHz, $CDCl_3$) δ: 1.06 (s, 6H), 1.28-1.34 (m, 6H), 2.01 (s, 3H), 2.46 (s, 2H), 3.06 (s, 3H), 3.10 (s, 2H), 3.66 (t, *J* = 5.9 Hz, 2H), 4.27 (t, *J* = 5.9 Hz, 2H), 4.50-4.58 (m, 4H), 6.71 (d, *J* = 9.0 Hz, 2H), 6.98 (d, *J* = 15.9 Hz, 1H), 7.07 (d, *J* = 15.9 Hz, 1H), 7.43 (d, *J* = 9.0 Hz, 2H), 8.39 (s, 1H). **^{13}C NMR** (100 MHz, $CDCl_3$) δ: 12.6, 20.9, 28.7, 31.9, 38.7, 39.1, 43.7, 45.0, 50.8, 61.3, 112.1, 124.6, 127.1, 127.5, 129.7, 137.8, 150.2, 159.2, 160.9, 161.2, 170.9, 171.2, 178.1. **HRMS (MALDI$^+$)** m/z 524.2564 $[M+H]^+$.; $[C_{29}H_{38}N_3O_4S]^+$ requires 524.2578. **Uv-Vis data** $\lambda_{max}(CH_2Cl_2)$ (nm): 563, molar extinction coefficient ε_{max}($ml^{-1}dm^3cm^{-1}$): 36. **Elemental analysis** found C 66.70, H 7.34, N 7.88, S 6.32 %; molecular formula $C_{29}H_{37}N_3O_4S$ requires C 66.51, H 7.12, N 8.02, S 6.12 %.

2-((4-formylphenyl)(methyl)amino)ethyl benzoate (Ald 3)

$POCl_3$ (1.0 mL, 10.92 mmol) was added dropwise to (2.0 mL, 25.83 mmol) of freshly distilled DMF at 0°C in argon atmosphere. A solution of (2.500 g, 9.80 mmol) of N-2-benzoxyethyl-N-methylaniline (20 mL) was added dropwise to the $POCl_3$ /DMF complex at room temperature. The reaction mixture was stirred at 90 °C for 6h. After

the completion of the reaction (monitored by TLC), the reaction mixture was cooled to rt and poured into ice water. The crude product was extracted with dichloromethane (3 x 100 ml) and the organic layer was washed with sodium acetate and water and dried over anhydrous sodium sulfate. After removing the solvent under reduced pressure, the residue was purified by column chromatography (eluent: dichloromethane/ethyl acetate, 95 : 5) on silica gel to afford the desired compound as an yellow oil (1.58 g, 57 % yield). Molecular weight (g/mol): 283.32.

IR (cm^{-1}): 1272 (C-O), 1678 (C=O), 1720 (C=O). **^{1}H NMR** (400 MHz, $CDCl_3$) δ: 3.15 (s, 3H), 3.84 (t, *J* = 5.9 Hz, 2H), 4.52 (t, *J* = 5.9 Hz, 2H), 6.80 (d, *J* = 9.0 Hz, 2H), 7.41 (t, *J* = 7,9 Hz, 2H), 7.55 (tt, J_1 = 7.5 Hz, J_2 = 1.3 Hz, 1H), 7.73 (dt, J_1 = 9.0 Hz, J_2 = 1.9 Hz, 2H), 7.94-7.96 (m, 2H), 9.74 (s, 1H) **^{13}C NMR** (100 MHz, $CDCl_3$) δ: 39.0; 50.8; 61.0; 111,3; 125.8; 128.5; 129.6; 132.1; 133.2; 153.4; 166.5; 190.3. **HRMS (HR-ESI^{+})** m/z 306.1104 $[M+Na]^{+}$; molecular formula $C_{17}H_{17}NNaO_3$ requires $[M+Na]^{+}$ 306.1100). **Elemental analysis** found C 72.15, H 6.04, N 4.92 %, molecular formula $C_{17}H_{17}NO_3$ requires C 72.07, H 6.05, N 4.94 %.

2-(methyl(4-(2-(thiophen-2-yl)vinyl)phenyl)amino)ethyl benzoate (6a) and 2-(methyl(4-(2-(thiophen-2-yl)vinyl)phenyl)amino)ethanol (6b)

To a dried, three-necked, 100 mL round-bottom flask were added 1,2-dimethoxyethane (15 mL) and sodium hydride, 60 %(156 mg, 4.06 mmol) under nitrogen. The mixture was stirred for 5 min, and compound **Ald 3** (575 mg, 2.03 mmol) in 1,2-dimethoxyethane (10 mL) was then added. The diethyl 2-thenylphosphonate (471 mg, 2.03 mmol) in 1,2-dimethoxyethane (10 mL) was added slowly to the reaction mixture. The resulting solution was overnight at room temperatura and then poured into crushed

ice (40 g) under nitrogen. The mixture was extracted with dichloromethane (3 × 30 mL). The organic layer was washed with water (3 × 50 mL). After removing the solvent, the crude product was chromatographed using hexane /diethyl ether (7: 3) to yield compound **6a** as yellow solid (143 mg, 0.39 mmol) yield: 19 %. Molecular weight (g/mol): 363.47.

m.p. (ºC) at 760 mmHg: 104. **I.R.** (Nujol) cm^{-1}: 1277 (C-O), 1713 (C=O). **^{1}H NMR** (400 MHz, $CDCl_3$) δ: 3.08 (s, 3H), 3.78 (t, *J* = 5.9 Hz, 2H), 4.51 (t, *J* = 5.9 Hz, 2H), 6.77 (d, *J* = 8.8 Hz, 2H), 6.86 (d, *J* = 16.0 Hz, 1H), 7.00-6.96 (m, 2H), 7.04 (d, *J* = 16.0 Hz, 1H), 7.12 (d, *J* = 4.8 Hz, 1H), 7.36 (d, *J* = 8.8 Hz, 2H), 7.42 (t, *J* = 7.7 Hz, 2H), 7.55 (t, *J* = 7.4 Hz, 1H), 7.97 (d, *J* = 7.4 Hz, 2H).**^{13}C NMR** (100 MHz, $CDCl_3$) δ: 38.8; 51.2; 62.1; 112.4; 117.9; 123.1; 124.6; 127.5; 127.6; 128.4; 128.5; 129.6; 133.0. **HRMS (HR-ESI^{+})** m/z 364.1367 $[M+H]^{+}$; molecular formula $C_{22}H_{22}NO_2S$: requires $[M+H]^{+}$ 364.1366). **Elemental analysis** found C 72.97, H 5.80, N 3.84, S 8.84 %, molecular formula $C_{22}H_{21}NO_3S$ requires C 72.70, H 5.82, N 3.85, S 8.82 %.

C**ompound 6b** was obtained as a yellow solid (164 mg, 0.63 mmol). Yield: 31 %. Molecular weight (g/mol): 259.36.

m.p. (ºC) at 760 mmHg: 124. **I.R.** (Nujol) cm^{-1}: 1604 (C=C), 3250 (O-H). **^{1}H NMR** (400 MHz, $CDCl_3$) δ: 3.01 (s, 3H), 3.51 (t, *J* = 5.6 Hz, 2H), 3.83 (t, *J* = 5.6 Hz, 2H), 6.80 (d, *J* = 8.6 Hz, 2H), 6.86 (d, *J* = 16.1 Hz, 1H), 6.97-7.00 (m, 2H), 7.06 (d, *J* = 16.1 Hz, 1H), 7.13 (d, *J* = 5.0 Hz, 1H), 7,36 (d, *J* = 8.6 Hz, 2H).**^{13}C NMR** (100 MHz, $CDCl_3$) δ: 39.0; 55.3; 60.1; 113.0; 118.1; 123.2; 124.7; 126.2; 127.4; 128.3; 143.7; 149.2. **HRMS (HR-ESI^{+})** m/z 260,1105 $[M+H]^{+}$; molecular formula $C_{15}H_{18}NOS$ requires $[M+H]^{+}$: 260,1104). **Elemental analysis** found C 69.63, H 6.62, N 5.39, S 12.39 %, molecular formula $C_{15}H_{17}NOS$ requires C 69.46, H 6.61, N 5.40, S 12.36 %.

2-((4-(2-(5-formylthiophene-2-yl)vinyl)phenyl)(methyl)amino)ethyl benzoate (Ald 4)

$POCl_3$ (0.05 mL, 0.58 mmol) was added dropwise to (0.29 mL, 3.77 mmol) of freshly distilled DMF at 0°C in argon atmosphere. A solution of (212 mg, 0.58 mmol) of compound **6a** was added dropwise to the $POCl_3$ /DMF complex at rt. The reaction mixture was stirred at 80 °C for 20 h. After the completion of the reaction (monitored by TLC), the reaction mixture was cooled to rt and poured into ice water. The crude product was extracted with dichloromethane (3 x 100 ml) and the organic layer was washed with sodium bicarbonate and water and dried over anhydrous sodium sulfate. After removing the solvent under reduced pressure, the residue was purified by column chromatography (eluent: hexane/dichloromethane, 1:1) on silica gel to afford an orange solid (188 mg, 0.48 mmol), 83% yield as a mixture Z/E (46/54). Molecular weight (g/mol): 391.48.

IR (KBr) cm^{-1}: 1262 (C-O), 1649 (C=O), 1714 (C=O). **^{1}H NMR** (400 MHz, $CDCl_3$) δ: 3.09-3.11 (m, 6H), 3.77-3.81 (m, 4H), 4.51-4.55 (m, 4H), 6.51 (d, *J* = 12.0 Hz, 1H), 6.68 (d, *J* = 12.0 Hz, 1H), 6.80 (m, 4H), 7.01 (d, *J* = 16.0 Hz, 1H), 7.07-7.11 (m, 3H), 7.27 (d, *J* = 8.9 Hz, 2H), 7.39-7.44 (m, 6H), 7,54-7,56 (m, 3H), 7,64 (d, *J* = 3.9 Hz, 1H), 7.95-8.00 (m, 4H), 9.79 (s, 1H), 9.82 (s, 1H). **HRMS (HR-ESI$^+$)** m/z 392,1321 $[M+H]^+$; molecular formula $C_{23}H_{22}NO_3S$ requires $[M+H]^+$ 392,1315). **Elemental analysis** found C 70.80, H 5.40, N 3.59, S 8.17 %, molecular formula $C_{22}H_{21}NO_3S$ requires C 70.56, H 5.41, N 3.58, S 8.19 %.

(*E*)-2-((4-(2-(5-((1,3-diethylthiobarbituric)-5(2H)-ylidene)methyl)thiophene-2-yl)vinyl)phenyl)(methyl)amino)ethyl benzoate (8)

A solution of the aldehyde, **Ald 4** (103 mg, 0.26 mmol) and 1,3-diethyl-2-thiobarbituric acid, **T** (53 mg, 0.26 mmol) was prepared in 25 mL ethanol. The mixture was refluxed under argon atmosphere with exclusion of light for 1 hour. After cooling, the residue was filtered and washed with cold ethanol. A dark blue solid was obtained (83 mg, 55%). Molecular weight (g/mol): 573.73.

m.p. (ºC) at 760 mmHg: 175. **IR** (KBr)(cm^{-1}): 1264 (C-O), 1685 (C=O), 1717 (C=O).**^{1}H NMR** (400 MHz, $CDCl_3$)) δ: 1.32 (t, *J* = 7.0 Hz, 3H), 1.37 (t, *J* = 7.0, 3H), 3.13 (s, 3H), 3.82 (t, *J* = 5.9 Hz, 2H), 4.53 (t, *J* = 5.9 Hz, 2H), 4.56-4.66 (m, 4H), 6.83 (d, *J* = 8.8 Hz, 2H), 7.08 (d, *J* = 16.0 Hz, 1H), 7,22 (d, *J* = 4.2 Hz, 1H), 7.38 (d, *J* = 16.0 Hz, 1H), 7.40-7.43 (m, 2H), 7.44-7.47 (m, 2H), 7.54-7.58 (m, 1H), 7.79 (d, *J* = 4.2 Hz, 1H), 7.95-7.97 (m, 2H), 8.60 (s, 1H).**^{13}C NMR** (100 MHz, $CDCl_3$) δ: 12.4, 12.6, 39.1, 43.1, 43.9, 51.1, 61.9, 108.7, 112.5, 116.7, 126.3, 128.4, 129.1, 129.6, 129.7, 133.2, 135.4, 135.8, 147.8, 150.0, 160.0, 161.3, 162.3, 166.5, 178.7. **HRMS (ESI^{+})** m/z 574.1809 $[M+H]^{+}$; $[C_{31}H_{32}N_3O_4S_2]^{+}$ requires 574.1829. **Uv-Vis data** $\lambda_{max}(CH_2Cl_2)$ (nm): 584, molar extinction coefficient ε_{max}($ml^{-1}dm^3cm^{-1}$): 51. **Elemental analysis** found C 65.01, H 5.56, N 7.11, S 11.25 %; molecular formula $C_{31}H_{31}N_3O_4S_2$ requires C 64.90, H 5.45, N 7.32, S 11.18 %.

(*E*)-1,3-diethyl-5-((5-(4-((2-hydroxyethyl)(methyl)amino)styryl)-2-thiophen-2-yl)methylen)-2-thiobarbituric acid (9)

To a solution of the **8** compound (67 mg, 0.12 mmol) in 2 mL ethanol, NaOH was added (0.5 mL, 20%). The reaction mixture was stirred at room temperature during 14 hours with exclusion of light. The residue was filtered and the solvent was removed. Chloroform (200 mL) was added and the organic phase was washed several times with both NH_4Cl and water and dried. After concentration under reduced pressure, a dark green solid was obtained (34 mg, 63%). Molecular weight (g/mol): 469.62.

m.p. (ºC) at 760 mmHg: 210. **IR** (Nujol)(cm^{-1}): 1377 (C=S), 1644 (C=O), 3497 (O-H).**^{1}H NMR** (400 MHz, $CDCl_3$) δ: 1.32 (t, *J* = 7.0 Hz, 3H), 1.36 (t, *J* = 7.0 Hz, 3H), 3,09 (s, 3H), 3.58 (t, *J* = 5.6 Hz, 2H), 3.87 (t, *J* = 5.6 Hz, 2H), 4.56-4.67 (m, 4H), 6.79-6.86 (m, 2H), 7.09 (d, *J* = 16.0 Hz, 1H), 7.21 (d, *J* = 4.3 Hz, 1H), 7.38 (d, *J* = 16.0 Hz, 1H), 7.45 (d, *J* = 8.9 Hz, 2H), 7.78 (d, *J* = 4.3 Hz, 1H), 8.60 (s, 1H).**^{13}C NMR**(100MHz, $CDCl_3$) δ: 12.4, 12.6, 29.7, 43.1, 44.0, 126.6, 129.0, 147.6, 149.0, 160.0, 161.2, 178.7. **HRMS (ESI^{+})** m/z 470.1552 $[M+H]^{+}$; $[C_{24}H_{28}N_3O_3S_2]^{+}$ requires 470.1567. **Uv-Vis data** $\lambda_{max}(CH_2Cl_2)$ (nm): 587, molar extinction coefficient ε_{max}($ml^{-1}dm^3cm^{-1}$): 41. **Elemental analysis** found C 61.28, H 5.76, N 9.10, S 13.50%; molecular formula $C_{24}H_{27}N_3O_3S_2$ requires C 61.38, H 5.80, N 8.95, S 13.65 %.

<u>*(E)*-5-((5-(4-((2-((*terc*-buthyldimethylsilyl)oxi)ethyl)(methyl)amino)styryl)thiophen-2-yl)methylen)-1,3-dimethyl-2-tioxodihydropyrimidine-4,6(1H,5H)-dione</u> (10).

To a stirred solution of 1,3-diethyl-2-thiobarbituric acid, **T** (50 mg, 0.250 mmol) in ethanol (6 mL), **Ald 5 (**100 mg, 0.250 mmol)solved in ethanol (12 mL) was added. The reaction mixture was heated at 70ºC during 2h with exclusion of light. The precipitated

was filtered and washed with cold ethanol. 0,120 g (0.205 mmol) of a dark blue solid were obtained with a yield of 82%. Molecular weight (g/mol): 583.88.

m.p. (^{o}C) at 760 mmHg: 140 (d). **IR** (Nujol)(cm^{-1}): 1266 (C-O), 1382 (C=S), 1652 (C=O). ^{1}**H NMR** (400 MHz, $CDCl_3$) δ: 0.02 (s, 6H), 0.88 (s, 9H), 1.31 (t, *J*=7.2 Hz, 3H), 1.36 (t, *J*=7.2 Hz, 3H), 3.07 (s, 3H), 3.53 (t, *J*=5.6 Hz, 2H), 3.80 (t, *J*=5.6 Hz, 2H), 4.58 (c, *J*=6.8 Hz 2H), 4.62 (c, *J*=6.8 Hz, 2H), 6.72 (d, *J*=8.8 Hz, 2H), 7.04 (d, *J*=16 Hz, 1H), 7.19 (d, *J*=4.4 Hz, 1H), 7.37 (d, *J*=16 Hz, 1H), 7.42 (d, *J*=8.8 Hz, 2H), 7.76 (d, *J*=4.4 Hz, 1H), 8.58 (s, 1H). **^{13}C NMR** (100 MHz, $CDCl_3$) -5.4, 12.4, 12.6, 25.8, 39.4, 43.1, 43.9, 54.7, 60.4, 108.4, 112.2, 116.0, 126.0, 129.1, 136.2, 147.9, 148.8, 150.2, 161.3, 162.8, 178.6. **HRMS (ESI^{+})** m/z 584.2392 $[M+H]^{+}$; $[C_{30}H_{42}N_3O_3S_2Si]^{+}$ requires 584.2431. **Uv-Vis data** $\lambda_{max}(CH_2Cl_2)$ (nm): 599, molar extinction coefficient ε_{max}(ml^{-1}dm^{3}cm^{-1}): 50. **Elemental analysis** found C 61.58, H 7.25, N 7.05, S 11.05 %, molecular formula $C_{30}H_{41}N_3O_3S_2Si$ requires C 61.71, H 7.08, N 7.20, S 10.98 %.

5-(3-((*E*)-2-(5-((*E*)-4-((2-((*terc*-buthyldimethylsilyl)oxi)ethyl)(methyl)amino)styryl)thiophen-2-yl)vinyl)-5,5-dimethylcyclohex-2-en-1-yliden)-1,3-diethyl-2-tioxodihydropyrimidine-4,6(1H,5H)-dione (11).

To a stirred solution of **Ald 5** (150 mg, 0.373 mmol) in dry acetonitrile (8 mL) piperidine (0.037 ml, 0.373 mmol) was added. After 15 min., the acceptor **IT** (119.68 mg, 0.373 mmol) was also added. The mixture was heated at 70 ^{o}C during 1 h. The solvent was removed and the residue was solved with dichloromethane (200 mL) and washed with H_2O-HCl (9:1) (2x70 ml) and twice with water. The residue was dried and purified with two consecutive column chromatography hexane-ethyl acetate (8:1) on

silicagel (40-60 μm). The desired product was obtained as a dark blue solid with a yield of 6%. Molecular weight (g/mol): 704.07.

m.p. (^{o}C) at 760 mmHg: 97. **IR** (KBr)(cm^{-1}): 1361 (C=S). ^{1}**H NMR** (400 MHz, $CDCl_3$) δ: 0.02 (s, 6H), 0.84 (s, 9H), 1.07 (s, 6H), 1.29-1.34 (m, 6H), 2.41 (s, 2H), 3.10 (s, 2H), 3.25 (s, 3H), 3.55 (t, 2H), 4.05 (t, 2H), 4.50-4.60 (m, 4H), 6.92 (d, *J*=16 Hz, 2H), 7.06 (d, *J*=4 Hz, 1H), 7.10 (d, *J*=4 Hz, 1H), 7.14 (d, *J*=16 Hz, 1H), 7.22 (d, *J*=16 Hz, 1H), 7.57 (d, *J*=8.4 Hz, 2H), 7.78 (d, *J*=8.4 Hz, 2H), 8.38 (s, 1H). ^{13}**C NMR** (100 MHz, $CDCl_3$) δ:-5.40, 12.6, 18.2, 25.9, 28.6, 29.7, 31.8, 38.9, 43.6, 43.7, 44.6, 60.0, 112.6, 124.1, 126.4, 128.0, 128.6, 129.4, 130.4, 131.0, 140.1, 156.8, 160.7, 161.1, 170.1, 178.1. **HRMS (HR-ESI^{+})** m/z 704.3351 $[M+H]^{+}$; $[C_{39}H_{54}N_3O_3S_2Si]^{+}$ requires 704.3370. **Uv-Vis data** $\lambda_{max}(CH_2Cl_2)$ (nm): 599, molar extinction coefficient ε_{max}(ml^{-1}dm^{3}cm^{-1}): 35. **Elemental analysis** found C 66.60, H 7.31, N 6.20, S 4.12 %; molecular formula $C_{39}H_{53}N_3O_3S_2Si$ requires C 66.53, H 7.59, N 5.97, S 3.99 %.

Acknowledgements

Financial support from MICINN-FEDER (CTQ2011-22727 and MAT2011-27978-C02-02) and Gobierno de Aragón-Fondo Social Europeo (E39 and E04) and also anonymous referees for helpful discussions are gratefully acknowledged.

Notes and references

[1] Dalton LR, Sullivan PA, Bale DH. Electric field poled organic electro-optic materials: state of the art and future prospects. Chem Rev 2010, 110, 25-55. DOI: 10.1021/cr9000429

[2] Cho MJ, Choi DH, Sullivan PA, Akelaitis AJP, Dalton LR. Recent progress in second-order non-linear optical polymers and dendrimers. Prog Polym Sci 2008; 33: 1013-58. DOI:10.1016/j.progpolymsci.2008.07.007

[3] Alicante R, Cases R, Forcén P, Oriol L, Villacampa B. Synthesis and nonlinear optical properties of side chain liquid crystalline polymers containing azobenzene push-pull chromophores. J Polym Sci Pol Chem 2010; 48: 232-42. DOI: 10.1002/pola.23776

[4] Piao X, Zhang X, Mori Y,Koishi M, Nakaya A, Inoue S, Aoki I, OtomoA,Yokoyama S. Nonlinear optical side-chain polymers post-functionalized with high-β chromophores exhibiting large electro-optic property. J Polym Sci Pol Chem 2011; 49: 47-54. DOI: 10.1002/pola.24410

[5] Ma H, Chen B, Sassa T, Dalton LR, Jen K-Y, Alex. Highly efficient and thermally stable nonlinear. Optical dendrimer for electrooptics. J Am Chem Soc 2001, 123, 986-7. DOI: 10.1021/ja003407c

[6] Kim T-D, Luo J, Cheng Y-J, Shi Z, Hau S, Jang S-H, Zhou X-H, Tian Y, Polishak B, Huang S, Ma H, Dalton LR, Jen AK-Y. Binary chromophore system in nonlinear optical dendrimers and polymers for large electrooptic activities. J Phys Chem C 2008, 112, 8091-8. DOI: 10.1021/jp712037j

[7] He M, Leslie MT, Sinicropi JA. α-Hydroxy ketone precursors leading to a novel class of electro-optic acceptors. Chem Mater 2002, 14:5, 2393-2400. DOI: 10.1021/cm011734t

[8] Prabhakar CH, Yesudas K, Bhanuprakash K, Jayathirtha Rao V, Sai Santosh R,Kumar, Narayana R D. Linear and nonlinear optical properties of mesoionic oxyallyl derivatives: enhanced non-resonant third order optical nonlinearity in croconate dyes. J Phys Chem C 2008; 112: 13272-80. DOI: 10.1021/jp803025v

[9] Scarpaci A, Cabanetos C, Blart E, Montembault V, Fontaine L, Rodriguez V, Odobel F. Postfunctionalization of poly(propargyl methacrylate) using copper catalyzed 1,3-dipolar Huisgen cycloaddition: An easy route to electro-optic materials. J Polym Sci Pol Chem 2009; 47: 5652-60. DOI: 10.1002/pola.23606

[10] Ramirez MA, Custodio R, Cuadro AM, Alvarez-Builla J, Clays K, Asselberghs I, Mendicuti F, Castaño O, Andrés JL, Vaquero JJ. Synthesis of charged bis-heteroaryl donor-acceptor (D-A+) NLO-phores coupling (π-deficient-π-excessive) heteroaromatic rings. Org Biomol Chem 2013; 11:41, 7145-54.DOI: 10.1039/C3OB41159A

[11] Wang A, Long L, Meng S, Li X, Zhao W, Song Y, Cifuentes MP, Humphreye MG, Zhang C. Cooperative enhancement of optical nonlinearities in a porphyrin derivative bearing a pyrimidine chromophore at the periphery. Org Biomol Chem 2013; 11: 4250-7. DOI: 10.1039/C3OB40323H

[12] Galán E, Andreu R, Garín J, Orduna J, Villacampa B, Diosdado BE. Cycloaddition reactions of polyenic donor-π-acceptor systems with an electron-rich alkyne: access to new chromophores with second-order optical nonlinearities. Org Biomol Chem 2012; 10: 8684-91. DOI: 10.1039/c3ob40323h

[13] Marco AB, Andreu R, Franco S, Garín J, Orduna J, Villacampa B, Diosdado BE, López Navarrete JT, Casado J. Push-pull systems bearing a quinoid/aromatic thieno[3,2-b]thiophene moiety: synthesis, ground state polarization and second-order nonlinear properties. Org Biomol Chem 2013; 11: 6338-49.DOI: 10.1039/c3ob41278d

[14] Fortuna CG, Bonaccorso C, Qamar F, Anu A, Ledoux I, Musumarraa G. Synthesis and NLO properties of new trans 2-(thiophen-2-yl)vinyl heteroaromatic iodides. Org Biomol Chem 2011; 9: 1608-13. DOI: 10.1039/c0ob00046a

[15] Andreu R, Franco S, Galán E, Garín J, Martínez de Baroja N, Momblona C, Orduna J, Alicante R, Villacampa B. Isophorone- and pyran-containing NLO-chromophores: a comparative study. Tetrahedron Lett 2010; 51: 3662-366.DOI: 10.1016/j.tetlet.2010.05.033

[16] Posner GH, Li Z, White MC, Vinadet V, Takenchi, K, Guggino SE, Dolan P, Kensler TW. 1.alpha.,25-Dihydroxyvitamin D3 analogs featuring aromatic and heteroaromatic rings: Design, synthesis, and preliminary biological testing. Journal of Medicinal Chemistry 1995, 38:22, 4529-37. DOI: 10.1021/jm00022a019

[17] Ito T, Hayashi A, Kondo A, Uchida T, Tanabe K, Yamada H, Nishimoto S. DNA hairpins containing a diaminostilbene derivative as a photoinduced electron donor for probing the effects of single-base mismatches on excess electron transfer in DNA. Org Lett 2009, 11:4, 927-30. DOI: 10.1021/ol802896y

[18] Brooker LGS, Craig AC, Heseltine DW, Jenkins PW, Lincoln LL. Color and constitution 1,3-merocyanines as solvent property indicators. J Am Chem Soc 1965; 87: 2443-50.DOI: 10.1021/ja01089a025

[19] Lemke R. Knoevenagel-kondensationen in dimethylformamid. Synthesis 1974, 359-61. DOI: 10.1055/s-1974-23322

[20] Andreu R, Garín, J, Orduna J, Alcalá R, Villacampa B. Novel NLO-phores with proaromatic donor and acceptor groups. Org Lett 2003; 5: 3143-46. DOI:10.1021/ol0352005

[21] Gubbelmansa E, Verbiest T, Van Beylen M, Persoons A, Samyn C. Chromophore-functionalised polymides with high-poling stabilities of the nonlinear optical effect at elevated temperature. Polymer 2002, 43: 5, 1581–5. DOI:10.1016/S0032-3861(01)00678-4

[22] Leroy-Lhez S, Baffreau J, Perrin L, Levillain E, Allain M, Blesa MJ, Hudhomme P. Tetrathiafulvalene in a perylene-3,4:9,10-bis(dicarboximide)-based dyad: A new reversible fluorescence-redox dependent molecular system. J Org Chem 2005; 70: 6313-20. DOI: 10.1021/jo050766n

[23] Yu L, Chan W, Bao Z, Cao SXF. Photorefractive polymers. 2. Structure design and property characterization. Macromolecules 1993; 26: 2216-21. DOI: 10.1021/ma00061a012

[24] Gao J, Cui Y, Yu J, Lin W, Wang Z, Qian G. Inorganic-organic hybrid nonlinear optical films containing thiophene-vinyl conjugated chromophore. Thin Solid Films 2011; 519: 5056-60. DOI: 10.1016/j.tsf.2011.01.127

[25] Briers D, Koeckelberghs G, Picard I, Verbiest T, Persoons A, Samyn C. Novel chromophore-functionalized poly[2-(trifluoromethyl) adamantyl acrylate-methyl vinyl urethane]s with high poling stabilities of the nonlinear optical effect. Macromol Rapid Commun 2003; 24: 841-46. DOI: 10.1002/marc.200350029

[26] Tan SX, Zhai J, Fang HJ, Jiu TG, Ge J, Li YL, Jiang L, Zhu DB. Tuning spectral properties of phenothiazine based donor-π-acceptor dyes for efficient dye-sensitized solar cells. J Mater Chem 2012; 22: 889-94. DOI: 10.1039/C1JM14024H

[27] Jang HN, No HJ, Lee JY, Rhee BK, Cho KH, Choi HD. The design, synthesis and nonlinear optical properties of a novel, Y-type polyurethane containing

tricyanovinylthiophene of high thermal stability. Dyes Pigments 2009; 82: 209-15. DOI: 10.1016/j.dyepig.2009.01.003

[28] Younes AH, Zhang L, Clark RJ, Davidson MW, Zhu L. Electronic structural dependence of the photophysical properties of fluorescent heteroditopic ligands - implications in designing molecular fluorescent indicators. Org Biomol Chem 2010; 8: 5431-41. DOI: 10.1039/C0OB00482K

[29] Ma X, Ma F, Zhao Z, Song N, Zhang J. Synthesis and properties of NLO with fine-tuned gradient electronic structures. J Mater Chem 2009, 19, 2975-2985. DOI: 10.1039/B817789A

[30] Abbotto A, Bradamante S, Facchetti A, Pagani GA. Facile, regioselective synthesis of highly solvatochromic thiophene-spaced N-alkylpyridinium dicyanomethanides for second-harmonic generation. J Org Chem 1997, 62:17, 5757. DOI: 10.1021/jo970059x

[31] Saadeh H, Wang L, Yu L. A new synthetic approach to novel polymers exhibiting large electrooptic coefficients and high thermal stability. Macromolecules 2000, 33:5, 1570-76. DOI: 10.1021/ma991097g

[32] Koeckelberghs G, Vangheluwe M, Picard I, De Groof L, Verbiest T, Persoons A, Samyn C. Synthesis and properties of new chiral donor-embedded polybinaphthalenes for nonlinear optical applications. Macromolecules 2004; 37: 8530-37. DOI: 10.1021/ma0491816

[33] Kim S-H, Lee S-Y, Gwon S-Y, Son Y-A, Bae J-S. D-π-A solvatochromic charge transfer dyes containing a 2-cyanomethylene-3-cyano-4,5,5-trimethyl-2,5-dihydrofuran acceptor. Dyes Pigments 2010; 84: 169-75.DOI: 10.1016/j.dyepig.2009.07.012

[34] Botrel A, Le Beuze P, Jacques H, Strub H. Solvatochromism of a typical merocyanine dye. J Chem Soc Faraday Trans 2 1984; 80: 1235-52. DOI: 10.1039/F29848001235

[35] Reichardt, C, Welton T. Solvents and Solvents Effects in Organic Chemistry, 4th ed. Weinheim: Wiley-VCH; 2010.

[36] Meier H, Gerold J, Kolshorn H, Muuhling J. Extension of conjugation leading to bathochromic or hypsochromic effects in OPV series. Chem Eur J 2004; 10: 360-70. DOI: 10.1002/chem.200305447

[37] Oudar JL, Chemla DS. Hyperpolarizabilities of the nitroanilines and their relations to the excited state dipole moment. J Chem Phys 1977; 66: 2664-68. DOI: 10.1063/1.434213

[38] Kanis DR, Ratner MA, Marks TJ. Design and construction of molecular assemblies with large second-order optical nonlinearities. Quantum chemical aspects. Chem Rev 1994; 94: 195-242.DOI: 10.1021/cr00025a007

[39] Ruiz Delgado MC, Casado J, Hernández V, López Navarrete JT, Orduna J, Villacampa B, Alicante R, Raimundo JM, Blanchard P, Roncali J. Electronic, optical, and vibrational properties of bridged dithienylethylene-based NLO chromophores. J Phys Chem C 2008; 112: 3109-20.DOI: 10.1021/jp710459c

[40] Alías S, Andreu R, Blesa MJ, Cerdán MA, Franco S, Garín J, LópezC, Orduna J, Sanz J, Alicante R, Villacampa B, Allain M. Iminium salts of ω-dithiafulvenylpolyenals: An easy entry to the corresponding aldehydes and doubly proaromatic nonlinear optic-phores. J Org Chem 2008; 73: 5890-8. DOI: 10.1021/jo800801q

[41] Burland DM, Miller RD, Walsh CA. Second-order nonlinearity in poled-polymer systems. Chem Rev 1994; 94: 31-75. DOI: 10.1021/cr00025a002

[42] Sahraoui B, Kityk IV, Phu XN, Hudhomme P, Gorgues A. Influence of hydrostatic pressure and temperature on two-photon absorption of a C_{60}-2-thioxo-1,3-dithiole cycloadduct. Phys Rev B, 1999; 59: 9229. DOI: 10.1103/PhysRevB.59.9229

[43] Shu CF, Shu YC, Gong ZH, Peng SM, Lee GH, Jen AKY. Nonlinear optical chromophores with configuration-locked polyenes possessing enhanced thermal stability and chemical stability. Chem Mater 1998; 10: 3284-86. DOI: 10.1021/cm980413n

[44] Zhang C, Ren AS, Wang F, Zhu J, Dalton LR, Woodford JN, Wang CH. Synthesis and characterization of sterically stabilized second-order nonlinear optical chromophores. Chem Mater 1999; 11: 1966-68. DOI: 10.1021/cm9902321

[45] Shu CF, Tsai WJ, Jen AKY. A new synthetic approach for nonlinear optical chromophores possessing enhanced thermal stability. Tetrahedron Lett 1996; 37: 7055-58. DOI: 10.1016/0040-4039(96)01550-X

[46] Shu YC, Gong ZH, Shu CF, Breitung EM, McMahon RJ, Lee GH, Jen AKY, Synthesis and characterization of nonlinear optical chromophores with conformationally locked polyenes possessing enhanced thermal stability. Chem Mater 1999; 11: 1628-32. DOI: 10.1021/cm990118i

[47] Dalton LR. Non linear optical polymeric materials: from chromophore design to commercial applications. Adv Polym Sci 2002; 158: 1-86. DOI: 10.1007/3-540-44608-7-1

[48] Jiang P, McFarland MJ. Large-scale fabrication of wafer-size colloidal crystals, macroporous polymers and nanocomposites by spin-coating. J Am Chem Soc 2004; 126: 13778-86.DOI: 10.1021/ja0470923

[49] Wang T, Keddie JL. Design and fabrication of colloidal polymer nanocomposites. Adv Colloid Interface Sci 2009; 147-148: 319-32. DOI: 10.1016/j.cis.2008.06.002

[50] Page RH, Jurich MC, Reck B, Sen A, Twieg RJ, Swalen JD, Bjorklund GC, and Willson CG. Electrochromic and optical waveguide studies of corona-poled electro-optic polymer films. J Opt Soc Am B 1990; 7: 1239-1250. DOI: 10.1364/JOSAB.7.001239

[51] Mortazavi MA, Knoesen A, Kowel S T, Higgins BG, Dienes A. Second-harmonic generation and absorption studies of polymer dye films oriented by corona-onset poling at elevated temperatures. J Opt Soc Am B 1989; 6: 733-741. DOI: 10.1364/JOSAB.6.000733

[52] Huang H, Deng G, Liu J, Wu J, Si P, Xu H,Bo S, Qiu L, Zhen Z, Liu X. A Nunchaku-like nonlinear optical chromophore for improved temporal stability of guest - host electro-optic materials. Dyes Pigments 2013; 99: 753-758. DOI: 10.1016/j.dyepig.2013.06.034

[53] Meredith GR, Vandusen JG, Williams DJ. In nonlinear optical properties of organic and polymeric materials, ed. D. J. Williams, ACS Symposium Series, Washington DC, 1983; 233: 109-1330.

CAPTIONS OF TABLES

Table 1. UV/Vis data of the chromophores **1-11**

Table 2. UV/Vis data of the chromophores **10** and **11** on hydrogen bond acceptor (HBA) solvents and on hydrogen bond acceptor (HBA)-hydrogen bond donor (HBD) solvents

Table 3. Electrochemical data [1], E_{HOMO} and E_{LUMO} values [2]

Table 4. Experimental and CPHF-calculated NLO properties and TDDFT-calculated [1] parameters of chromophores **1-11**

Table 5. Refractive indices n_o and n_e measured at *1306 nm* before film poling

Table 6. Nonlinear coefficients of poled films with compounds **4** and **10**

CAPTIONS OF ILLUSTRATIONS

Fig. 1. a) Isosbestic plot: Titration of 0.01 M HCl to a blue solution of chromophore **9** in EtOH ($2\ 10^{-5}$ M). b) Solution color: blue (pH=3.04), green (pH= 2.85), yellow (pH=2.72).

Fig. 2. Absorption spectra of thin films with different content of compound **10** embedded in polycarbonate **PC_10_X %** (**X**=**4** (green), **8** (blue), **12** (red) and **20** (pink))

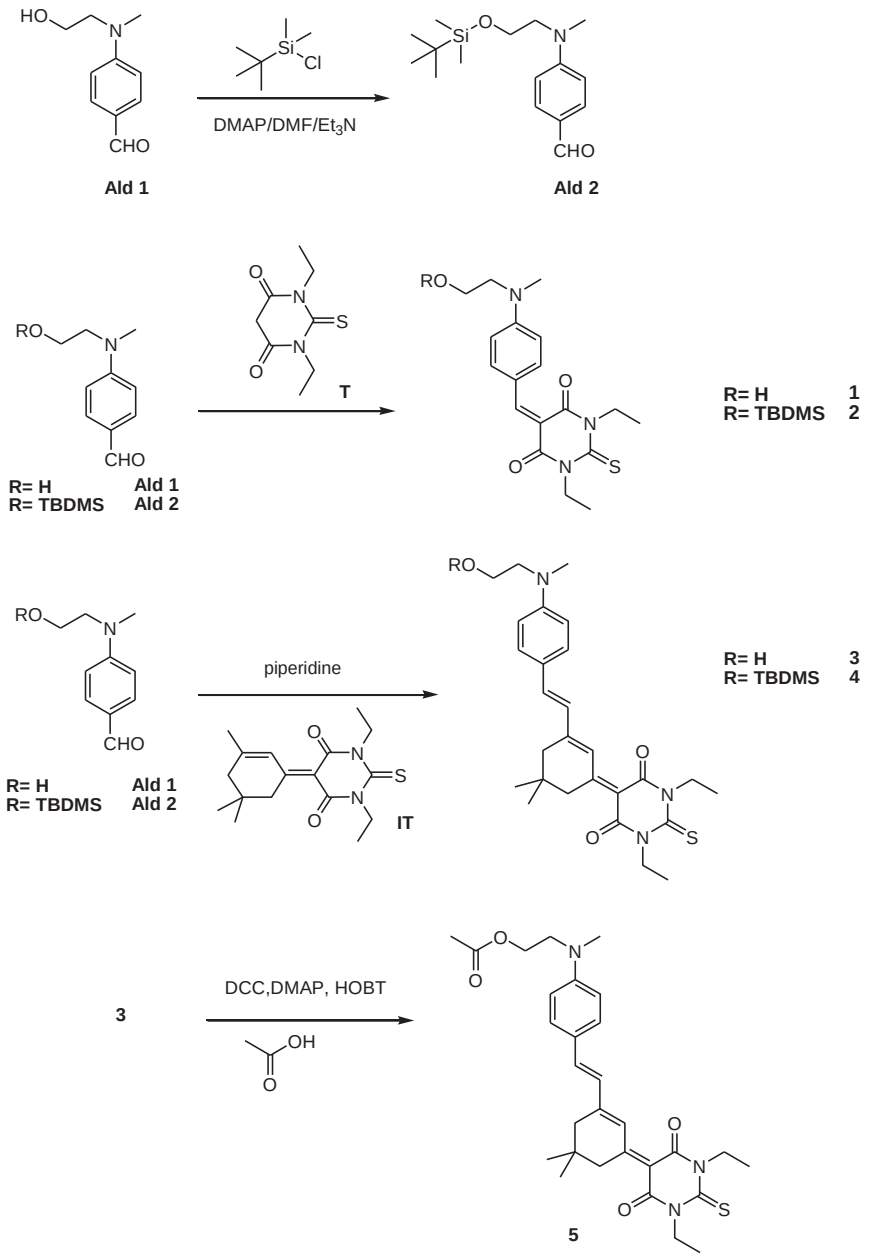
HO
N
CHO
Ald 1
Si
Cl
DMAP/DMF/Et3N
Si
O
N
CHO
Ald 2
RO
N
CHO
R= H
R= TBDMS
Ald 1
Ald 2
O
N
S
N
O
T
RO
N
O
N
O
N
S
R= H 1
R= TBDMS 2
RO
N
CHO
R= H
R= TBDMS
Ald 1
Ald 2
piperidine
O
N
S
N
O
IT
RO
N
R= H 3
R= TBDMS 4
3
DCC,DMAP, HOBT
OH
O
O
O
N
O
N
S
5

Scheme 1

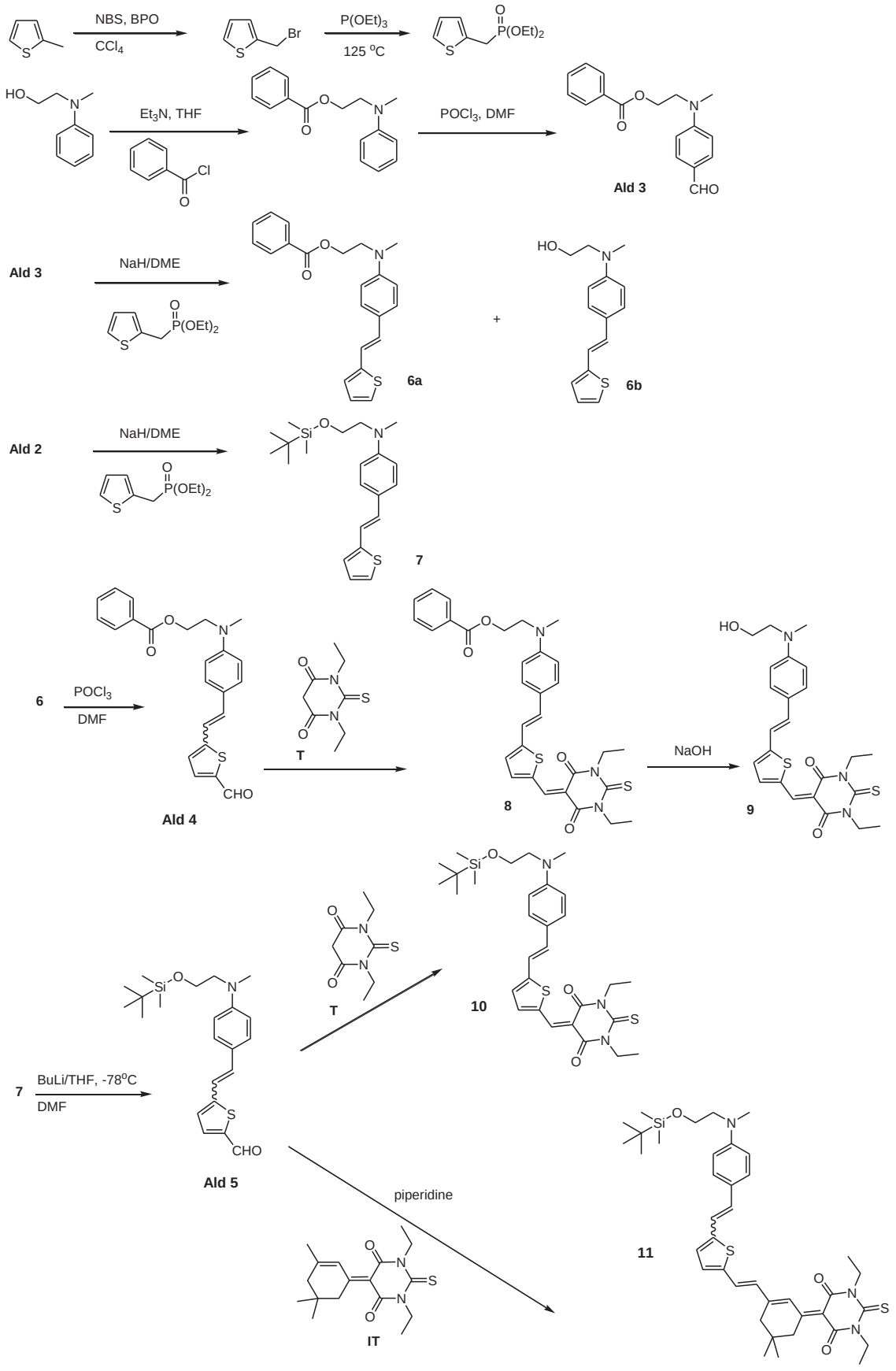
NBS, BPO
CCl4
P(OEt)3
125 °C
Et3N, THF
POCl3, DMF
Ald 3
NaH/DME
6a
6b
Ald 2
7
6
POCl3
DMF
T
8
NaOH
9
Ald 4
7
BuLi/THF, -78°C
DMF
Ald 5
10
piperidine
IT
11

Scheme 2

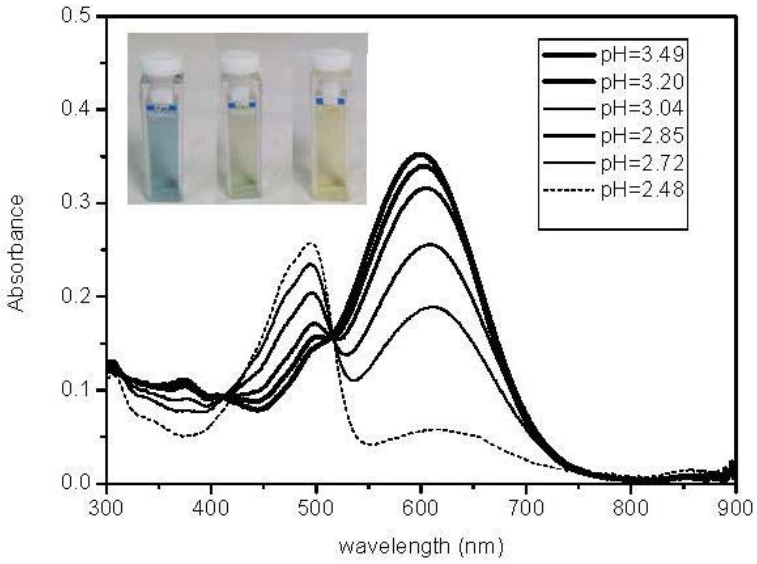

Fig. 1. a) Isosbestic plot: Titration of HCl to a blue solution of chromophore **9** in EtOH ($2\ 10^{-5}$ M). b) Solution color: blue (pH=3.04), green (pH= 2.85), yellow (pH=2.72).

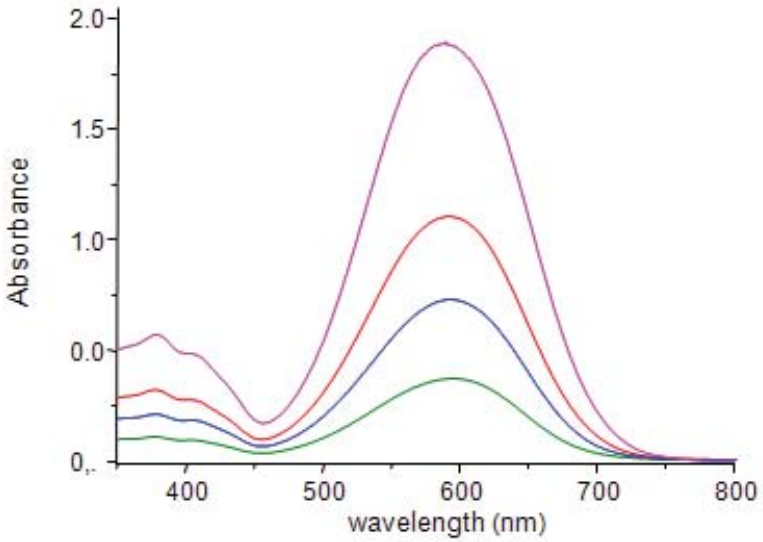

Fig. 2. Absorption spectra of thin films with different content of compound **10** embedded in polycarbonate **PC_10_X %** (**X=4** (green), **8** (blue), **12** (red) and **20** (pink))

Table 1. UV/Vis data of the chromophores **1-11**

	Experimental						Theoretical calc. [3]		
	CH_2Cl_2			DMF			CH_2Cl_2		
	λ_{max} [1]	ΔE_{01} [2]	log ε	λ_{max} [1]	ΔE_{01} [2]	log ε	λ_{max} [1]	ΔE_{01} [2]	*f*
1	493	2.51	4.88	504	2.46	4.72	425	2.92	1.37
2	496	2.50	4.89	503	2.46	4.84	432	2.87	1.63
3	564	2.20	4.42	597	2.08	4.64	536	2.31	1.96
4	579	2.14	4.66	593	2.09	4.62	536	2.31	1.95
5	563	2.20	4.56	579	2.14	4.54	523	2.38	1.94
8	584	2.12	4.71	589	2.10	4.63	518	2.39	1.69
9	587	2.11	4.61	602	2.06	4.56	548	2.26	1.69
10	599	2.07	4.70	599	2.07	4.68	548	2.26	1.72
11	599	2.07	4.55	599	2.07	4.48	566	2.19	1.81

[1] nm. [2] eV. [3] td-PCM-M06-2X/6-311+G(2d,p) on M06-2X/6-31G* PCM CH_2Cl_2 geometries

Table 2. UV/Vis data of the chromophores **10** and **11** on hydrogen bond aceptor (HBA) solvents and on hydrogen bond acceptor (HBA)-hydrogen bond donor (HBD) solvents

	1,4-dioxane			ethyl acetate			DMSO			acetonitrile			ethanol		
	λ_{max} [1]	ΔE_{01} [2]	log ε	λ_{max} [1]	ΔE_{01} [2]	log ε	λ_{max} [1]	ΔE_{01} [2]	log ε	λ_{max} [1]	ΔE_{01} [2]	log ε	λ_{max} [1]	ΔE_{01} [2]	log ε
10	576	2.15	4.73	579	2.14	4.74	609	2.04	4.15	585	2.12	4.56	596	2.08	4.30
11	567	2.19	4.14	570	2.17	4.23	*	*	*	573	2.16	4.49	598	2.07	4.45

[1] nm. [2] eV; * decomposed.

Table 3. Electrochemical data [1], E_{HOMO} and E_{LUMO} values [2]

	$E_{1/2}$ [3] (V)	ΔE_p (mV)	$E_{p,c}$ (V)	E_{HOMO}/E_{LUMO} (eV)
1	1.13	80	-1.08	-6.95/-1.94
2	1.16	130	-0.93	-6.77/-1.84
3	0.74	80	-0.85	-6.26/-2.14
4	0.77	130	-0.89	-6.26/-2.14
5	0.84	80	-0.88	-6.35/-1.98
8	0.80	65	-0.88	-6.30/-2.24
9	0.74	90	-0.81	-6.19/-2.22
10	0.77	135	-0.83	-6.20/-2.22
11	0.65	115	-0.77	-6.01/-2.26

[1] 10^{-3} M in CH_2Cl_2 versus Ag/AgCl (KCl 3M), glassy carbon working electrode, Pt counter electrode, 20 ºC, 0.1 M NBu_4PF_6, 100 mVs^{-1} scan rate. Ferrocene internal reference E_{ox}=+0.51 V. ΔE_p=0.160 V. [2] Calculated at the PCM M06-2X/6-31G level in CH_2Cl_2. [3] E_{ox}= $E_{1/2,}$ net oxidation

Table 4. Experimental and CPHF-calculated NLO properties and TDDFT-calculated[1] parameters.

	Experimental			Theoretical calc.		
	$\mu\beta$[2] [10^{-48}esu]	$\mu\beta_0$[3] [10^{-48}esu]	$\mu\beta_0$[4] [10^{-48}esu]	μ_g [D]	E [eV]	$\Delta\mu_{ge}(z)$ [D]
1	340	230	184	8.90	2.92	8.60
2	330	220	358	12.99	2.87	7.39
3	1320	780	1254	15.96	2.31	13.35
4	1900	1090	1321	16.23	2.31	13.11
5	1100	650	1085	11.29	2.37	13.60
8	1880	1060	1221	13.80	2.39	11.41
9	1400	790	1549	14.04	2.26	14.38
10	2500	1375	1647	13.68	2.26	14.70
11	2540	1390	1744	13.23	2.19	16.24

[1] Calculated at the M06-2X/6-311+G(2d,p) level in CH_2Cl_2//PCM-M06-2X/6-31G*. [2] $\mu\beta$ values determined in dichloromethane at 1907 nm (experimental accuracy ±10%). [3] Experimental $\mu\beta_0$ values calculated using the two level model and the λmax values gathered in **Table 1**. [4] Calculated at the CPHF/6-31G* level in gas phase //M06-2X/6-31G*

Table 5. Refractive indices n_o and n_e measured at *1306 nm* before film poling

PC film	Chromophore amount (% wt)	n_o	n_e	$\Delta n=(n_e-n_o)$
PC_10	4	1.564	1.550	-0.014
PC_10	12	1.579	1.567	-0.012
PC_10	4	1.571	1.558	-0.013
PC_10	12	1.585	1.572	-0.013
PC_10	20	1.604	1.594	-0.020

Table 6. Nonlinear coefficients of poled films with compounds **4** and **10**

compound	**numberdensity** **N**[1]	$\mu\beta$[2]	d_{31}[3]	d_{33}[3]
4_4%	0.48 x 10^{20}	1900	0.9	2.8
4_12%	1.45 x 10^{20}		2.4	7.2
10_4%	0.49 x 10^{20}	2500	1.1	3.3
10_12%	1.48 x 10^{20}		3.0	9.0
10_20%	2.22 x 10^{20}		5.7	17

[1] Chromophore molecules cm^{-3}.[2] From EFISH at 1.9 μm, in CH_2Cl_2, in x10^{-48}esu. [3] In pm V^{-1}, d_{ij}coefficients have been calculated from the Maker fringes measured at about 24 hours after the poling (experimental accuracy±15%)

ELECTRONIC SUPPLEMENTARY INFORMATION FOR: **Using functionalized nonlinear optical chromophores to prepare NLO-active polycarbonate films**

M. González-Lainez [a], M.T. Jiménez-Ruiz [a], N. Martínez de Baroja [a], J. Garín [a], J. Orduna[a*], B. Villacampa[b*], M.J. Blesa[a*]

Address:

[a] Departamento de Química Orgánica, ICMA
Universidad de Zaragoza-CSIC
50009, Zaragoza (Spain)
Phone: (+34) 876 553507
FAX: (+34) 976 761194

E-mail: mjblesa@unizar.es

[b] Departamento de Física de la Materia Condensada, ICMA
Universidad de Zaragoza-CSIC
50009, Zaragoza (Spain)

Corresponding author: mjblesa@unizar.es

TABLE OF CONTENTS

3. UV/Vis

1. General Experimental Methods

Infrared measurements were carried out in nujol mulls using a Perkin –Elmer Fourier Transform Infrared 1600 spectrometer. Melting points were obtained on a Gallenkamp apparatus in open capillaries and are uncorrected. Elemental analysis was performed with a Perkin-Elemer 240C microanalyzer. ^{1}H and ^{13}C NMR spectra were recorded on a Bruker AV400 at 400 MHz and 100 MHz, respectively; δ values are given in ppm (relative to TMS) and *J* values in Hz. The apparent resonance multiplicity is described as a s (singlet), br s (broad singlet), d (doublet), t (triplet), q (quartet) and m (multiplet). ^{1}H-^{1}H COSY experiments were recorded at 400 MHz in order to establish peaks assignment and spacial relationships. Electrospray mass spectra (HRMS-ESI^{+}) were recorded on a Bruker MicroTOF-Q spectrometer; accurate mass measurements were achieved using sodium formate as external reference. MALDI+ spectra were recorded on Bruker Microflex and Bruker Autoflex III spectrometers. Electronic spectra were recorded with an UV-Vis UNICAM UV spectrometer. The absorption wavelengths are reported in nm. Cyclic Voltammetry measurements were performed with a μ-Autolab ECO-Chemie potenciostat, using a glassy carbon working electrode, Pt counter electrode, and Ag/AgCl reference electrode. The experiments were carried out under argon, in CH_2Cl_2 with Bu_4NPF_6 as supporting electrolyte (0.1mol L^{-1}). Scan rate was 100 mV s^{-1}.

2. NMR studies

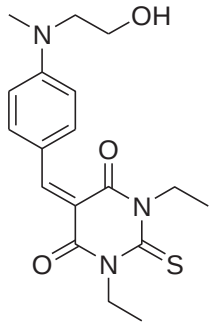

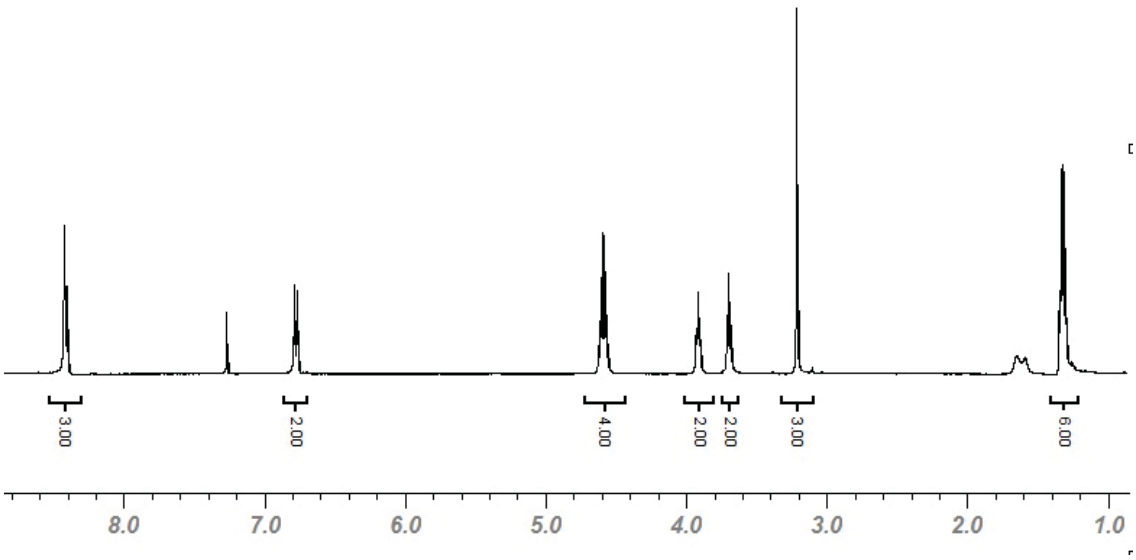

Figure S-1. ^{1}H-NMR spectrum of compound **1** (400 MHz, $CDCl_3$).

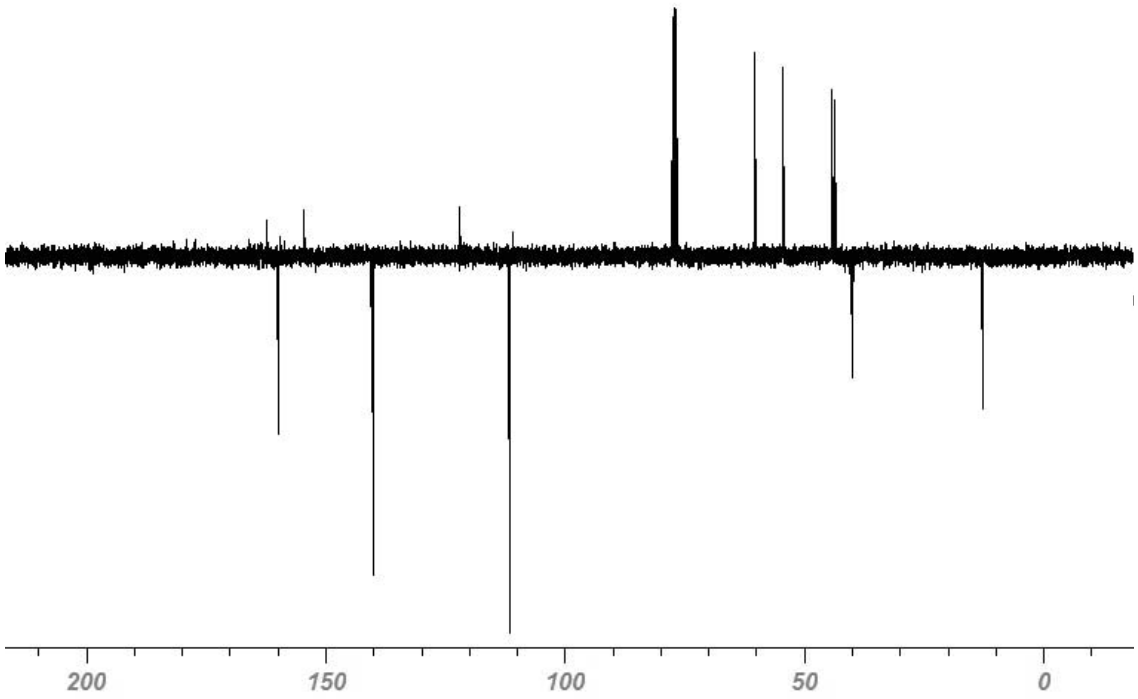

Figure S-2. ^{13}C-NMR (APT) spectrum of compound **1** (100 MHz, $CDCl_3$).

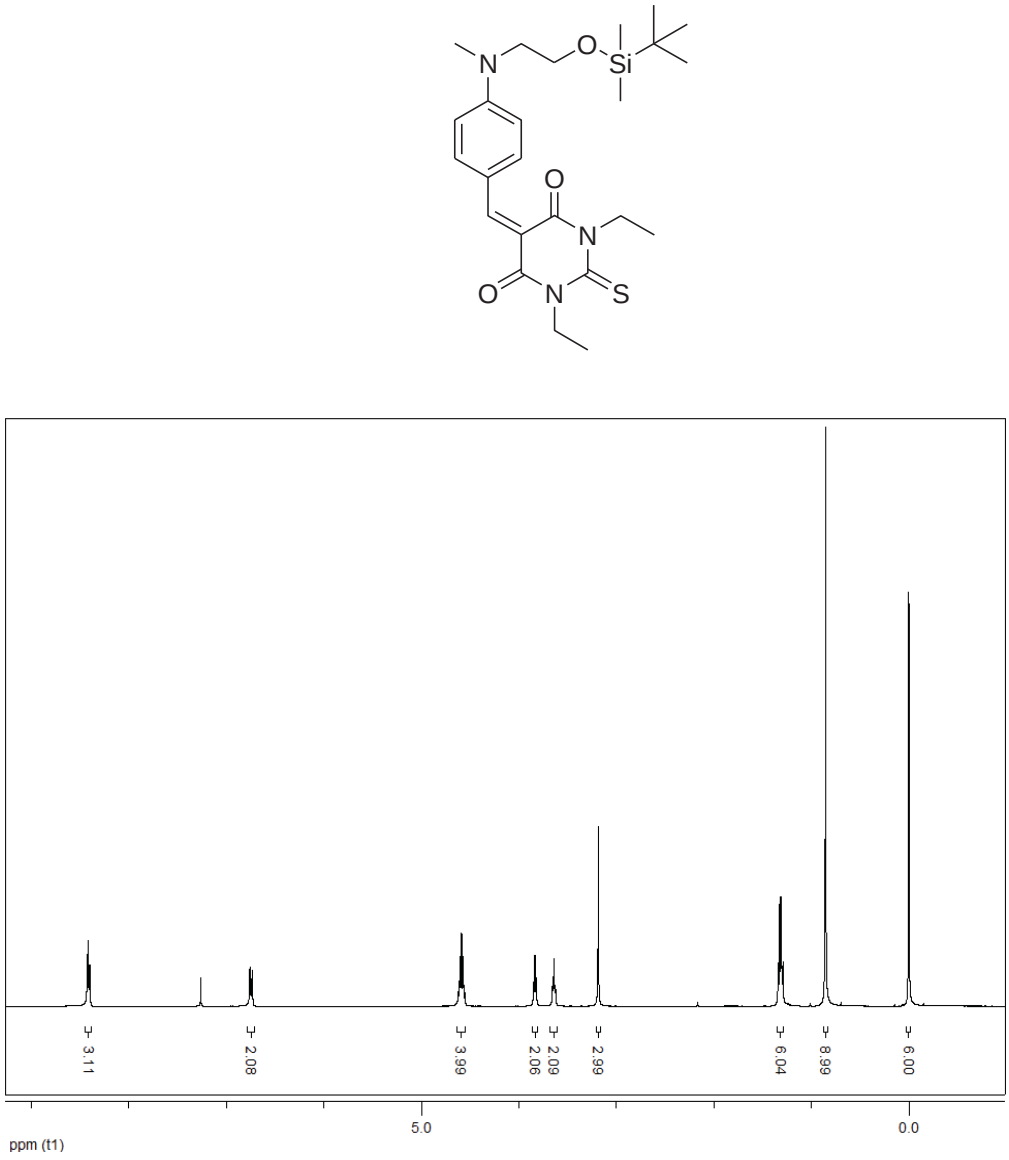

Figure S-3. ^{1}H-NMR spectrum of compound **2** (400 MHz, $CDCl_3$).

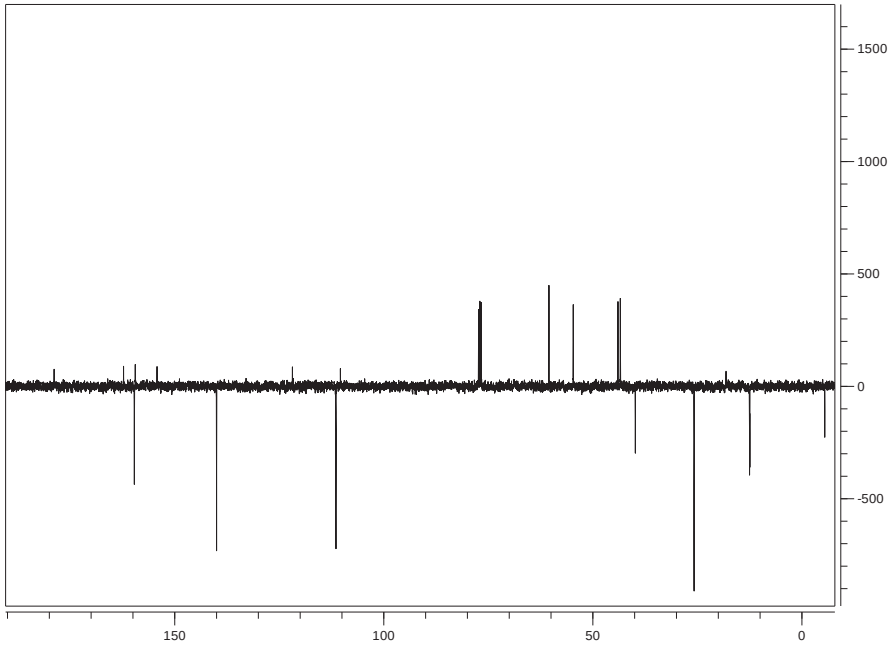

Figure S-4. ^{13}C-NMR (APT) spectrum of compound **2** (100 MHz, $CDCl_3$).

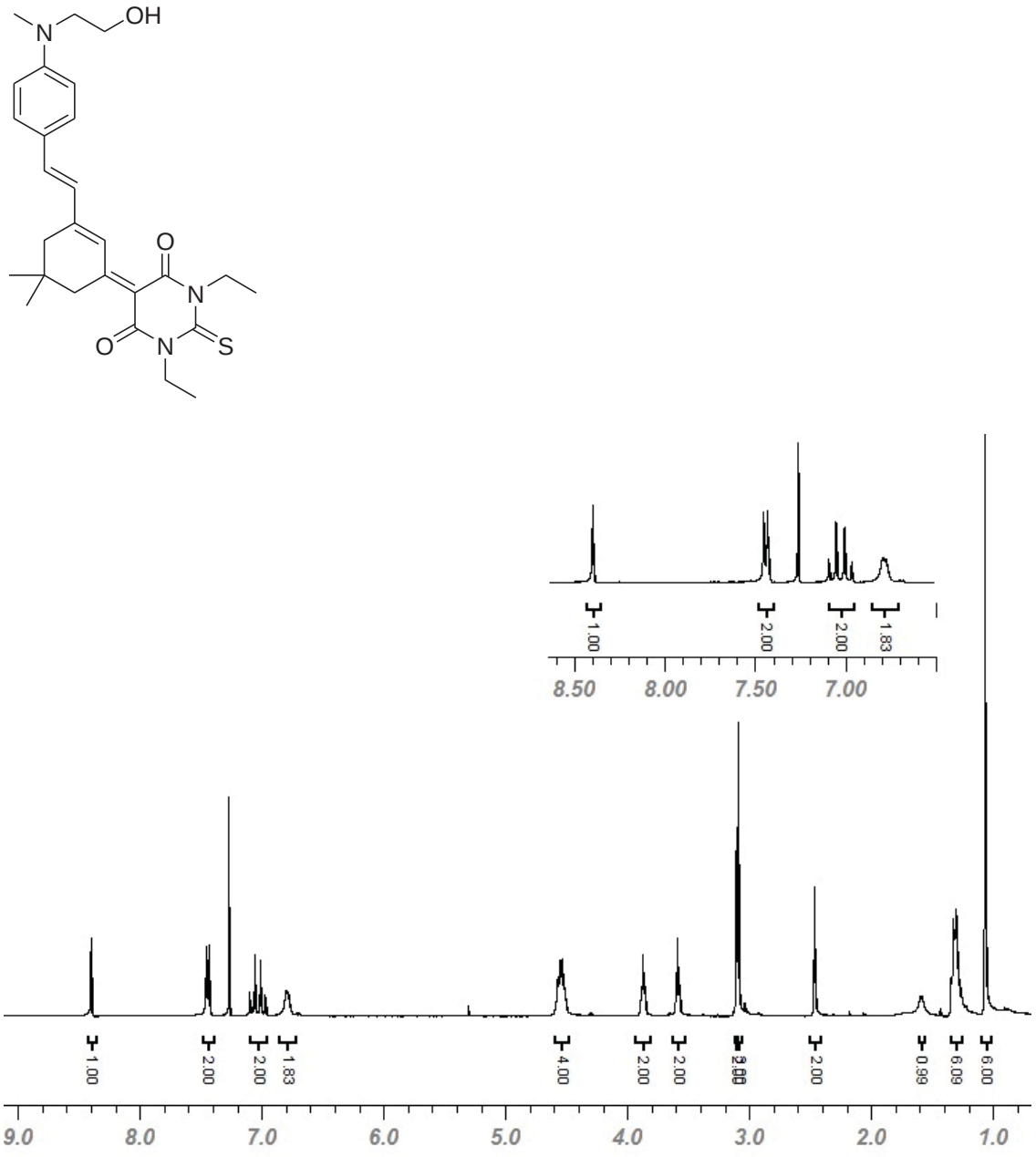

Figure S-5. ^{1}H-NMR spectrum of compound **3** (400 MHz, $CDCl_3$).

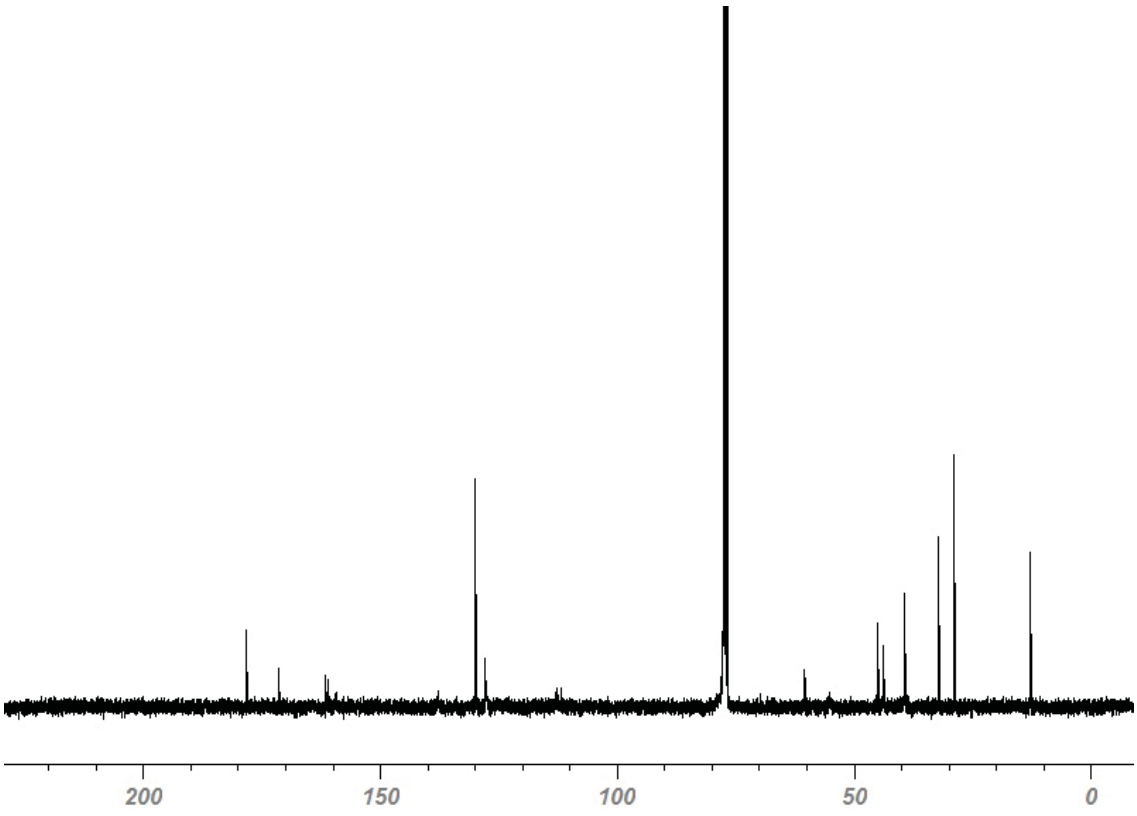

Figure S-6. ^{13}C-NMR spectrum of compound **3** (100 MHz, $CDCl_3$).

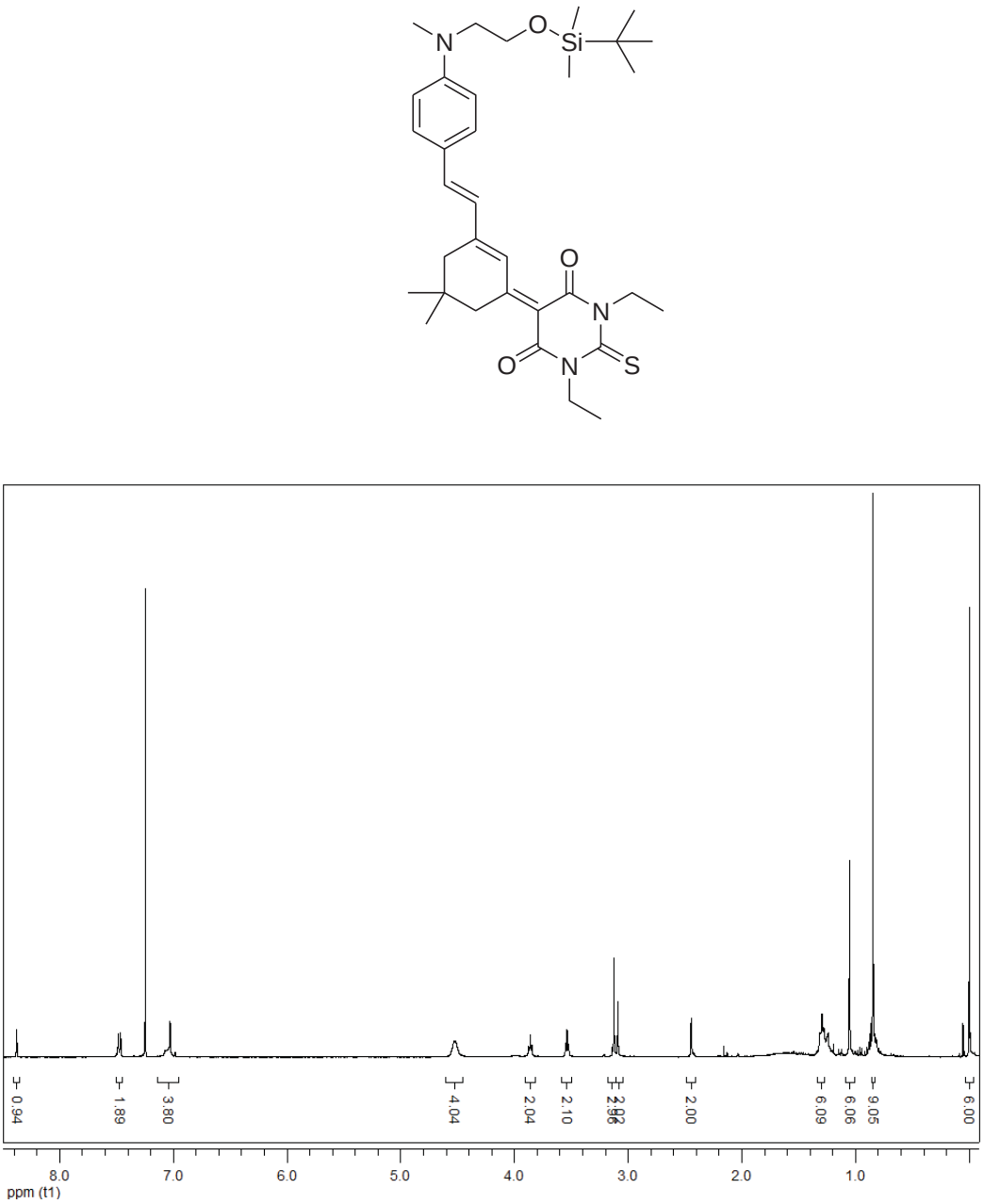

Figure S-7. ^{1}H-NMR spectrum of compound **4** (400 MHz, $CDCl_3$).

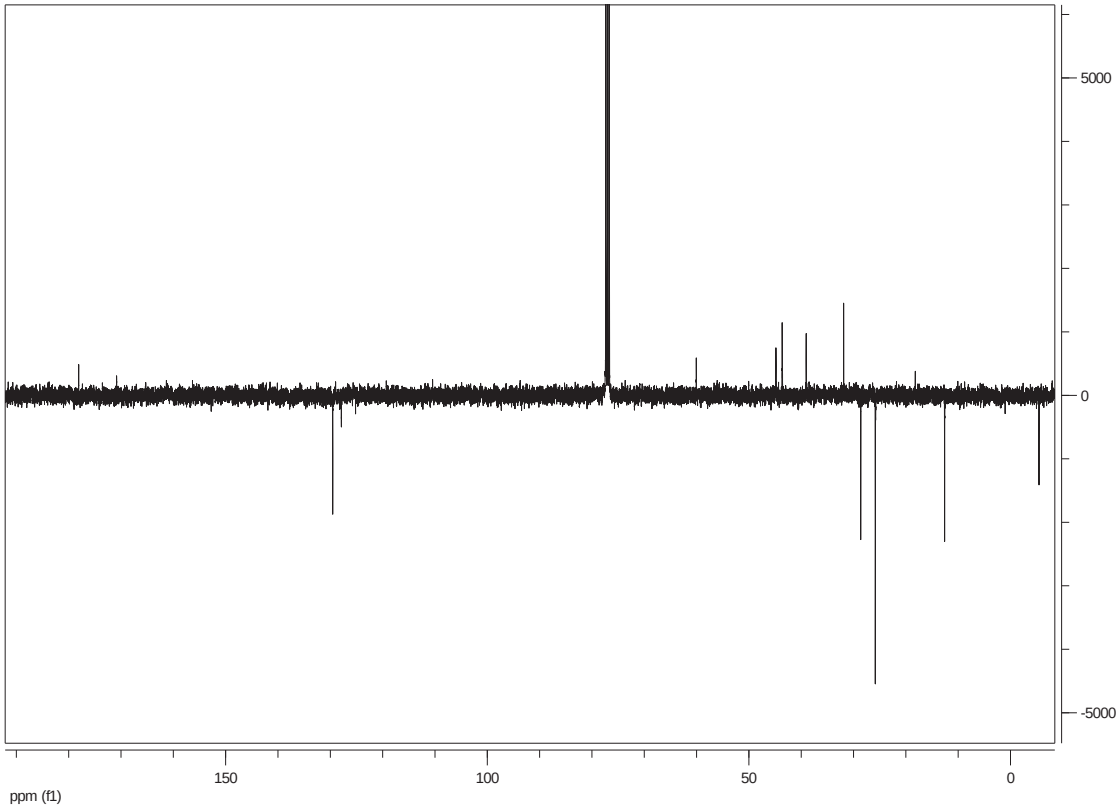

Figure S-8 ^{13}C-NMR (APT) spectrum of compound **4** (100 MHz, $CDCl_3$).

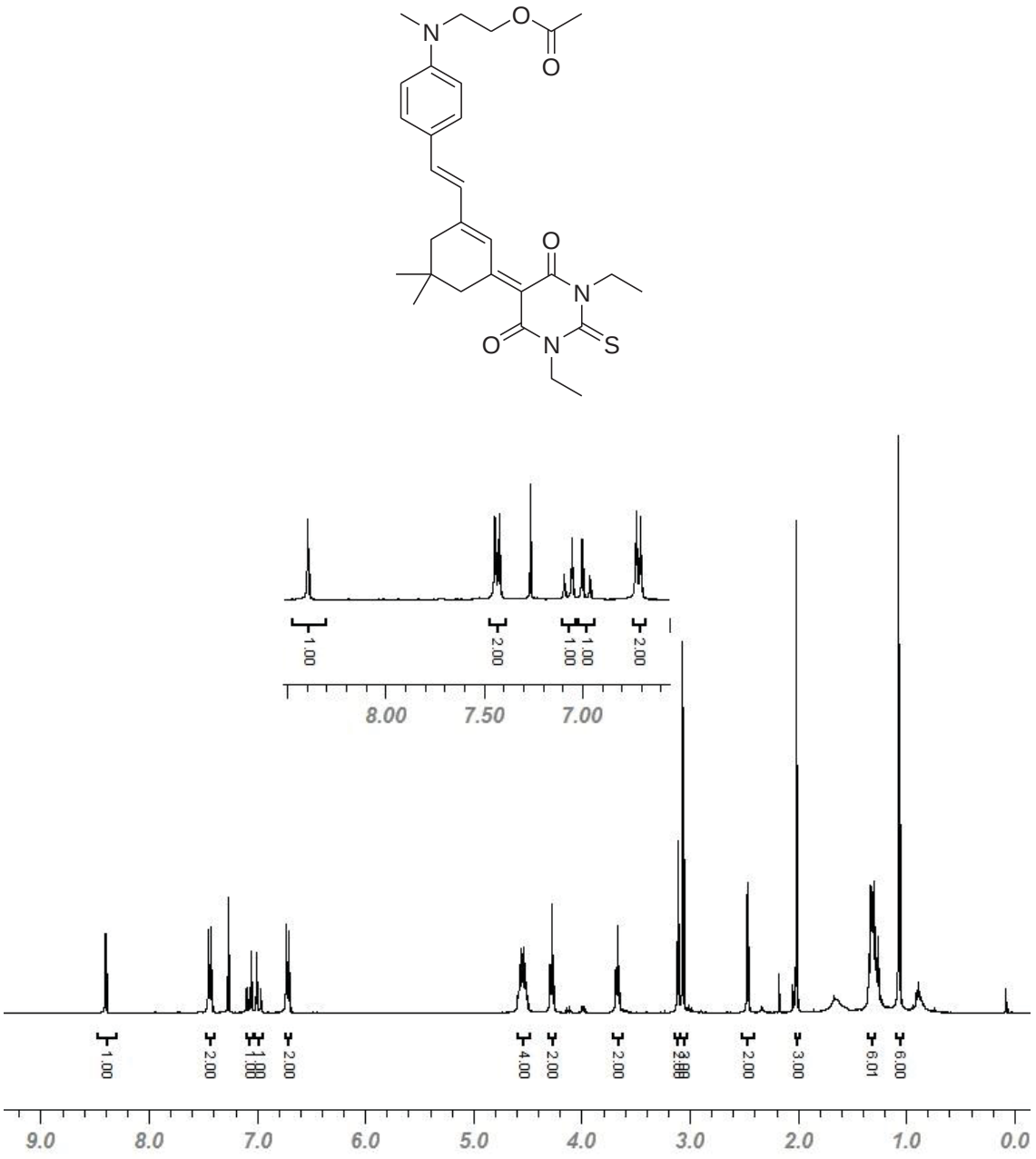

Figure S-9. ^{1}H-NMR spectrum of compound **5** (400 MHz, $CDCl_3$).

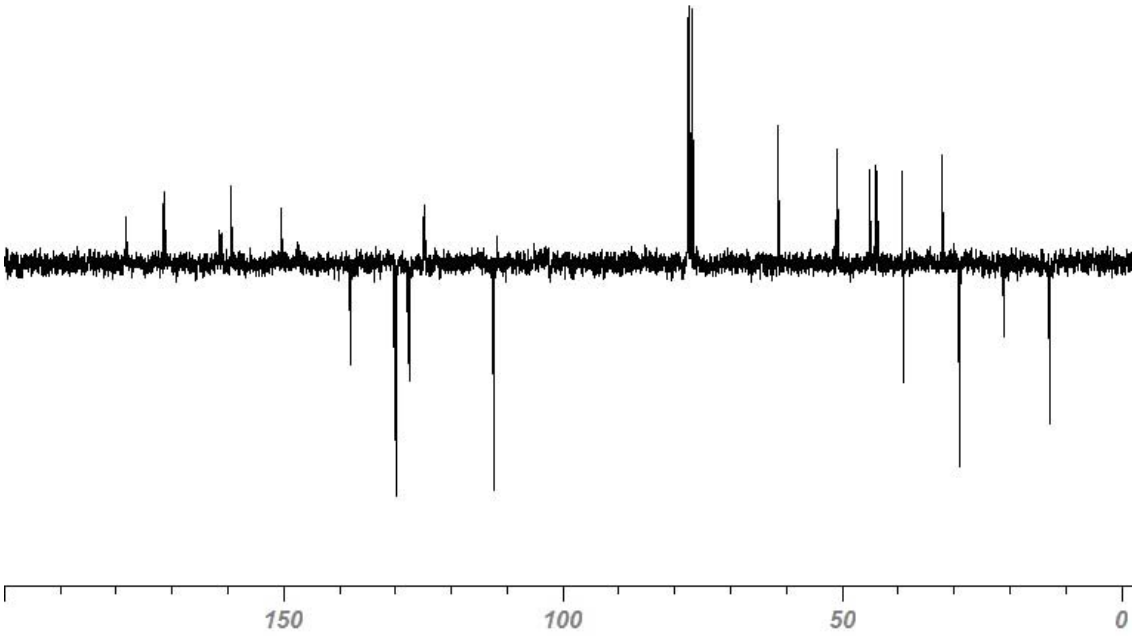

Figure S-10. ^{13}C-NMR (APT) spectrum of compound **5** (100 MHz, $CDCl_3$).

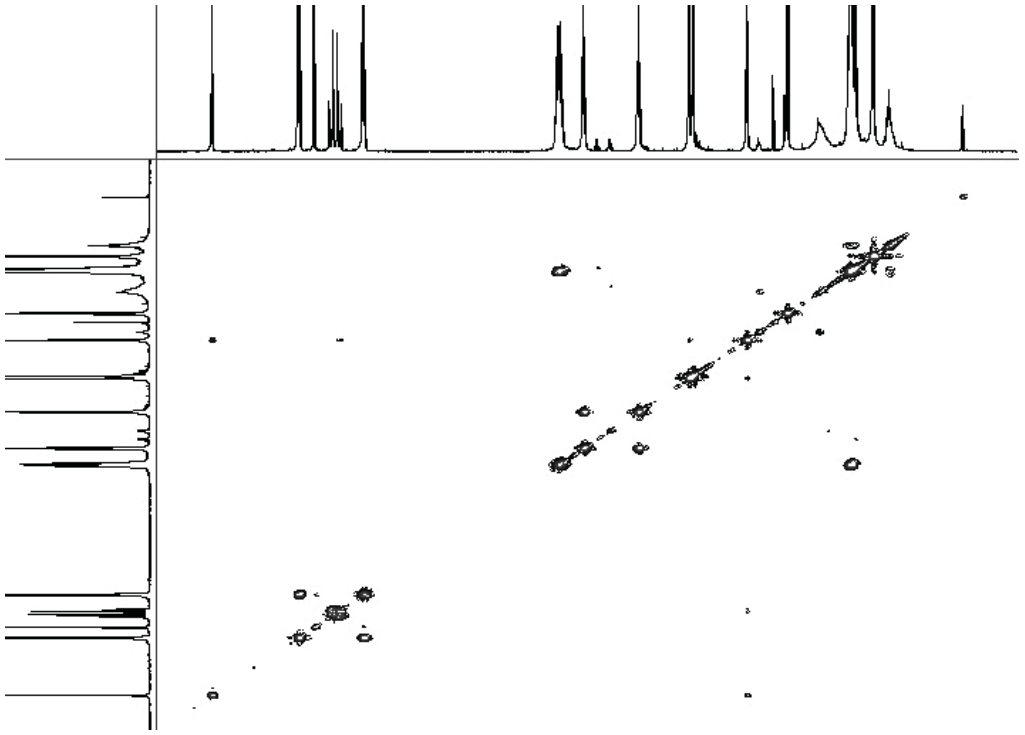

Figure S-11. ^{1}H-^{1}H COSY spectrum of compound **5** (400 MHz, $CDCl_3$).

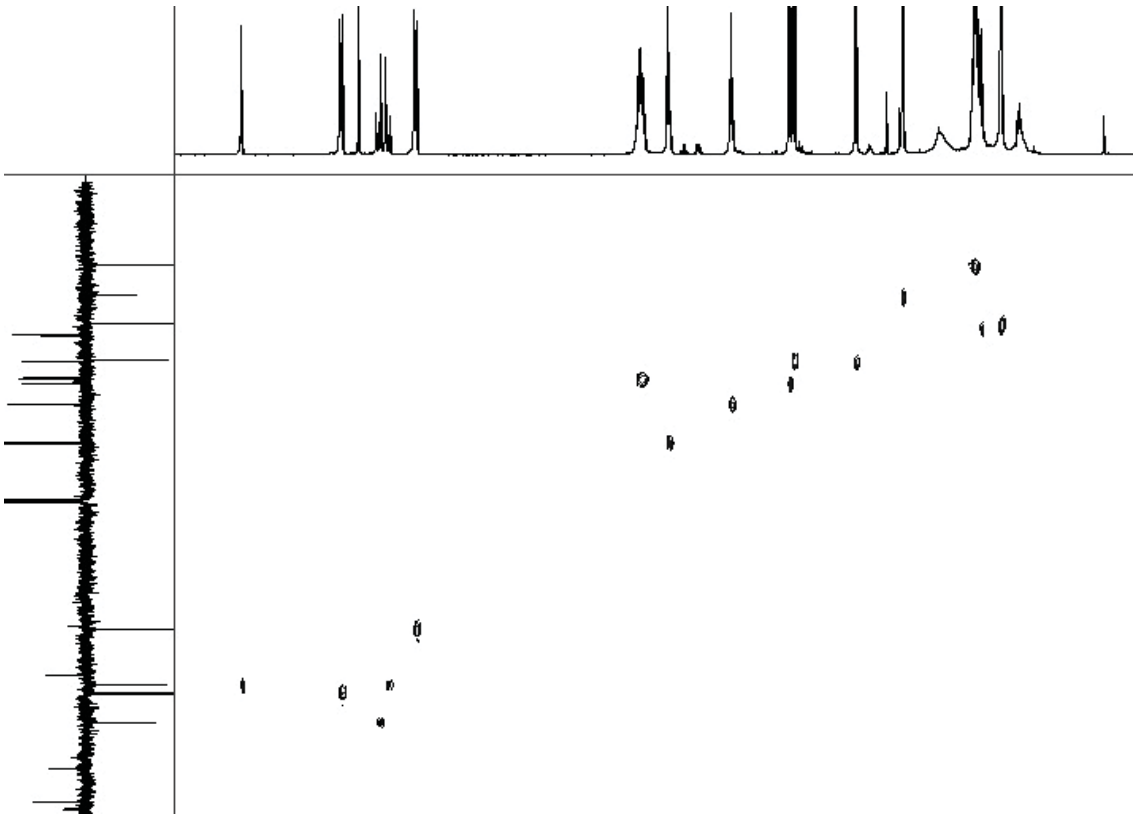

Figure S-12. ^{1}H-^{13}C HSQC spectrum of compound **5**.

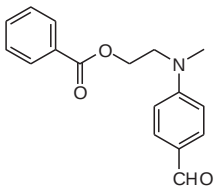

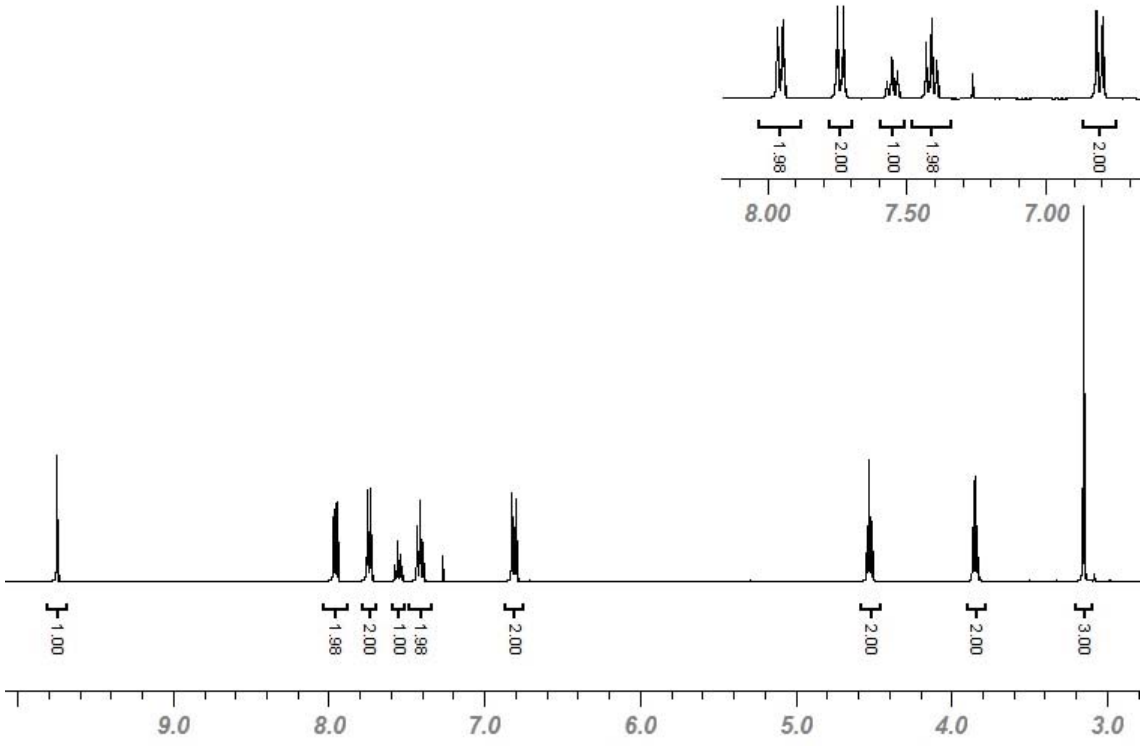

Figure S-13. ^{1}H-NMR spectrum of compound **Ald 3** (400 MHz, $CDCl_3$).

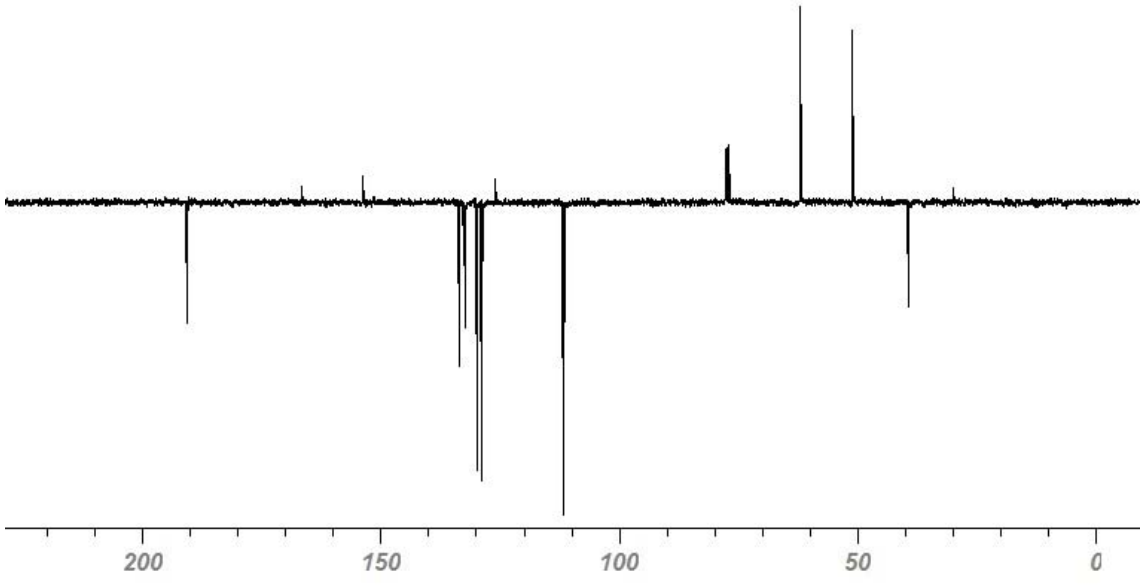

Figure S-14. ^{13}C-NMR (APT) spectrum of compound **Ald 3** (400 MHz, $CDCl_3$).

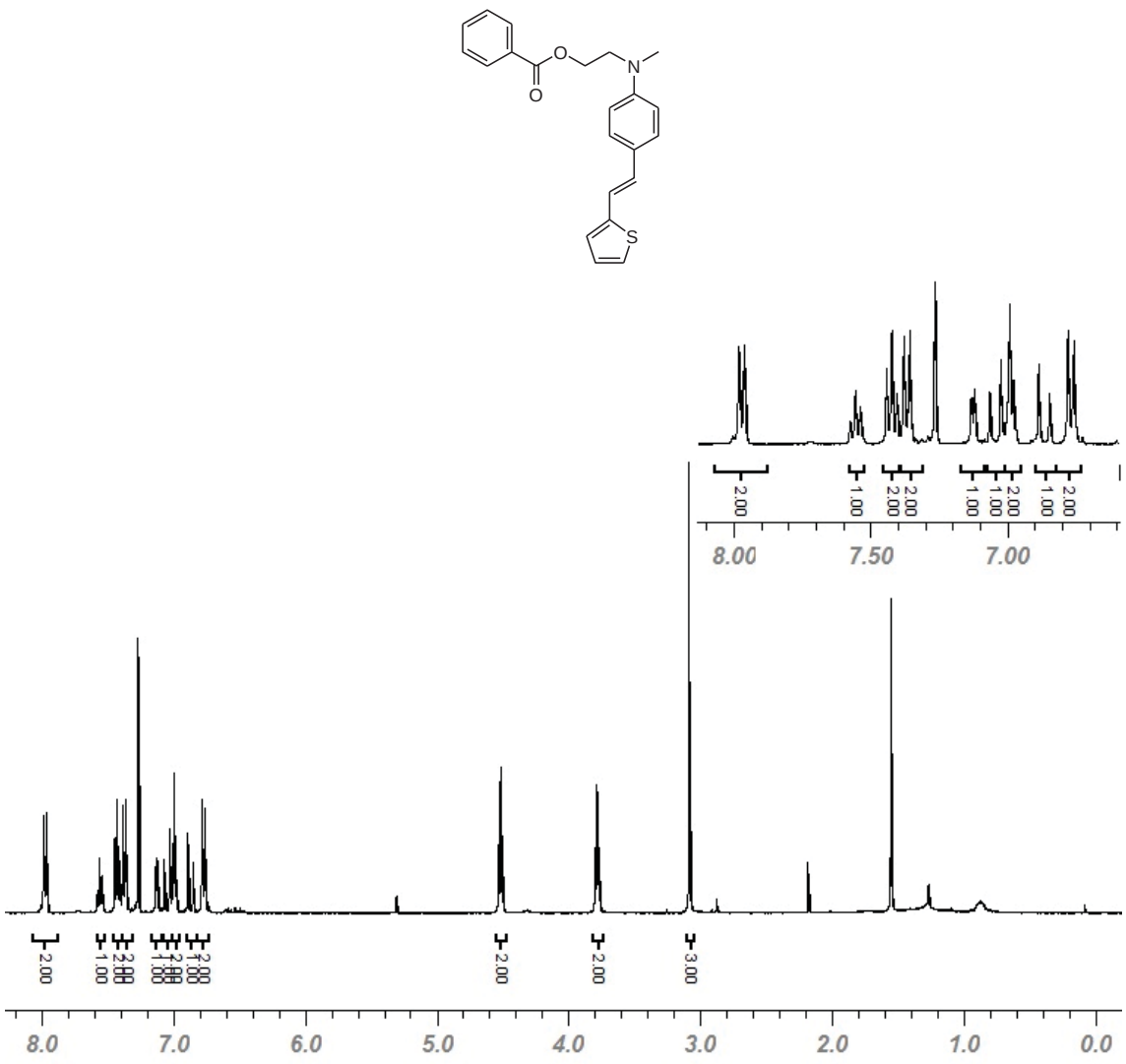

Figure S-15. ^{1}H-NMR spectrum of compound **6a** (400 MHz, $CDCl_3$).

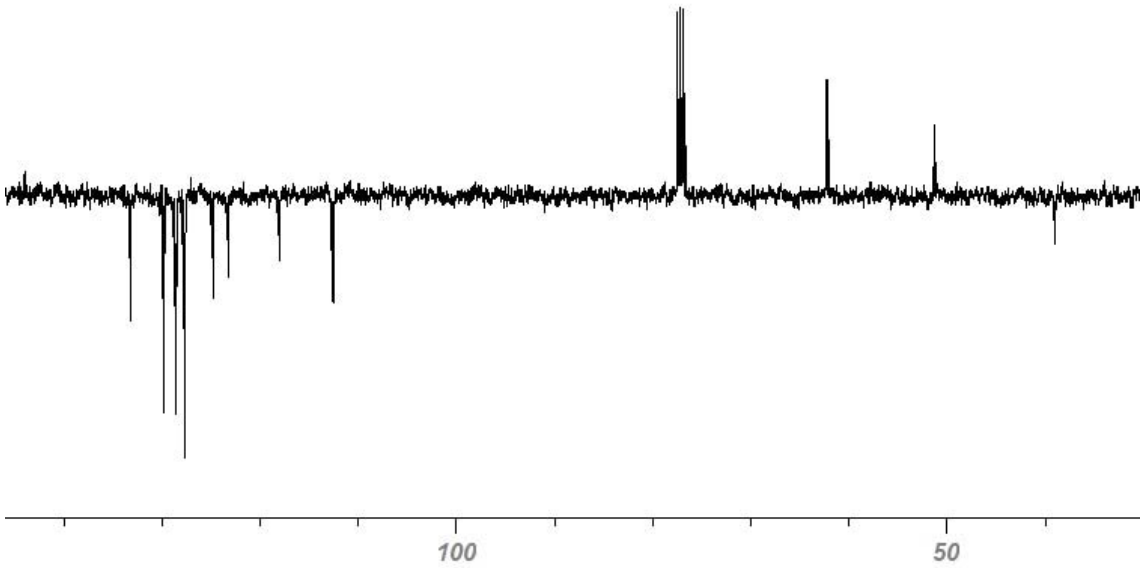

Figure S-16. ^{13}C-NMR (APT) spectrum of compound **6a** (400 MHz, $CDCl_3$).

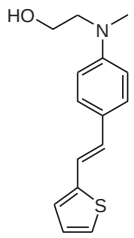

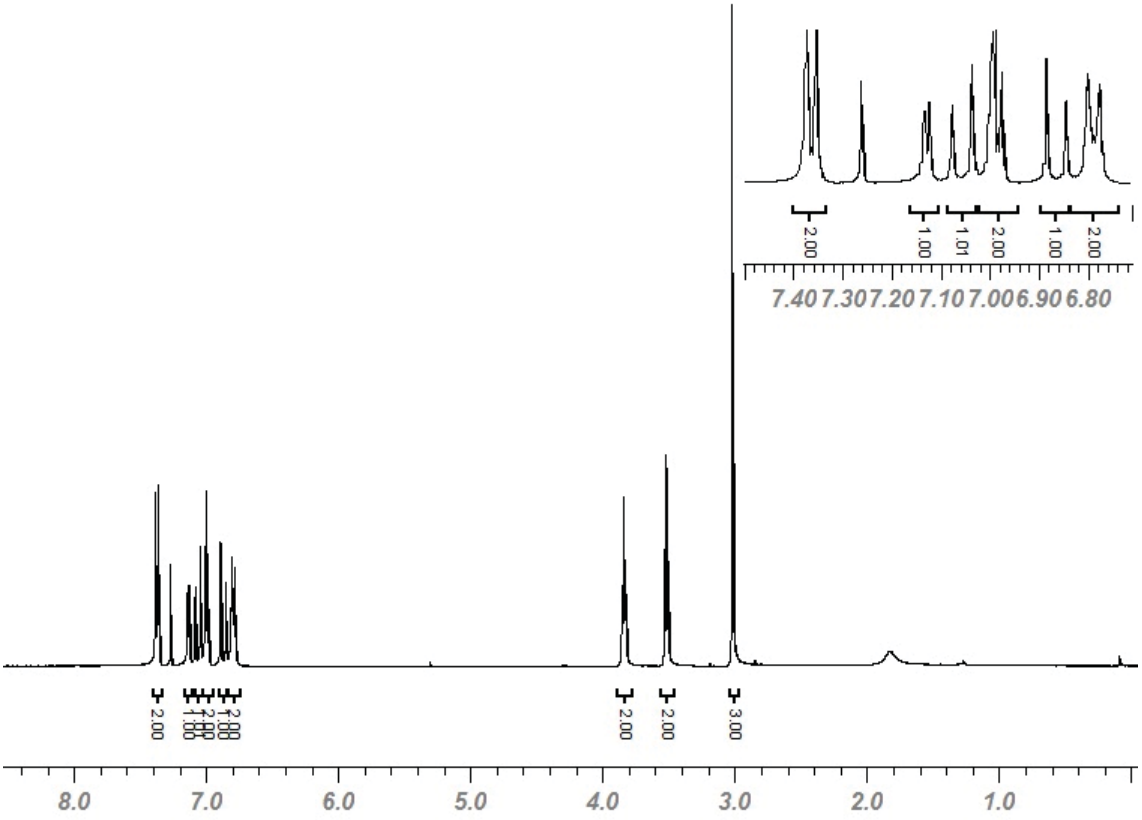

Figure S-17. ^{1}H-NMR spectrum of compound **6b** (400 MHz, $CDCl_3$).

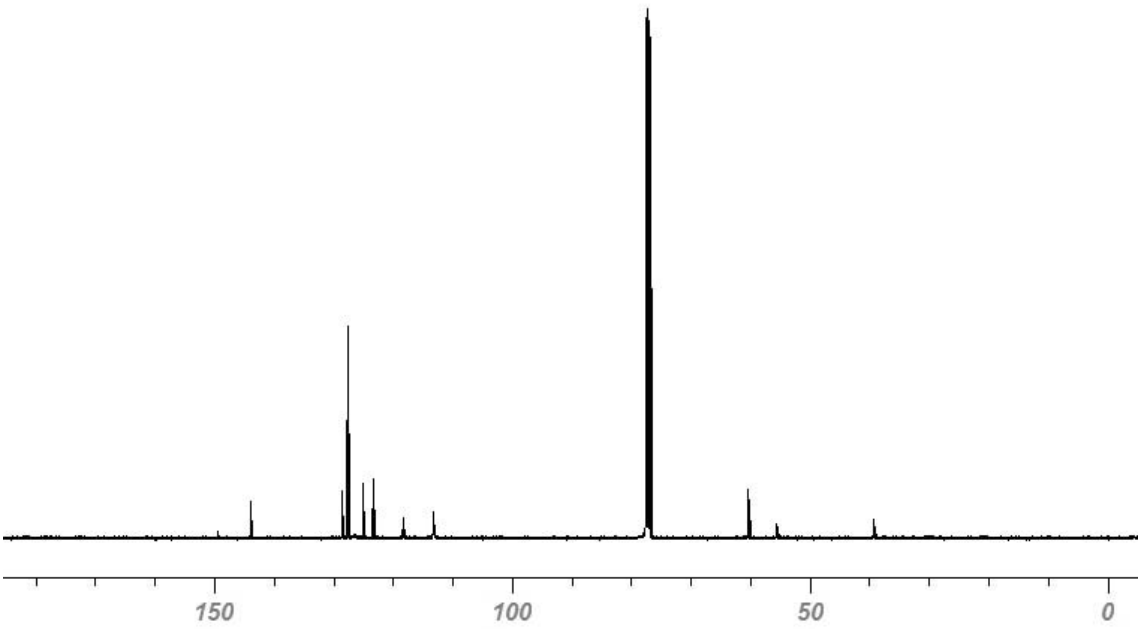

Figure S-18. ^{13}C-NMR spectrum of compound **6b** (1 00 MHz, $CDCl_3$).

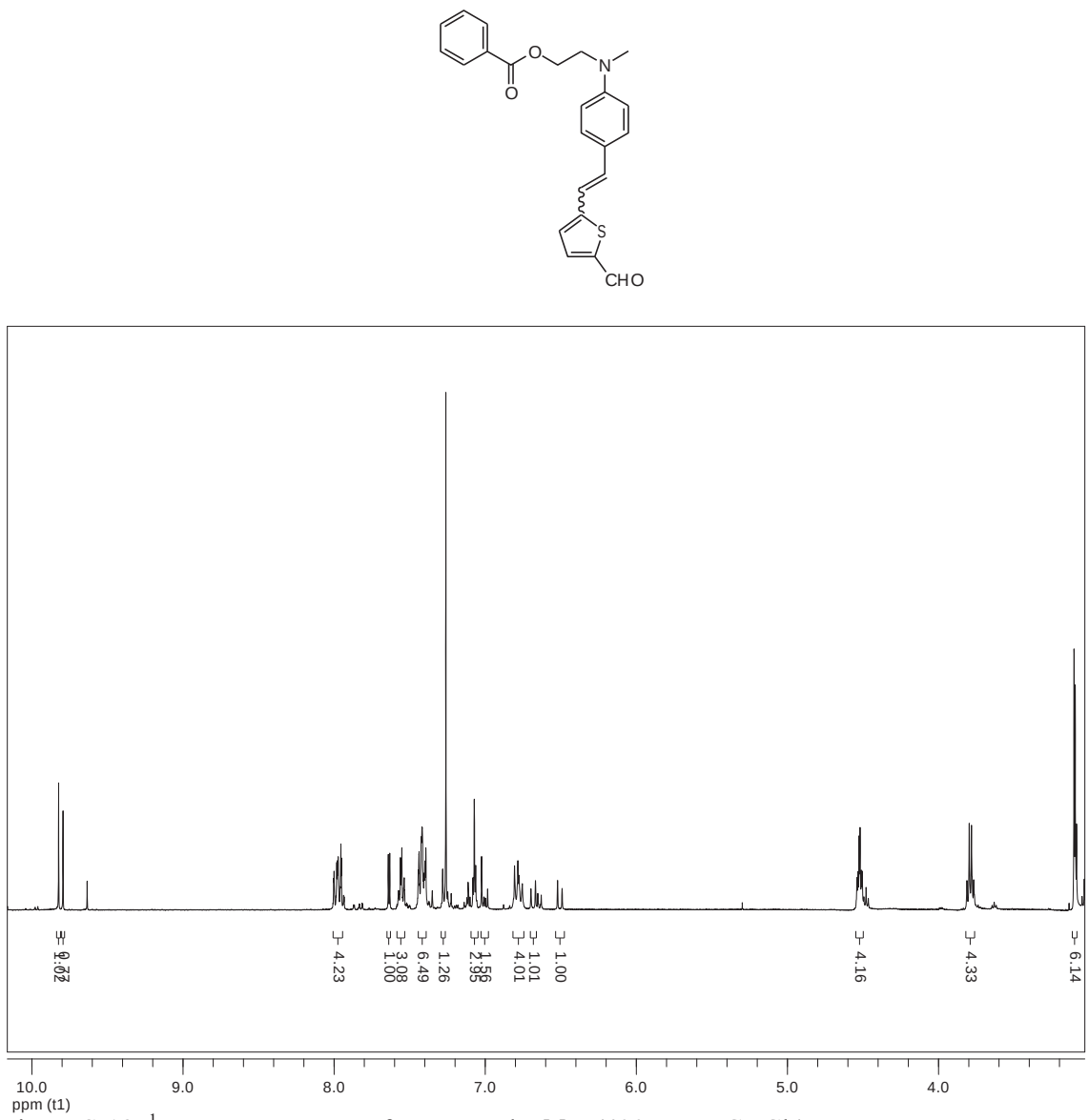

Figure S-19. ^{1}H-NMR spectrum of compound **Ald 4** (400 MHz, $CDCl_3$).

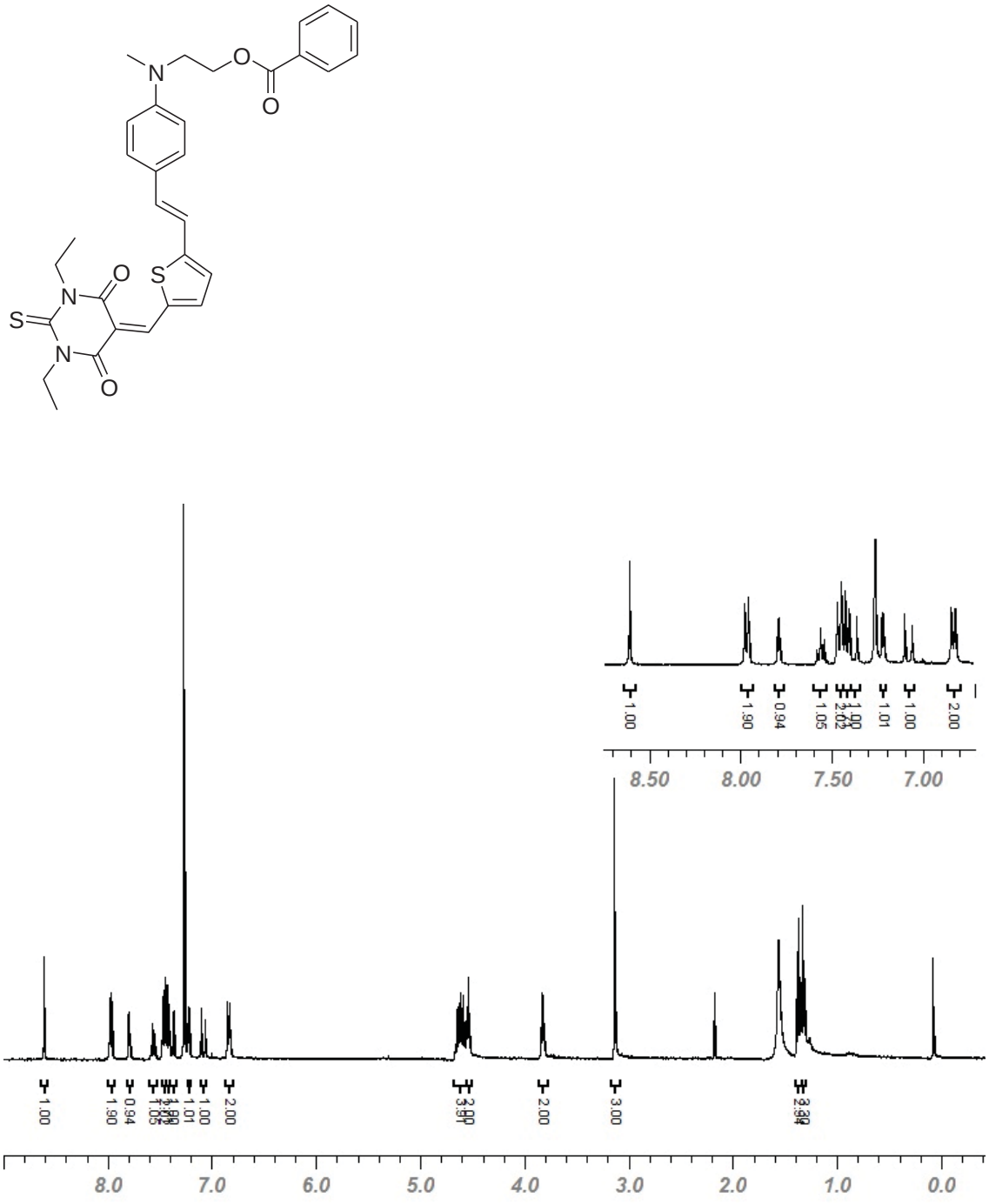

Figure S-20. ^{1}H-NMR spectrum of compound **8** (400 MHz, $CDCl_3$).

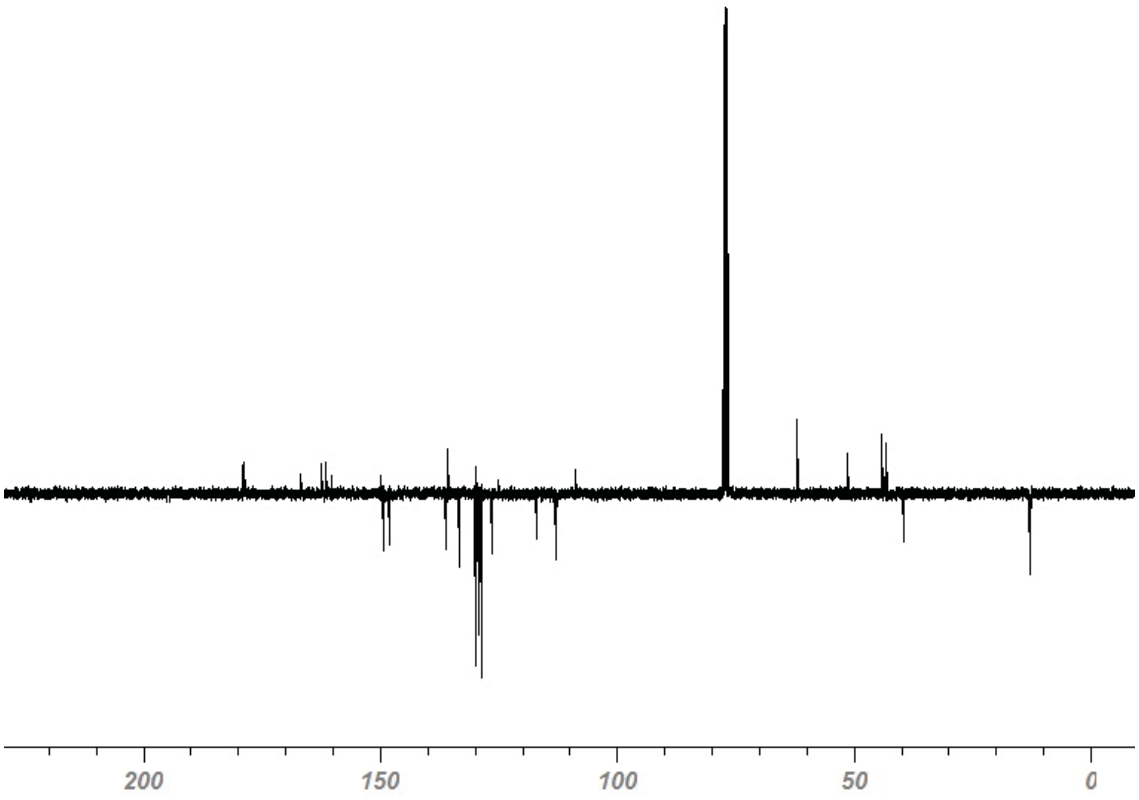

Figure S-21. ^{13}C-NMR (APT) spectrum of compound **8** (100 MHz, $CDCl_3$).

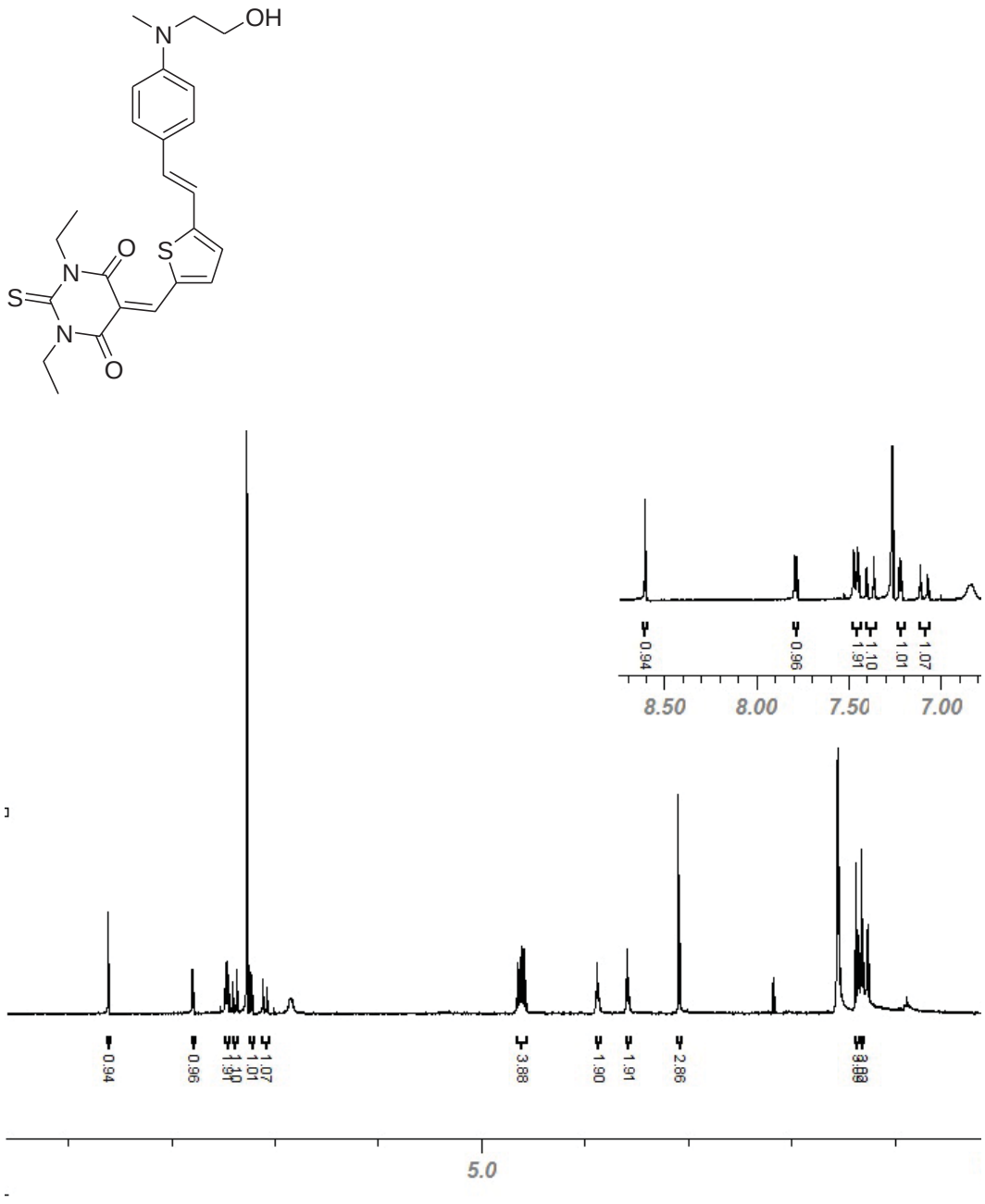

Figure S-22. ^{1}H-NMR spectrum of compound **9** (400 MHz, $CDCl_3$).

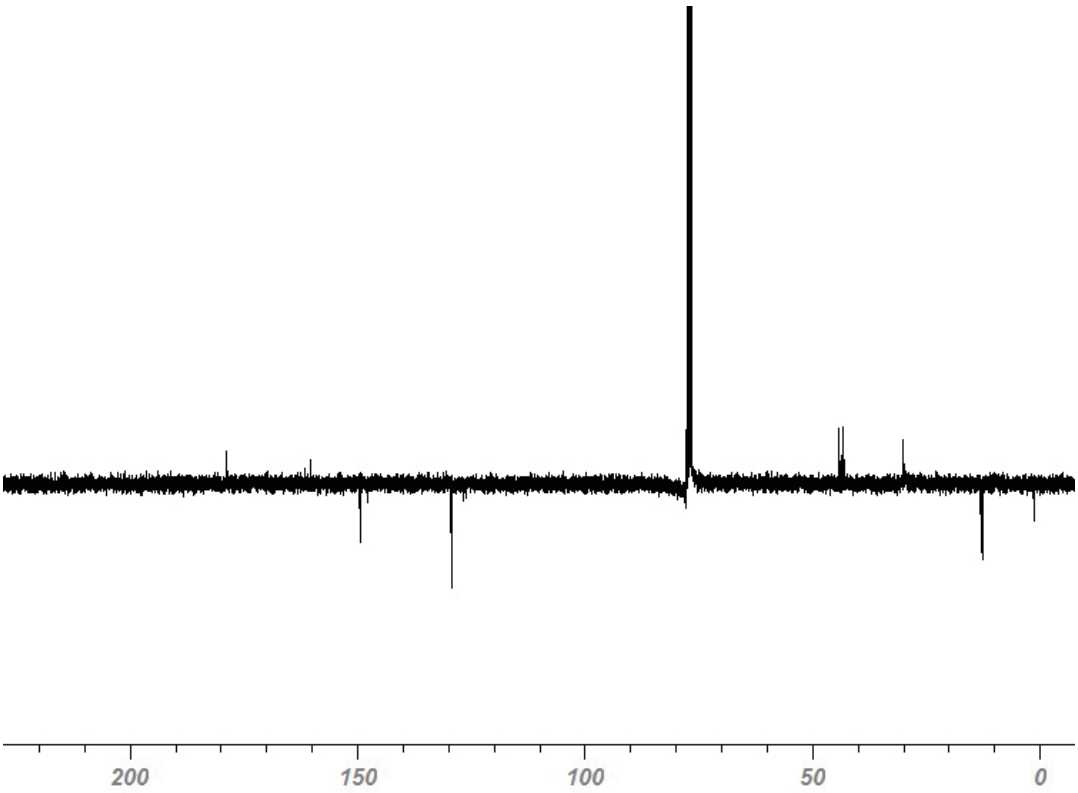

Figure S-23. ^{13}C-NMR (APT) spectrum of compound **9** (100 MHz, $CDCl_3$).

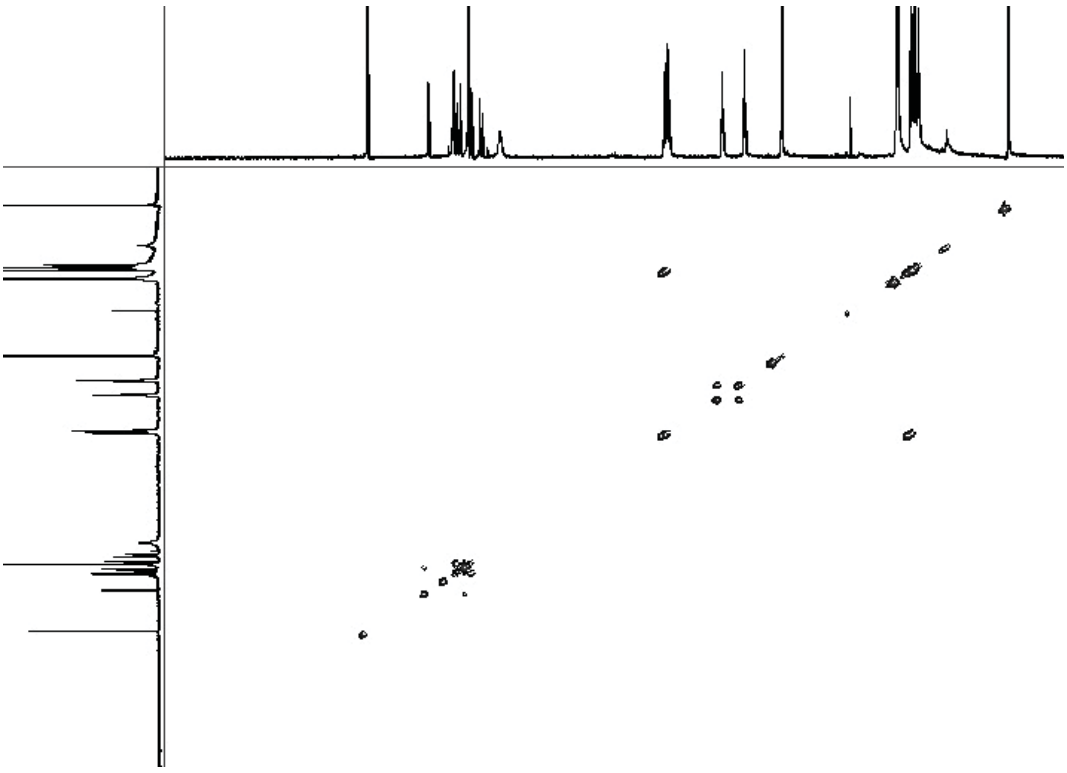

Figure S-24. ^{1}H-^{1}H COSY spectrum of compound **9** (400 MHz, $CDCl_3$).

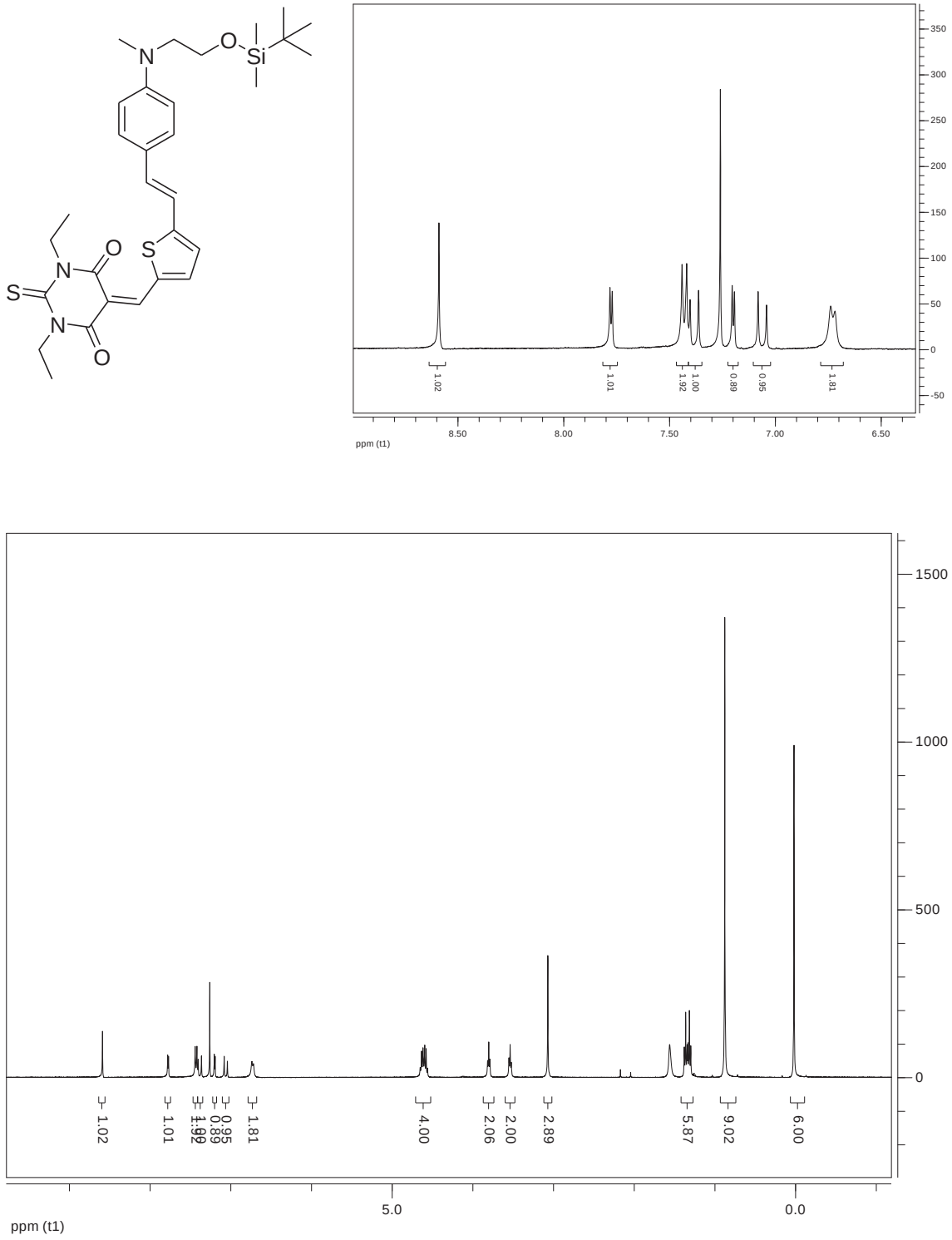

Figure S-25. ^{1}H-NMR spectrum of compound **10** (400 MHz, $CDCl_3$).

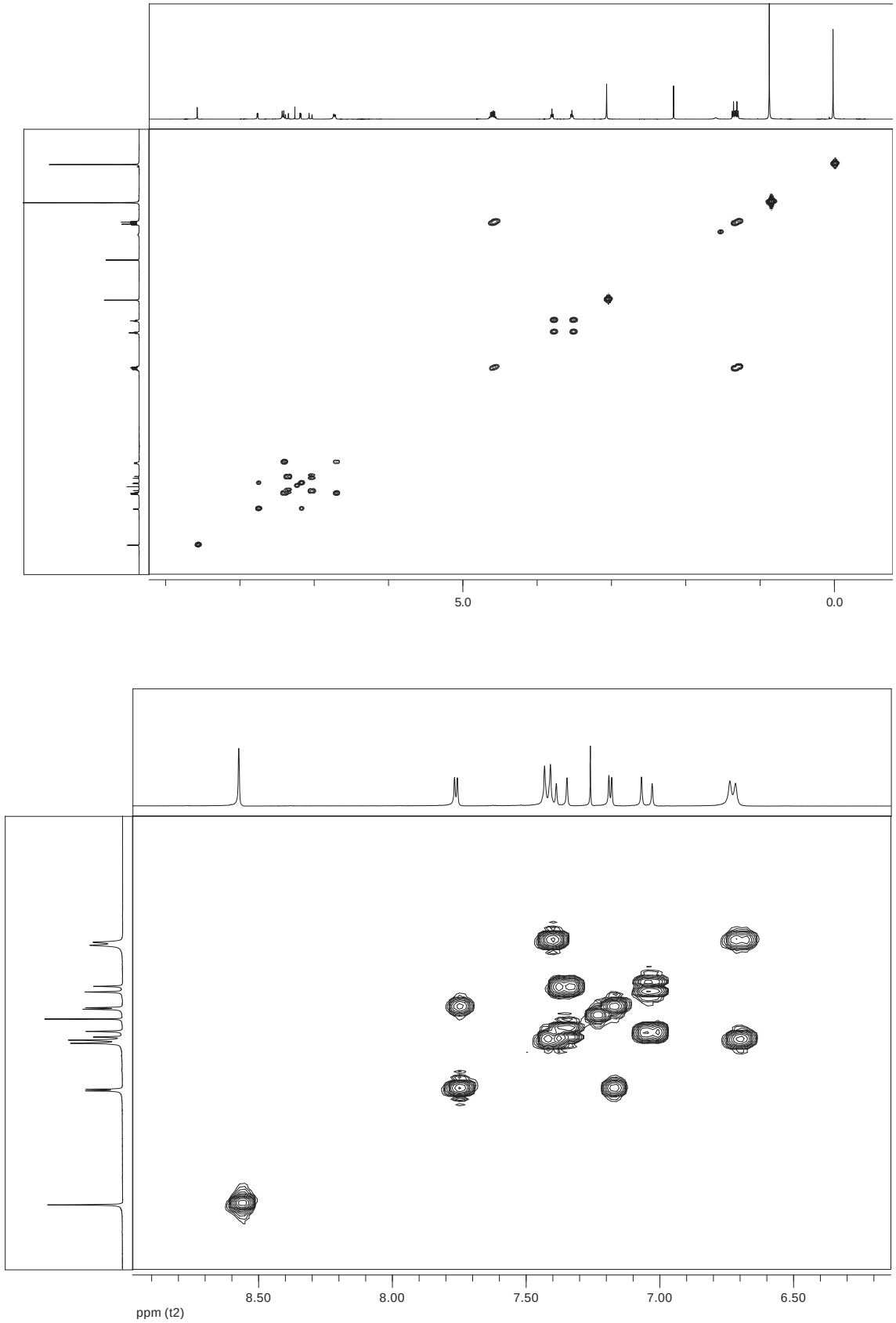

Figure S-26. ^{1}H-^{1}H COSY spectrum of compound **10** (400 MHz, $CDCl_3$).

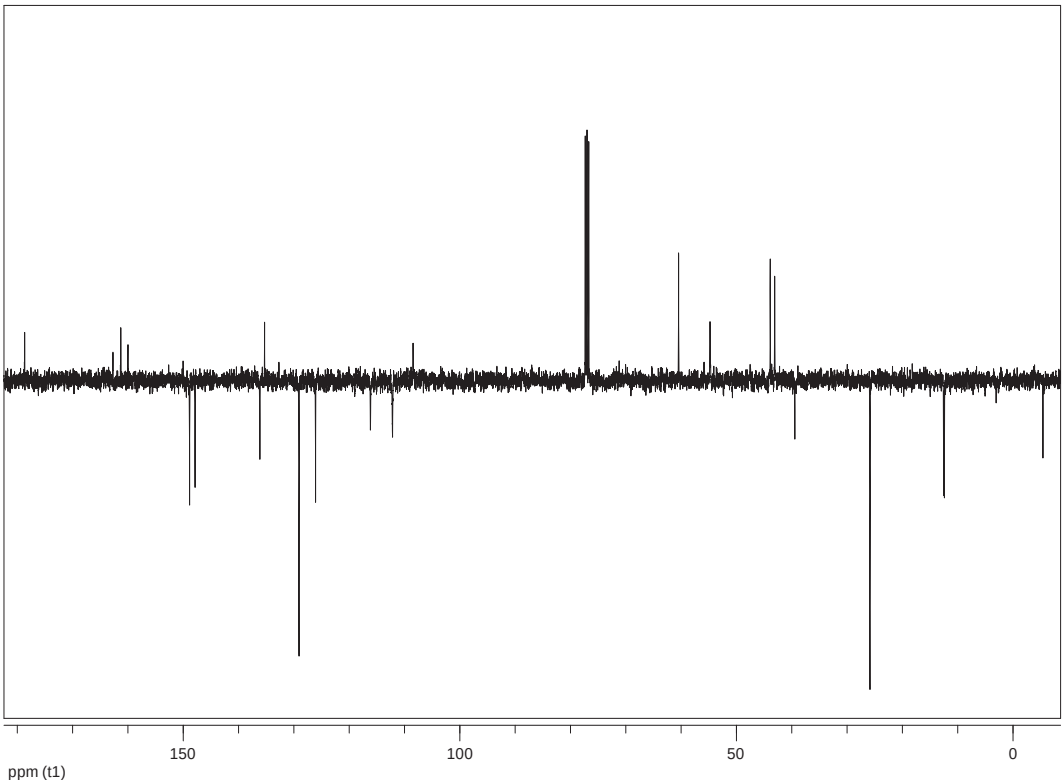

Figure S-27. ^{13}C-NMR (APT) spectrum of compound **10** (100 MHz, $CDCl_3$).

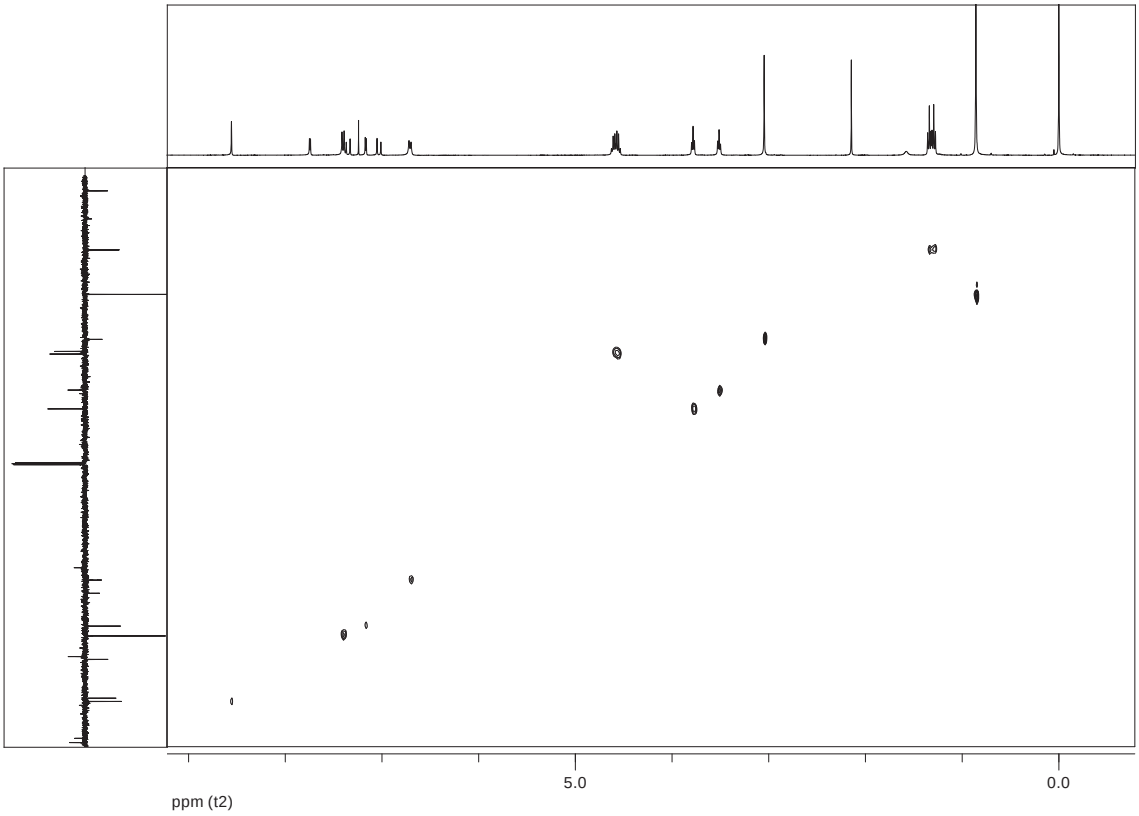
5.0
0.0
ppm (t2)

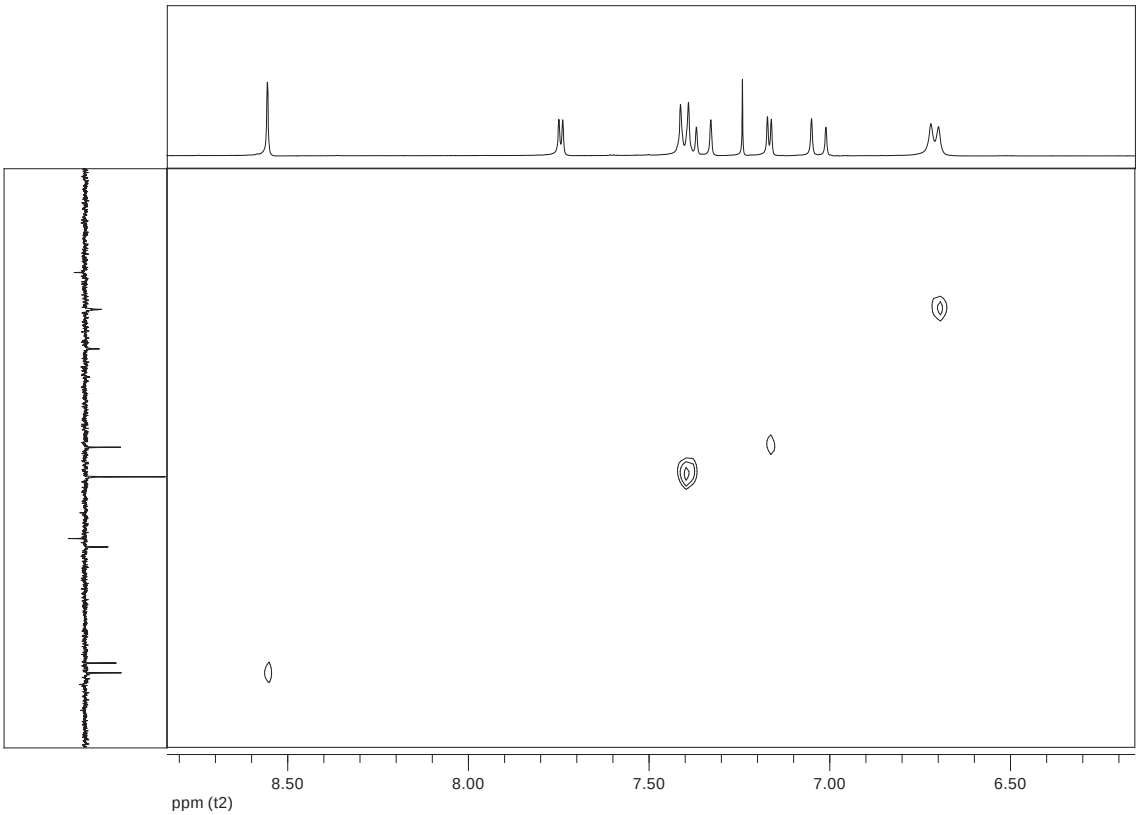
8.50
8.00
7.50
7.00
6.50
ppm (t2)

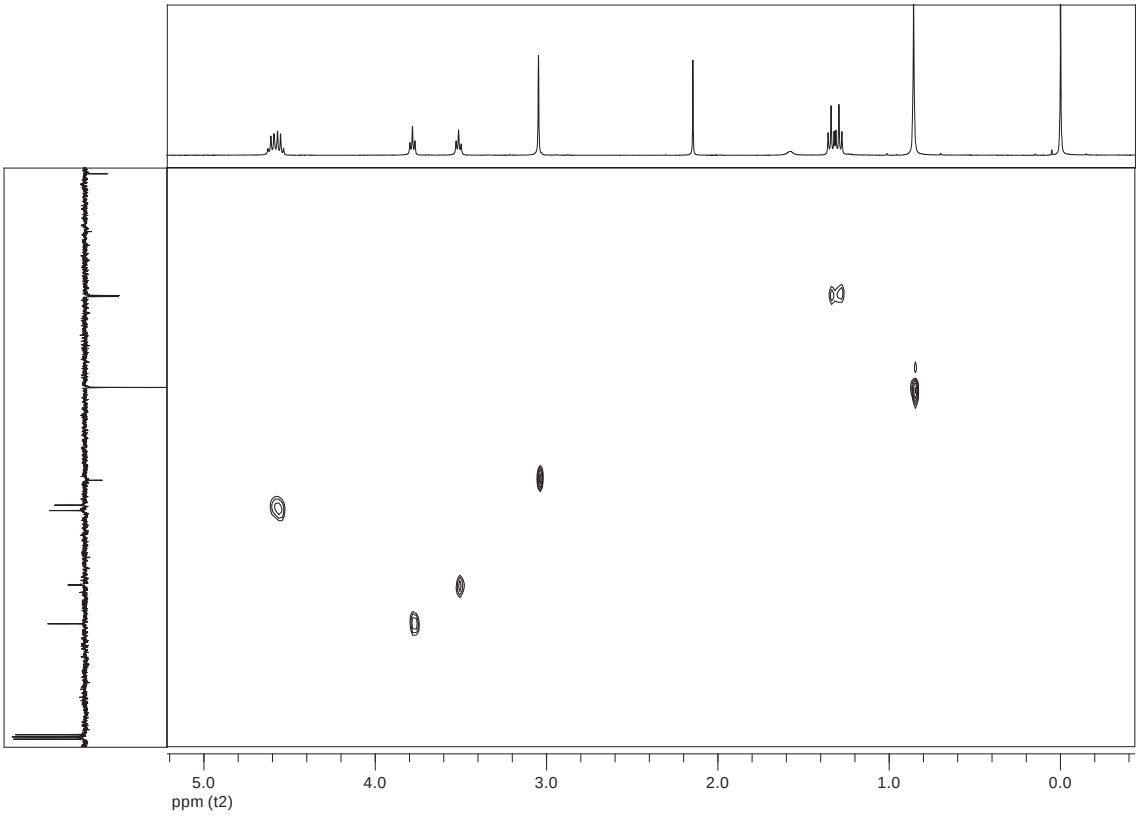

Figure S-28. ^{1}H-^{13}C. HSQC spectrum of compound **10**

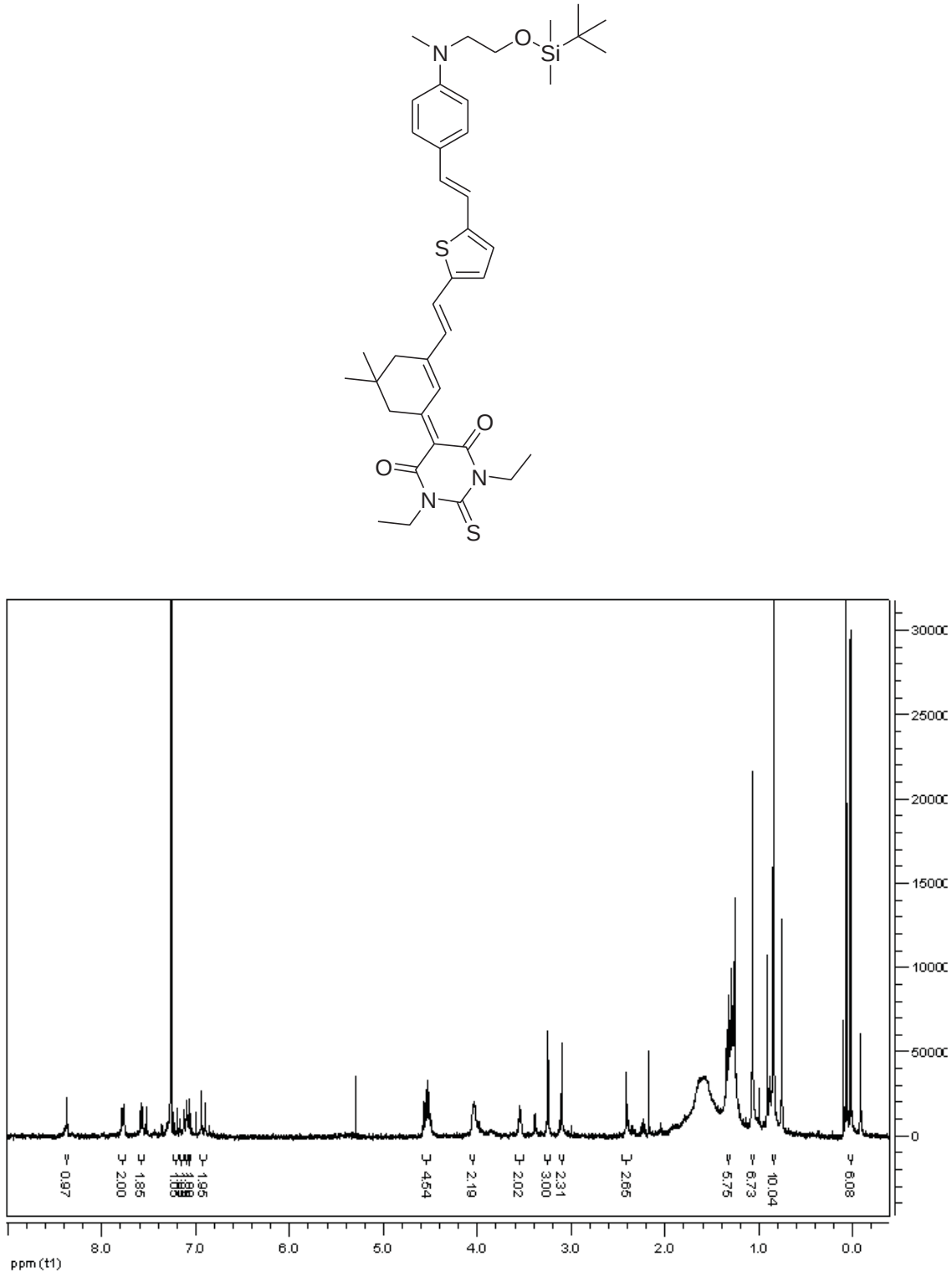

Figure S-29. ^{1}H-NMR spectrum of compound **11** (400 MHz, $CDCl_3$).

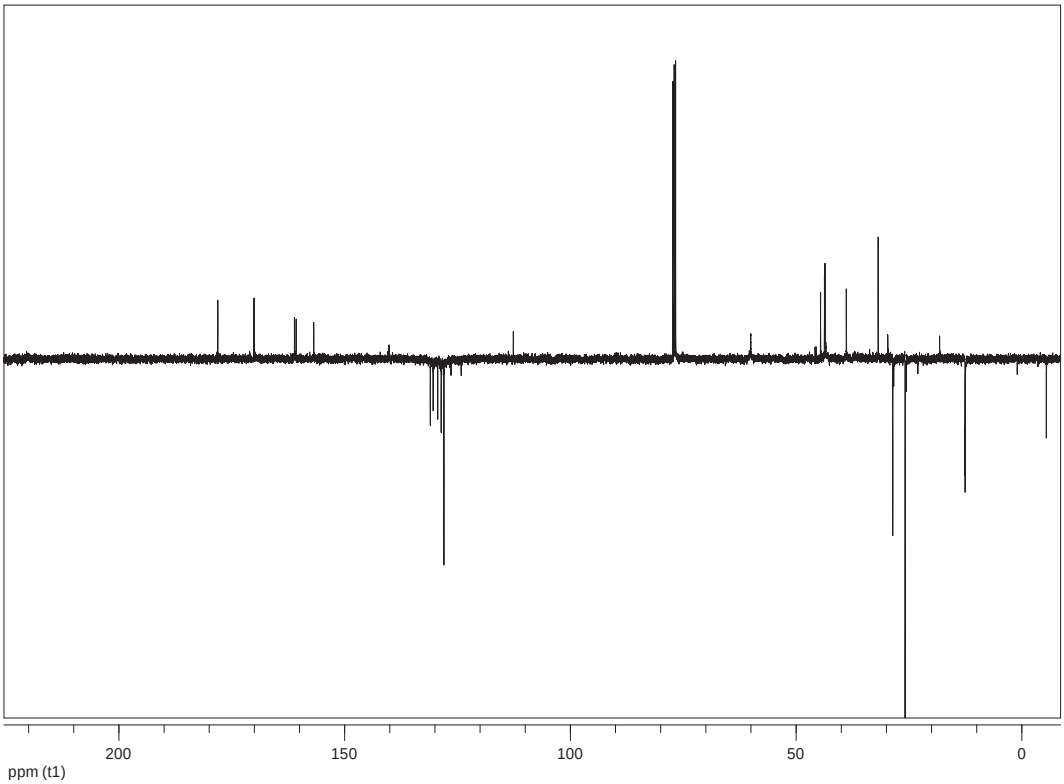

Figure S-30. ^{13}C-NMR (APT) spectrum of compound **11** (100 MHz, $CDCl_3$).

3. UV-vis spectra

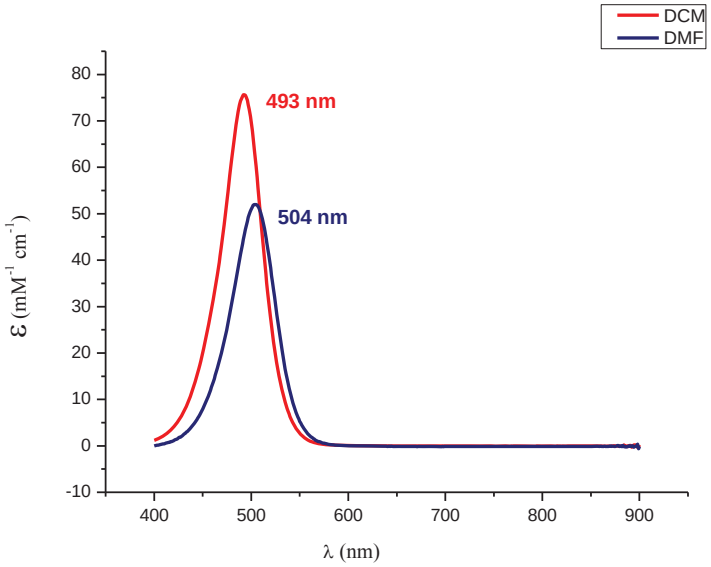

Figure S-31: UV-vis absorption of compound **1** (10^{-5}M) in DMF and CH_2Cl_2

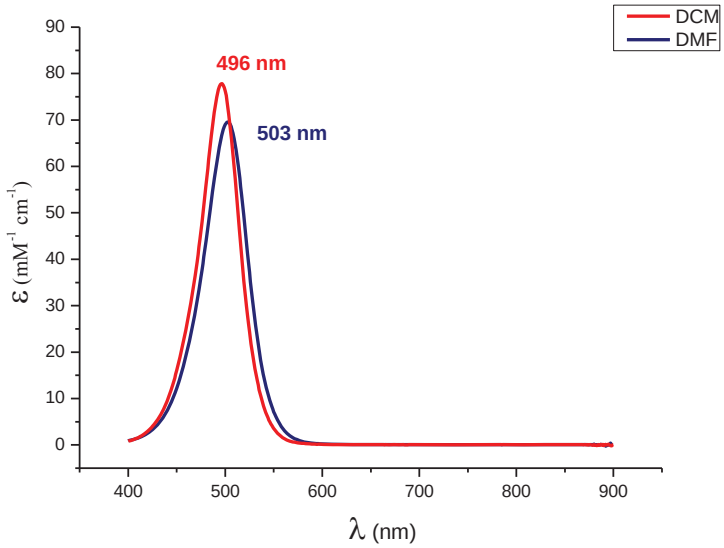

Figure S-32: UV-vis absorption of compound **2** (10^{-5}M) in DMF and CH_2Cl_2

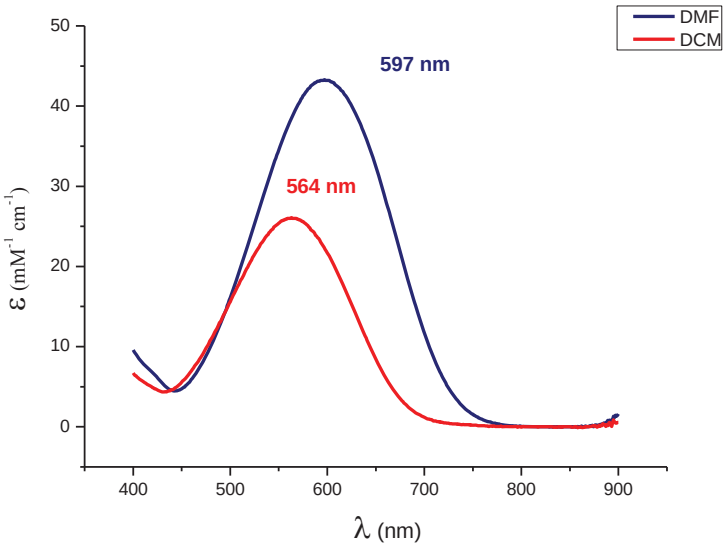

Figure S-33: UV-vis absorption of compound **3** (10^{-5}M) in DMF and CH_2Cl_2

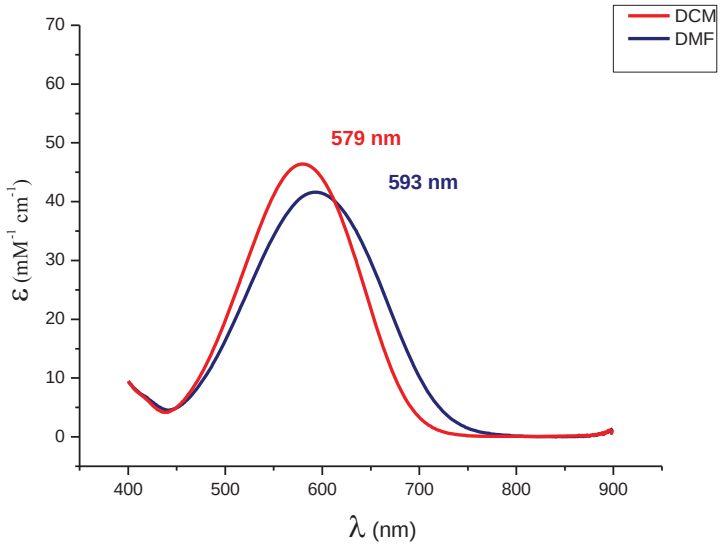

Figure S-34: UV-vis absorption of compound **4** (10^{-5}M) in DMF and CH_2Cl_2

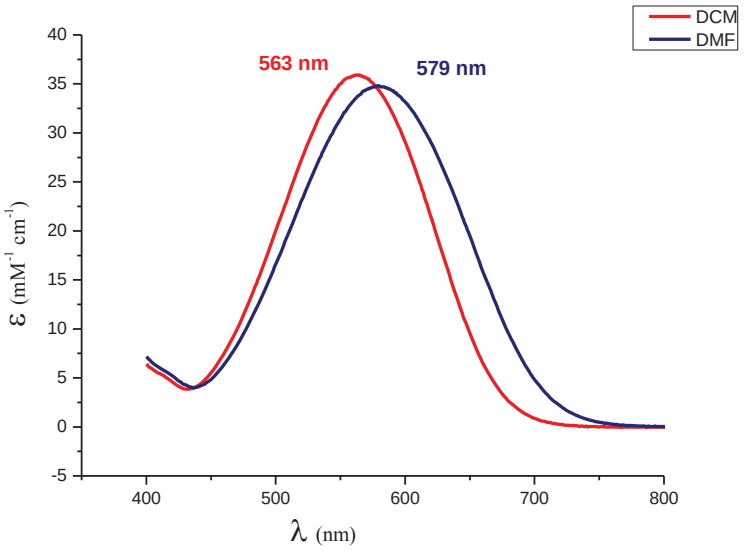

Figure S-35: UV-vis absorption of compound **5** (10^{-5}M) in DMF and CH_2Cl_2

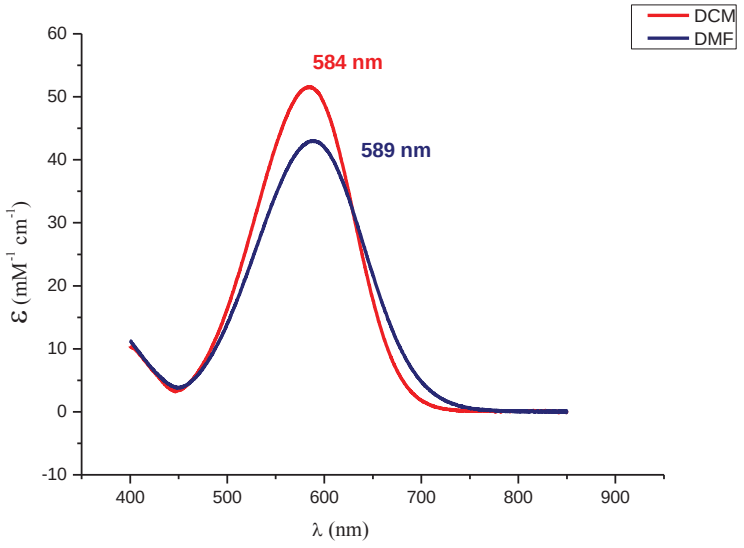

Figure S-36: UV-vis absorption of compound **8** (10^{-5}M) in DMF and CH_2Cl_2

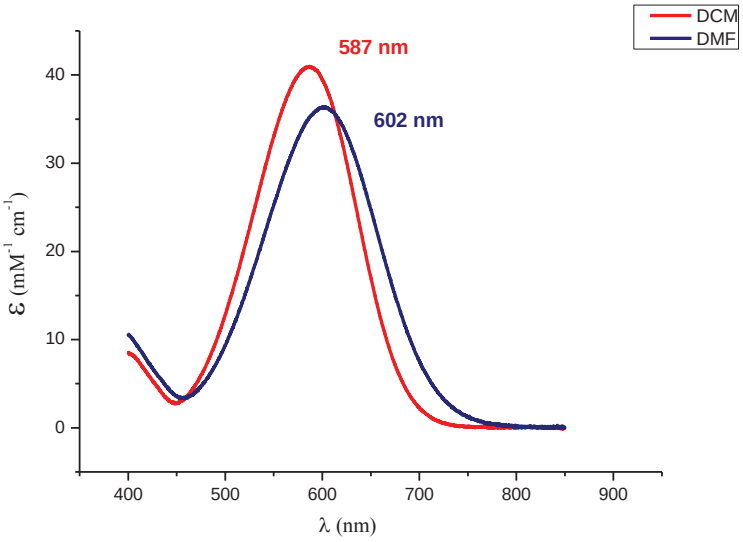

Figure S-37: UV-vis absorption of compound **9** (10^{-5}M) in DMF and CH_2Cl_2

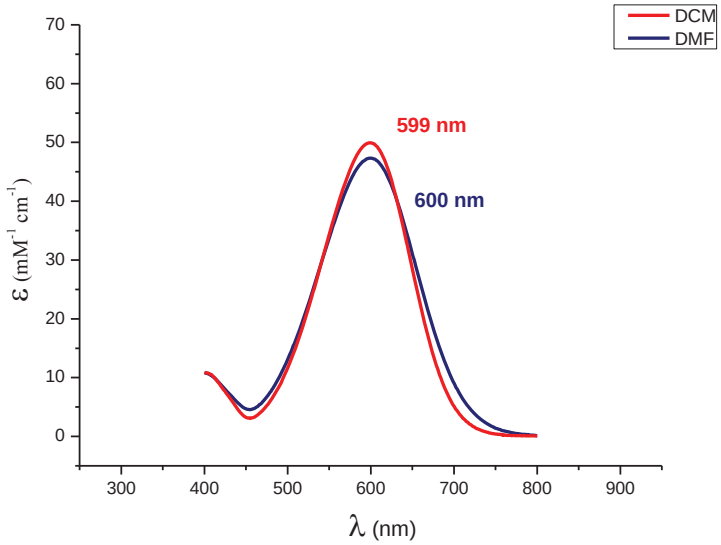

Figure S-38: UV-vis absorption of compound **10** (10^{-5}M) in DMF and CH_2Cl_2

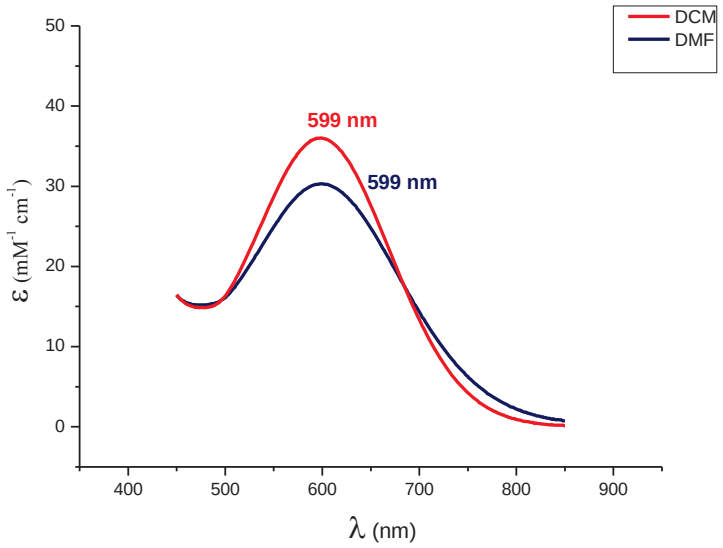

Figure S-39: UV-vis absorption of compound **11** (10^{-5}M) in DMF and CH_2Cl_2

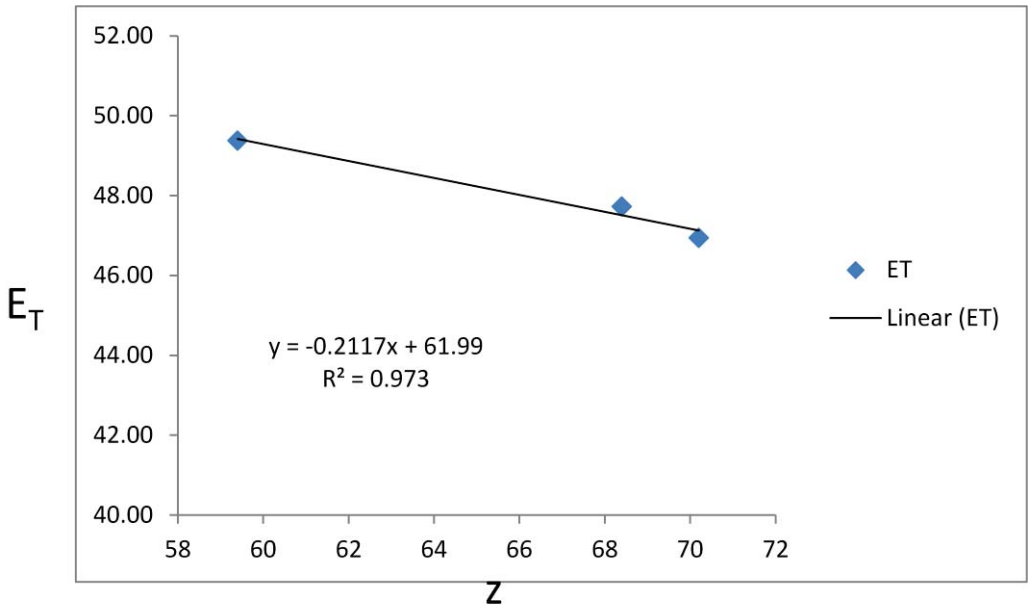

Figure S-40: Transition energy plot of compound **10**. Z-scale

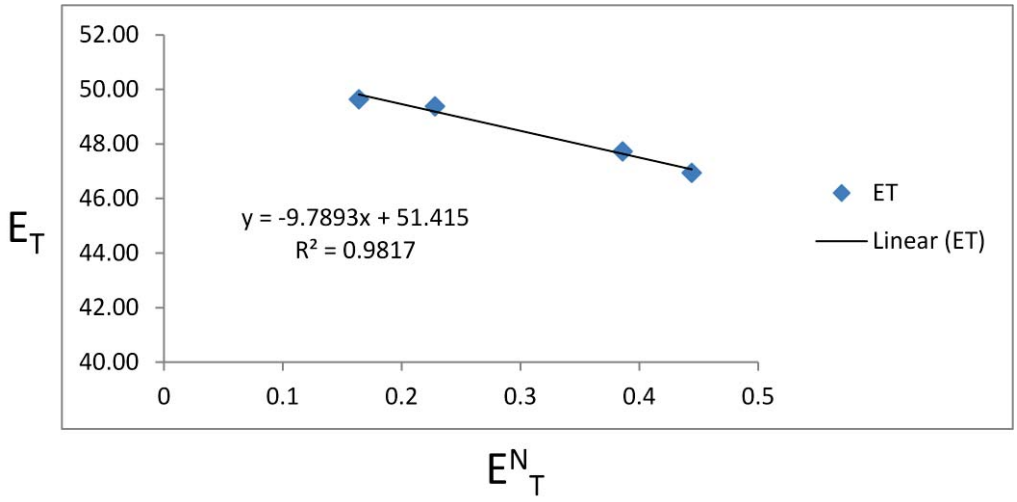

Figure S-41: Transition energy plot. Scale E^{N}_{T} of compound **10**

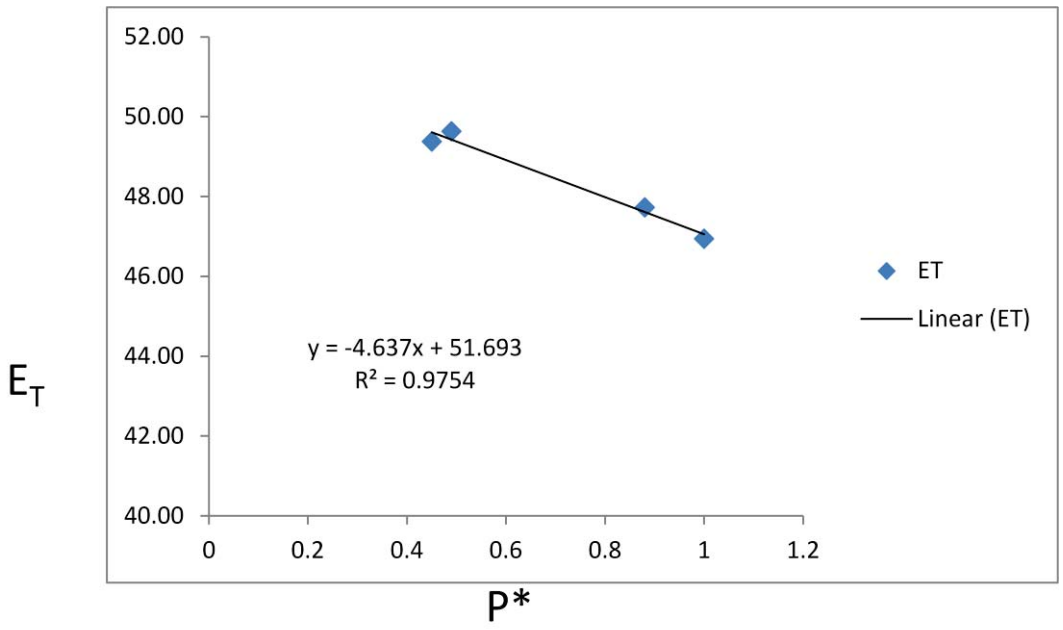

Figure S-42: Transition energy plot. Scale p* of compound **10**

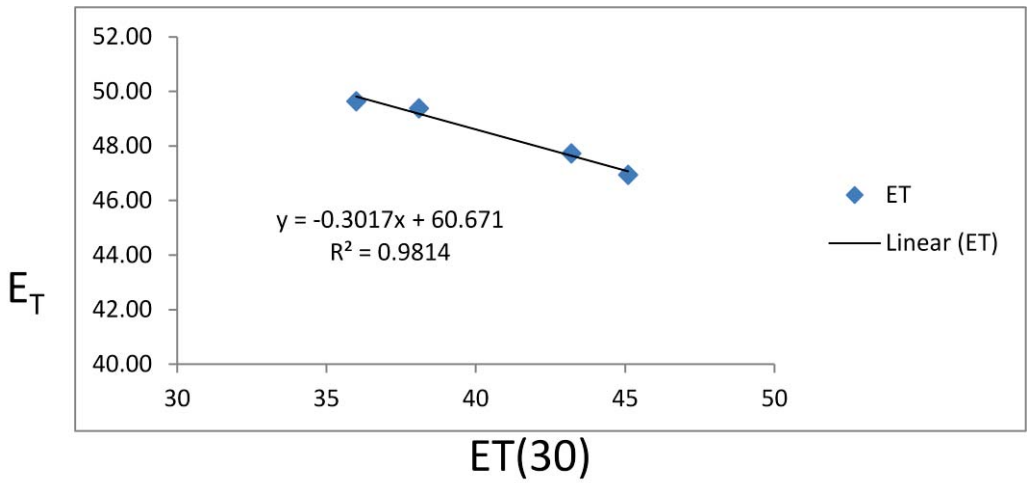

Figure S-43: Transition energy plot. Scale ET(30) of compound **10**

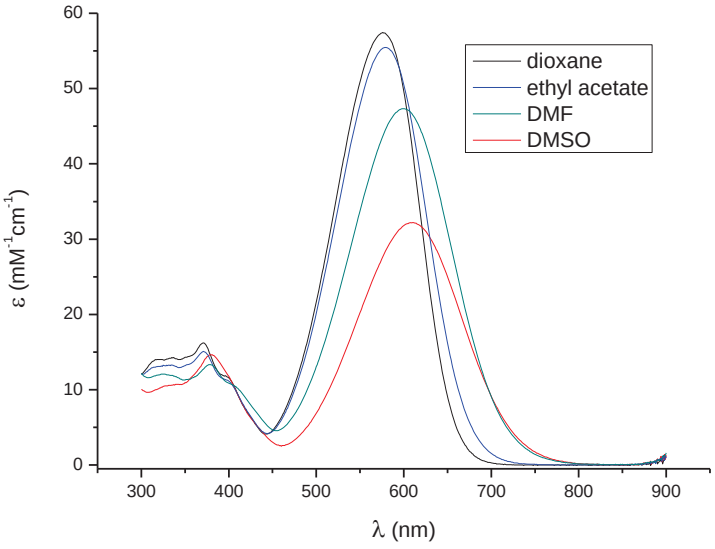

Figure S-44. UV/Vis spectra of the **10** chromophore in different solvents: 1,4-dioxane (black), ethyl acetate (blue), DMF (green), DMSO (red) of compound **10**

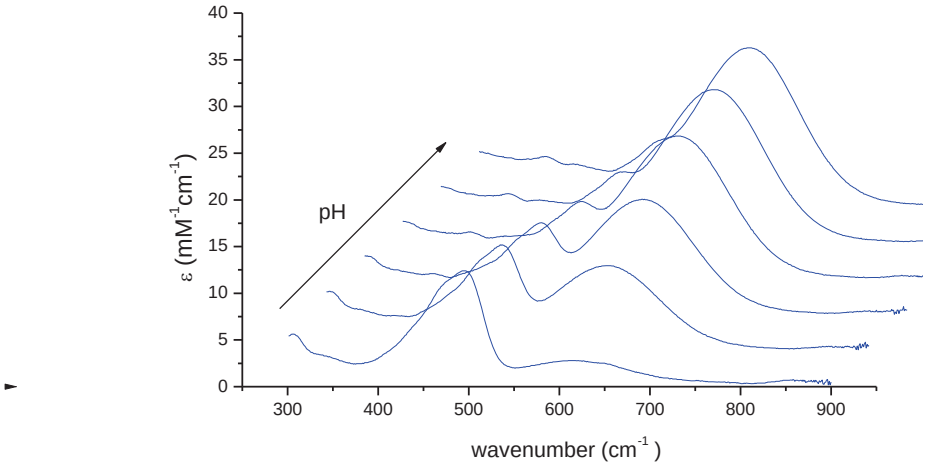

Figure S-45: a) Titration of HCl to a blue solution of chromophore **9** in EtOH (2 10^{-5} M).

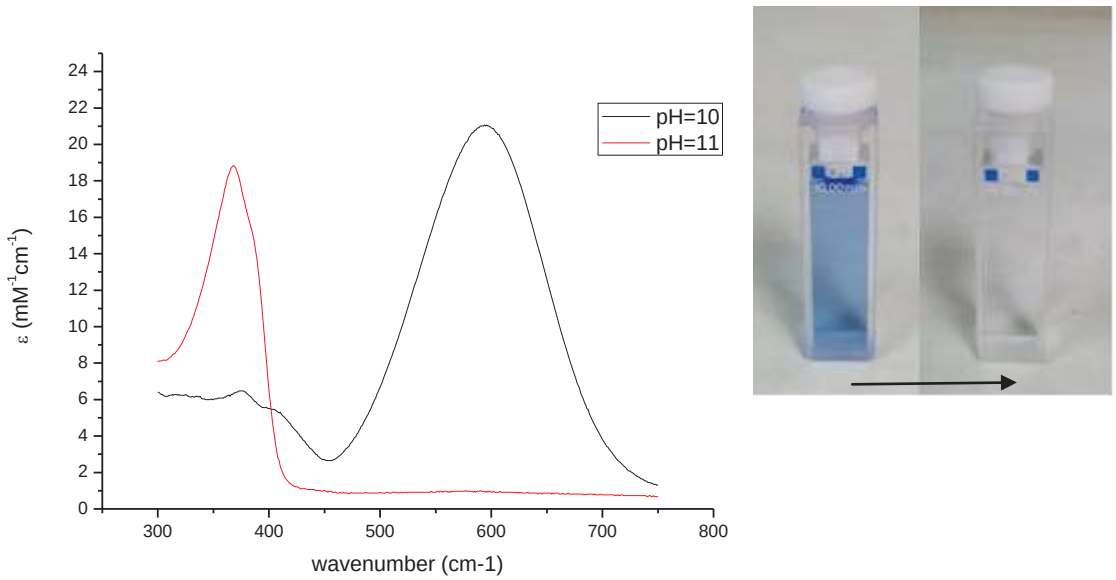

Figure S-46: Titration of KOH to a blue solution of chromophore **9** in EtOH (2 10^{-5} M)

4. Theoretical calculations

All theoretical calculations were performed by using the Gaussian 09 [1] program. The molecular geometries were optimized using the M06-2X [2] functional and the 6-31G* [3] basis set. M06-2X/6-311+G(2d,p) was used for TD-DFT calculations and the excited state dipole moments. Solvent effect was studied by placing the solute in a cavity within the solvent reaction field and using the Polarizable Continuum Model (PCM) [4]. Molecular hyperpolarizabilities were calculated by the Coupled Perturbed Hartree Fock method (CPHF) using the HF/6-31G* model. The default Gaussian 09 parameters were used in every case. Molecular orbital contours were plotted using Molekel 4.3 [5].

[1] Gaussian 09, Revision A.02, Frisch, M. J.; Trucks, G. W.; Schlegel, H. B.; Scuseria, G. E.; Robb, M. A.; Cheeseman, J. R.; Scalmani, G.; Barone, V.; Mennucci, B.; Petersson, G. A.; Nakatsuji, H.; Caricato, M.; Li, X.;
Hratchian, H. P.; Izmaylov, A. F.; Bloino, J.; Zheng, G.; Sonnenberg, J. L.; Hada, M.; Ehara, M.; Toyota, K.; Fukuda, R.; Hasegawa, J.; Ishida, M.; Nakajima, T.; Honda, Y.; Kitao, O.; Nakai, H.; Vreven, T.; Montgomery, Jr. J. A.; Peralta, J. E.; Ogliaro, F.; Bearpark, M.; Heyd, J. J.; Brothers, E.; Kudin, K. N.; Staroverov, V. N.; Kobayashi, R.; Normand, J.; Raghavachari, K.; Rendell, A.; Burant, J. C.; Iyengar, S. S.; Tomasi, J.; Cossi, M.; Rega, N.; Millam, J. M.; Klene, M.; Knox, J. E.; Cross, J. B.; Bakken, V.; Adamo, C.; Jaramillo, J.; Gomperts, R.; Stratmann, R. E.; Yazyev, O.; Austin, A. J.; Cammi, R.; Pomelli, C.; Ochterski, J. W.; Martin, R. L.; Morokuma, K.; Zakrzewski, V. G.; Voth, G. A.; Salvador, P.; Dannenberg, J. J.; Dapprich, S.; Daniels, A. D.; Farkas, O.; Foresman, J. B.; Ortiz, J. V.; Cioslowski, J.; Fox, D. J. Gaussian, Inc., Wallingford CT, 2009

[2] Yan Zhao, Donald G. Truhla, *Theor Chem Account* **2008**, 120, 215–241.

[3] Hariharan, P. C.; Pople, J. A. *Theor. Chim. Acta* **1973**, *28*, 213-222.

[4] Tomasi, J.; Mennucci, B.; Cammi, R. *Chem. Rev*. **2005**, 105, 2999-3093.

[5] Portmann, S.; Lüthi, H. P. *Chimia* **2000**, *54*, 766–770.

Cartesian coordinates and energies of optimized geometries

1 (CH_2Cl_2//PCM-M06-2X/6-31G*)

Standard orientation:

Center Number	Atomic Number	Atomic Type	Coordinates (Angstroms) X	Y	Z
1	6	0	-3.552914	-1.964026	0.110581
2	6	0	-2.179334	-2.113101	0.097996
3	6	0	-1.304878	-1.027496	-0.123162
4	6	0	-1.899107	0.224099	-0.407355
5	6	0	-3.269071	0.373941	-0.427650
6	6	0	-4.137084	-0.704260	-0.134638
7	1	0	-4.171730	-2.827101	0.323386
8	1	0	-1.758563	-3.097329	0.286604
9	1	0	-1.272885	1.069017	-0.651280
10	1	0	-3.702919	1.319603	-0.730788
11	7	0	-5.517487	-0.534353	-0.186800
12	6	0	-6.321842	-1.744971	-0.263458
13	1	0	-6.383253	-2.280353	0.697151
14	1	0	-7.335603	-1.467425	-0.561621
15	1	0	-5.913654	-2.418324	-1.019495
16	6	0	-6.192998	0.463897	0.659100
17	1	0	-7.204005	0.574356	0.253913
18	1	0	-6.291964	0.066650	1.682970
19	6	0	-5.592093	1.849866	0.764439
20	1	0	-4.584392	1.813411	1.196613
21	1	0	-6.228975	2.410404	1.461919
22	8	0	-5.592914	2.450798	-0.517290
23	1	0	-5.263304	3.356509	-0.424406
24	6	0	0.098684	-1.355910	-0.113706
25	1	0	0.268993	-2.431981	-0.138525
26	6	0	1.288250	-0.676267	-0.080346
27	6	0	2.488676	-1.525890	-0.180061
28	6	0	3.911566	0.471527	0.015650
29	16	0	5.442509	1.158424	0.025414
30	8	0	2.451801	-2.741635	-0.262707
31	8	0	0.544814	1.552613	0.265915
32	7	0	2.784723	1.224017	0.256297
33	6	0	1.458881	0.757141	0.136797
34	7	0	3.729878	-0.870453	-0.228618
35	6	0	2.903532	2.665257	0.562120
36	1	0	2.071700	2.904302	1.222239
37	1	0	3.837820	2.807500	1.099226
38	6	0	4.891049	-1.754022	-0.461996
39	1	0	4.537509	-2.550406	-1.114509

40	1	0	5.643714	-1.170314	-0.986267
41	6	0	2.850772	3.512154	-0.701337
42	1	0	3.674890	3.256032	-1.372148
43	1	0	1.902064	3.358713	-1.221836
44	1	0	2.934219	4.570496	-0.439264
45	6	0	5.431505	-2.322548	0.841900
46	1	0	4.660545	-2.908595	1.348434
47	1	0	6.283473	-2.975685	0.634165
48	1	0	5.765205	-1.519306	1.504158

E (M062X)= -1487.4128439 AU

2 (CH_2Cl_2//PCM-M06-2X/6-31G*)

Standard orientation:

Center Number	Atomic Number	Atomic Type	Coordinates (Angstroms) X	Y	Z
1	6	0	0.408149	3.138279	0.137368
2	6	0	-0.928371	2.884933	-0.057013
3	6	0	-1.470101	1.573737	-0.076546
4	6	0	-0.545661	0.512197	0.093409
5	6	0	0.795783	0.747824	0.283141
6	6	0	1.321553	2.068448	0.329412
7	1	0	0.753425	4.164078	0.151172
8	1	0	-1.599425	3.728897	-0.194947
9	1	0	-0.900336	-0.506773	0.065663
10	1	0	1.455200	-0.105354	0.385845
11	7	0	2.639939	2.313474	0.549234
12	6	0	3.154077	3.673171	0.462916
13	1	0	2.733524	4.307641	1.250973
14	1	0	4.236928	3.646809	0.583893
15	1	0	2.927819	4.123123	-0.509516
16	6	0	3.594669	1.237859	0.765681
17	1	0	3.140350	0.437051	1.355397
18	1	0	4.419492	1.637252	1.365188
19	6	0	4.127719	0.673533	-0.554105
20	1	0	4.660185	1.467255	-1.097847
21	1	0	3.284401	0.357076	-1.178591
22	8	0	4.953722	-0.446440	-0.338932
23	6	0	-2.886788	1.508042	-0.272862
24	1	0	-3.313678	2.498667	-0.425659
25	14	0	6.531714	-0.376854	0.239697
26	6	0	6.536241	-0.589310	2.106027
27	1	0	5.976326	0.211978	2.599407
28	1	0	6.084327	-1.542127	2.400288
29	1	0	7.559133	-0.565129	2.497646
30	6	0	7.291001	1.280195	-0.216744
31	1	0	7.226119	1.479034	-1.291568
32	1	0	6.805659	2.109450	0.310154
33	1	0	8.350258	1.295610	0.062919
34	6	0	7.424340	-1.813733	-0.605257
35	6	0	6.662853	-3.118575	-0.332350

36	1	0	5.631481	-3.063298	-0.696876
37	1	0	7.156923	-3.957664	-0.841315
38	1	0	6.633409	-3.353865	0.738013
39	6	0	8.855804	-1.937933	-0.066343
40	1	0	9.376959	-2.765849	-0.566069
41	1	0	9.439491	-1.026984	-0.245874
42	1	0	8.868288	-2.142507	1.010459
43	6	0	7.468976	-1.563111	-2.118781
44	1	0	8.044260	-0.662288	-2.362762
45	1	0	7.947348	-2.409775	-2.629940
46	1	0	6.462009	-1.445718	-2.534747
47	6	0	-3.885161	0.558804	-0.312962
48	6	0	-5.230896	1.104167	-0.547956
49	6	0	-3.734512	-0.874577	-0.116492
50	6	0	-6.188545	-1.142653	-0.244376
51	8	0	-5.460389	2.287247	-0.743010
52	8	0	-2.672100	-1.445254	0.070838
53	7	0	-6.305142	0.197146	-0.529187
54	7	0	-4.915886	-1.648597	-0.130498
55	6	0	-7.634759	0.806124	-0.738778
56	1	0	-8.277100	0.043760	-1.172193
57	1	0	-7.487790	1.604575	-1.463879
58	6	0	-4.708360	-3.093405	0.099881
59	1	0	-5.519891	-3.620418	-0.395197
60	1	0	-3.768816	-3.344391	-0.389037
61	6	0	-8.209692	1.353703	0.559315
62	1	0	-9.186202	1.807302	0.368949
63	1	0	-8.336980	0.553731	1.293272
64	1	0	-7.547790	2.118643	0.973155
65	6	0	-4.649838	-3.421919	1.584367
66	1	0	-3.823107	-2.888071	2.059809
67	1	0	-5.585969	-3.146414	2.076954
68	1	0	-4.491020	-4.495398	1.718894
69	16	0	-7.543271	-2.116709	-0.045719

E (M062X)= -2013.9101508AU

3 (CH_2Cl_2//PCM-M06-2X/6-31G*)

Standard orientation:

Center Number	Atomic Number	Atomic Type	Coordinates (Angstroms) X	Y	Z
1	6	0	6.464212	-1.453359	-0.428491
2	6	0	5.153096	-1.875249	-0.303013
3	6	0	4.078352	-0.974041	-0.244599
4	6	0	4.392850	0.396297	-0.309908
5	6	0	5.694320	0.838574	-0.430027
6	6	0	6.775964	-0.076180	-0.503147
7	1	0	7.250836	-2.196322	-0.470745
8	1	0	4.950087	-2.942334	-0.248630
9	1	0	3.602355	1.138729	-0.250379
10	1	0	5.875229	1.906188	-0.456001

11	7	0	8.073943	0.344141	-0.650421
12	6	0	9.152868	-0.624831	-0.559836
13	1	0	9.097547	-1.354765	-1.375198
14	1	0	10.104624	-0.099079	-0.639011
15	1	0	9.135879	-1.168745	0.393071
16	6	0	8.420676	1.753736	-0.606868
17	1	0	7.704521	2.340512	-1.189070
18	1	0	9.392309	1.878543	-1.095823
19	6	0	8.492715	2.299202	0.821308
20	1	0	9.236524	1.728767	1.395902
21	1	0	7.525046	2.169464	1.315759
22	8	0	8.769691	3.685292	0.832867
23	6	0	2.729121	-1.489262	-0.107021
24	1	0	2.668866	-2.572250	-0.009506
25	6	0	1.576783	-0.776390	-0.102887
26	1	0	1.606911	0.303530	-0.232224
27	6	0	0.260149	-1.354003	0.029664
28	6	0	-0.828638	-0.527848	-0.087292
29	6	0	-2.182607	-1.000265	-0.089482
30	1	0	-0.652937	0.525207	-0.245150
31	6	0	-1.261284	-3.180788	0.868882
32	6	0	-1.473114	-4.694419	0.808959
33	1	0	-0.685464	-5.214728	1.365245
34	1	0	-2.437362	-4.967261	1.251591
35	1	0	-1.457243	-5.055688	-0.225107
36	6	0	-1.322326	-2.729490	2.333860
37	1	0	-2.301742	-2.967178	2.763222
38	1	0	-0.559260	-3.249328	2.923471
39	1	0	-1.157130	-1.652924	2.438748
40	6	0	-2.366884	-2.496247	0.053770
41	1	0	-3.334752	-2.718549	0.505271
42	1	0	-2.404365	-2.932289	-0.955251
43	6	0	-3.281803	-0.149617	-0.226345
44	6	0	-4.616216	-0.703021	-0.466007
45	6	0	-3.165695	1.307782	-0.146028
46	6	0	-5.631882	1.502047	-0.067991
47	8	0	-2.121281	1.936978	-0.072392
48	8	0	-4.838945	-1.840345	-0.849502
49	16	0	-7.000758	2.455422	0.159859
50	6	0	-7.038348	-0.519272	-0.277969
51	1	0	-7.696152	0.011253	0.406644
52	1	0	-6.884850	-1.533699	0.086334
53	6	0	-7.598047	-0.532949	-1.692982
54	1	0	-6.927297	-1.080427	-2.359608
55	1	0	-8.573805	-1.026740	-1.699427
56	1	0	-7.724980	0.486245	-2.067417
57	6	0	-4.197322	3.512141	-0.057218
58	1	0	-5.069868	3.965947	-0.520584
59	1	0	-3.315878	3.742548	-0.652502
60	6	0	-4.018579	3.987736	1.377224
61	1	0	-4.894853	3.732415	1.978628
62	1	0	-3.131259	3.529920	1.821444
63	1	0	-3.892402	5.073880	1.393250
64	6	0	0.097821	-2.831391	0.259068

65	1	0	0.897630	-3.205641	0.908019
66	1	0	0.213697	-3.344484	-0.708059
67	7	0	-5.720002	0.143198	-0.218394
68	7	0	-4.374123	2.047430	-0.130383
69	1	0	9.680138	3.810380	0.528202

E (M062X)= -1837.4471447 AU

4 (CH_2Cl_2//PCM-M06-2X/6-31G*)

Standard orientation:

Center Number	Atomic Number	Atomic Type	Coordinates (Angstroms) X	Y	Z
1	6	0	3.614662	-3.658289	-0.351941
2	6	0	2.242305	-3.739276	-0.195710
3	6	0	1.413197	-2.608257	-0.261777
4	6	0	2.043145	-1.371210	-0.493298
5	6	0	3.409825	-1.267852	-0.649162
6	6	0	4.242748	-2.414137	-0.588066
7	1	0	4.201964	-4.566343	-0.295157
8	1	0	1.792538	-4.713105	-0.016267
9	1	0	1.453783	-0.460462	-0.539650
10	1	0	3.838370	-0.285253	-0.805005
11	7	0	5.602119	-2.332042	-0.756641
12	6	0	6.427573	-3.503301	-0.516723
13	1	0	6.221737	-4.292355	-1.249216
14	1	0	7.476325	-3.218823	-0.608861
15	1	0	6.268902	-3.913609	0.488048
16	6	0	6.265302	-1.052517	-0.928050
17	1	0	5.694417	-0.412310	-1.607710
18	1	0	7.230009	-1.235022	-1.413472
19	6	0	6.482852	-0.325224	0.401220
20	1	0	7.132146	-0.934908	1.045950
21	1	0	5.522433	-0.211928	0.916837
22	8	0	7.021130	0.961853	0.199368
23	6	0	-0.018630	-2.759333	-0.075270
24	1	0	-0.344147	-3.777350	0.134773
25	6	0	-0.951543	-1.779393	-0.143697
26	1	0	-0.647291	-0.761546	-0.378470
27	6	0	-2.369623	-1.971193	0.048120
28	6	0	-3.196360	-0.891545	-0.130583
29	6	0	-4.627251	-0.970608	-0.071290
30	1	0	-2.745813	0.056938	-0.379612
31	6	0	-4.301363	-3.236999	1.056750
32	6	0	-4.919268	-4.634104	1.133225
33	1	0	-4.287145	-5.300682	1.730500
34	1	0	-5.907741	-4.593311	1.603964
35	1	0	-5.033557	-5.073137	0.136180
36	6	0	-4.190950	-2.665950	2.476448
37	1	0	-5.183995	-2.584820	2.931559
38	1	0	-3.583253	-3.325397	3.105512
39	1	0	-3.731642	-1.672741	2.483742

40	6	0	-5.205017	-2.344754	0.193732
41	1	0	-6.184904	-2.264381	0.665852
42	1	0	-5.382381	-2.829880	-0.777311
43	6	0	-5.454224	0.139420	-0.250113
44	6	0	-6.901102	-0.033015	-0.399354
45	6	0	-4.937120	1.509247	-0.301801
46	6	0	-7.243759	2.385398	-0.107586
47	8	0	-3.758363	1.826499	-0.344321
48	8	0	-7.448856	-1.082866	-0.695006
49	16	0	-8.277390	3.692257	0.130929
50	6	0	-9.163597	0.828886	-0.122117
51	1	0	-9.606224	1.551544	0.559314
52	1	0	-9.274639	-0.170474	0.294818
53	6	0	-9.790749	0.908893	-1.506201
54	1	0	-9.335795	0.171085	-2.171532
55	1	0	-10.862379	0.701773	-1.438336
56	1	0	-9.659039	1.906943	-1.932518
57	6	0	-5.315632	3.914563	-0.318728
58	1	0	-6.063096	4.568913	-0.760315
59	1	0	-4.453548	3.858295	-0.980591
60	6	0	-4.903728	4.395221	1.065276
61	1	0	-5.769188	4.431246	1.732031
62	1	0	-4.149584	3.727940	1.489765
63	1	0	-4.477672	5.399953	0.995714
64	6	0	-2.917579	-3.324263	0.408516
65	1	0	-2.229136	-3.847267	1.082328
66	1	0	-2.974915	-3.928651	-0.509761
67	7	0	-7.712472	1.099171	-0.163505
68	7	0	-5.892295	2.554962	-0.275486
69	14	0	8.631910	1.272226	-0.169932
70	6	0	8.857687	1.370109	-2.032763
71	1	0	8.660014	0.404666	-2.510498
72	1	0	8.181203	2.107412	-2.477055
73	1	0	9.884170	1.657335	-2.286044
74	6	0	9.709437	-0.098646	0.532250
75	1	0	9.555253	-0.228999	1.608524
76	1	0	9.514044	-1.060968	0.045435
77	1	0	10.767058	0.137315	0.370914
78	6	0	9.000481	2.938220	0.643350
79	6	0	8.010152	3.988576	0.120378
80	1	0	6.974392	3.702960	0.334025
81	1	0	8.198302	4.958682	0.600861
82	1	0	8.106862	4.132346	-0.962292
83	6	0	10.432682	3.385256	0.320540
84	1	0	10.644780	4.348050	0.805518
85	1	0	11.176213	2.664837	0.682062
86	1	0	10.585914	3.519596	-0.756610
87	6	0	8.839503	2.807018	2.164106
88	1	0	9.563691	2.101389	2.587797
89	1	0	9.002983	3.779658	2.648122
90	1	0	7.833991	2.463421	2.431319

E (M062X)= -2363.9352955AU

5 (CH_2Cl_2//PCM-M06-2X/6-31G*)

Standard orientation:

Center Number	Atomic Number	Atomic Type	Coordinates (Angstroms) X	Y	Z
1	6	0	9.072519	4.521926	0.248740
2	1	0	10.016768	4.346321	-0.272897
3	1	0	8.362694	4.924468	-0.478153
4	1	0	9.219148	5.230300	1.062264
5	6	0	8.550279	3.224243	0.805345
6	8	0	8.329609	2.988332	1.964807
7	8	0	8.352245	2.321588	-0.178859
8	6	0	7.855309	1.052830	0.248360
9	1	0	8.525377	0.627074	1.002961
10	1	0	6.869439	1.173093	0.709784
11	6	0	7.791219	0.170980	-0.992762
12	1	0	8.794302	0.071485	-1.417364
13	1	0	7.178448	0.649403	-1.762174
14	7	0	7.282601	-1.152707	-0.698496
15	6	0	8.226588	-2.156782	-0.247632
16	1	0	8.136701	-3.077870	-0.835304
17	1	0	9.238978	-1.771689	-0.377788
18	1	0	8.086447	-2.409428	0.812021
19	6	0	5.929572	-1.379997	-0.543409
20	6	0	5.452504	-2.646514	-0.149735
21	6	0	4.967933	-0.371411	-0.783616
22	6	0	4.094059	-2.882850	-0.023424
23	1	0	6.145084	-3.454264	0.052017
24	6	0	3.617192	-0.626924	-0.649507
25	1	0	5.276641	0.625677	-1.073978
26	1	0	3.761667	-3.873396	0.278384
27	1	0	2.919469	0.180417	-0.850712
28	6	0	1.722945	-2.202815	-0.105079
29	6	0	0.683843	-1.348731	-0.222822
30	1	0	1.517073	-3.246343	0.128922
31	1	0	0.869250	-0.302545	-0.457792
32	6	0	3.136628	-1.888951	-0.264406
33	6	0	-0.713080	-1.713035	-0.086798
34	6	0	-1.657105	-0.752985	-0.307264
35	6	0	-1.095041	-3.127903	0.252102
36	6	0	-3.077208	-1.016872	-0.311105
37	1	0	-1.327697	0.246696	-0.548353
38	6	0	-2.505381	-3.228319	0.837464
39	1	0	-1.027026	-3.736223	-0.662963
40	1	0	-0.376453	-3.554627	0.961967
41	6	0	-3.483274	-2.453328	-0.055371
42	6	0	-4.019770	-0.027556	-0.543541
43	6	0	-3.667228	1.399364	-0.646047
44	6	0	-5.442996	-0.371100	-0.690481
45	6	0	-6.040458	1.978395	-0.245457
46	8	0	-5.855823	-1.487829	-0.952630
47	8	0	-2.546128	1.843373	-0.824188

48	7	0	-6.374318	0.666112	-0.496718
49	7	0	-4.722728	2.317816	-0.466479
50	6	0	-7.788015	0.244892	-0.495351
51	1	0	-8.381355	1.107620	-0.789569
52	1	0	-7.872334	-0.532332	-1.253655
53	6	0	-8.212988	-0.281764	0.867712
54	1	0	-8.096990	0.493098	1.629672
55	1	0	-9.263733	-0.583822	0.838222
56	1	0	-7.613649	-1.154369	1.141425
57	6	0	-4.309195	3.733931	-0.416366
58	1	0	-3.514509	3.842910	-1.152834
59	1	0	-5.167990	4.329509	-0.717048
60	6	0	-3.818640	4.127506	0.969325
61	1	0	-3.519112	5.179458	0.971255
62	1	0	-4.612596	3.993245	1.708230
63	1	0	-2.952176	3.523384	1.250671
64	16	0	-7.170944	3.095946	0.262921
65	1	0	-3.574138	-2.952709	-1.031293
66	1	0	-4.481440	-2.499661	0.381431
67	6	0	-2.935363	-4.695713	0.878762
68	1	0	-2.942327	-5.134236	-0.125294
69	1	0	-2.250730	-5.282058	1.502260
70	1	0	-3.942274	-4.794840	1.298382
71	6	0	-2.531553	-2.661707	2.262834
72	1	0	-3.542951	-2.725252	2.678909
73	1	0	-1.863402	-3.234824	2.915364
74	1	0	-2.217376	-1.613939	2.292281

E (M062X)= -1990.056859AU

8 (CH_2Cl_2//PCM-M06-2X/6-31G*)

Standard orientation:

Center Number	Atomic Number	Atomic Type	Coordinates (Angstroms) X	Y	Z
1	6	0	8.012194	1.554246	0.293859
2	6	0	7.707180	-0.880279	0.521295
3	6	0	5.729268	0.636786	0.158826
4	8	0	8.240259	-1.968372	0.664342
5	8	0	4.543201	0.871256	-0.017150
6	16	0	9.045667	2.866562	0.139322
7	7	0	8.492920	0.285346	0.528291
8	7	0	6.646635	1.701637	0.189904
9	6	0	6.265977	-0.698735	0.329891
10	6	0	5.511684	-1.845876	0.316891
11	1	0	6.120491	-2.739738	0.452310
12	6	0	9.941230	0.054507	0.708466
13	1	0	10.028587	-0.783792	1.397689
14	1	0	10.356966	0.944545	1.174125
15	6	0	6.049396	3.039121	-0.004358
16	1	0	5.075894	3.006231	0.482259
17	1	0	6.682691	3.756196	0.512054

18	6	0	10.625152	-0.259053	-0.614083
19	1	0	11.691831	-0.430765	-0.446232
20	1	0	10.195900	-1.160673	-1.058540
21	1	0	10.514295	0.573956	-1.313247
22	6	0	5.904515	3.377981	-1.480766
23	1	0	5.260423	2.647218	-1.976756
24	1	0	5.452058	4.367365	-1.589666
25	1	0	6.880896	3.388155	-1.972208
26	6	0	4.137539	-2.167370	0.177441
27	6	0	3.732475	-3.503095	0.216939
28	16	0	2.741838	-1.130166	-0.041418
29	6	0	2.356527	-3.687615	0.078054
30	1	0	4.447507	-4.308399	0.346922
31	6	0	1.671159	-2.487705	-0.067487
32	1	0	1.858921	-4.650311	0.084115
33	6	0	0.239867	-2.362932	-0.222634
34	6	0	-0.427817	-1.194633	-0.331488
35	1	0	-0.295207	-3.309760	-0.241752
36	1	0	0.144769	-0.266423	-0.299383
37	6	0	-1.863772	-1.017327	-0.485496
38	6	0	-2.393440	0.280782	-0.547654
39	6	0	-2.777059	-2.080988	-0.568717
40	6	0	-3.750102	0.518097	-0.681182
41	1	0	-1.718636	1.130807	-0.481539
42	6	0	-4.135476	-1.864093	-0.704725
43	1	0	-2.424240	-3.107356	-0.525659
44	6	0	-4.664469	-0.553668	-0.771178
45	1	0	-4.094277	1.544892	-0.709760
46	1	0	-4.794444	-2.721561	-0.761534
47	7	0	-6.019651	-0.350910	-0.936301
48	6	0	-6.932695	-1.473983	-0.775915
49	1	0	-7.958780	-1.107830	-0.859147
50	1	0	-6.774998	-2.220538	-1.560480
51	1	0	-6.818814	-1.965600	0.199578
52	6	0	-6.597727	0.968566	-0.778523
53	1	0	-7.582213	0.957782	-1.256134
54	1	0	-6.006293	1.719301	-1.307406
55	6	0	-6.752794	1.339976	0.699521
56	1	0	-7.146118	0.486676	1.255537
57	1	0	-5.793559	1.620267	1.138830
58	8	0	-7.583715	2.496326	0.858755
59	6	0	-8.891269	2.458184	0.519029
60	8	0	-9.453065	3.490529	0.247923
61	6	0	-9.600407	1.137604	0.510941
62	6	0	-9.545869	0.261285	1.597755
63	6	0	-10.381004	0.823096	-0.604058
64	6	0	-10.251825	-0.937491	1.555462
65	1	0	-8.971127	0.524296	2.481342
66	6	0	-11.066914	-0.386722	-0.651920
67	1	0	-10.437236	1.526449	-1.429675
68	6	0	-11.000051	-1.267790	0.426470
69	1	0	-10.217573	-1.612682	2.404152
70	1	0	-11.659205	-0.638132	-1.525627
71	1	0	-11.540181	-2.208589	0.391214

E (M062X)= -2460.7783378 AU

9 (CH_2Cl_2//PCM-M06-2X/6-31G*)

Standard orientation:

Center Number	Atomic Number	Atomic Type	Coordinates (Angstroms) X	Y	Z
1	6	0	-5.869183	1.399851	-0.226779
2	6	0	-5.472983	-1.028762	-0.359848
3	6	0	-3.546143	0.579896	-0.155412
4	8	0	-5.966863	-2.142421	-0.428064
5	8	0	-2.364289	0.869462	-0.045016
6	16	0	-6.950289	2.675616	-0.089414
7	7	0	-6.306104	0.103633	-0.382820
8	7	0	-4.508248	1.605537	-0.186024
9	6	0	-4.033501	-0.781758	-0.247540
10	6	0	-3.232461	-1.897678	-0.227783
11	1	0	-3.810858	-2.818781	-0.296602
12	6	0	-7.750343	-0.192501	-0.482365
13	1	0	-7.833056	-1.071307	-1.119519
14	1	0	-8.223325	0.652284	-0.976570
15	6	0	-3.959468	2.972403	-0.066828
16	1	0	-3.006485	2.960310	-0.593119
17	1	0	-4.642547	3.643740	-0.581249
18	6	0	-8.361535	-0.456771	0.885715
19	1	0	-9.426837	-0.677787	0.777082
20	1	0	-7.876952	-1.314527	1.359174
21	1	0	-8.253899	0.418351	1.531944
22	6	0	-3.768170	3.372713	1.388809
23	1	0	-3.074715	2.687482	1.883228
24	1	0	-3.352556	4.382626	1.442232
25	1	0	-4.722979	3.362938	1.920811
26	6	0	-1.842302	-2.160045	-0.146892
27	6	0	-1.382806	-3.479417	-0.158114
28	16	0	-0.481790	-1.059981	-0.038556
29	6	0	0.004386	-3.602471	-0.083148
30	1	0	-2.067994	-4.318216	-0.221599
31	6	0	0.645421	-2.370922	-0.014872
32	1	0	0.541651	-4.543543	-0.078769
33	6	0	2.074790	-2.180871	0.067615
34	6	0	2.688545	-0.978878	0.124811
35	1	0	2.654576	-3.101062	0.079252
36	1	0	2.066554	-0.082601	0.108197
37	6	0	4.115955	-0.719377	0.206895
38	6	0	4.567984	0.609258	0.242300
39	6	0	5.096005	-1.725370	0.246357
40	6	0	5.910900	0.930789	0.314825
41	1	0	3.839362	1.415708	0.203752
42	6	0	6.442895	-1.425373	0.319934
43	1	0	4.803846	-2.771364	0.218234
44	6	0	6.894485	-0.083509	0.365714

45	1	0	6.192922	1.976521	0.323256
46	1	0	7.155578	-2.240323	0.346792
47	7	0	8.235070	0.201464	0.470266
48	6	0	9.207781	-0.869425	0.335917
49	1	0	10.209061	-0.440958	0.387787
50	1	0	9.108310	-1.598919	1.147320
51	1	0	9.106976	-1.399473	-0.619850
52	6	0	8.717003	1.568639	0.391957
53	1	0	9.713111	1.603077	0.845724
54	1	0	8.082968	2.229265	0.990097
55	6	0	8.789705	2.090531	-1.045020
56	1	0	9.464404	1.453819	-1.635181
57	1	0	7.799452	2.037027	-1.507933
58	8	0	9.180748	3.448436	-1.084401
59	1	0	10.103145	3.501568	-0.794570

E (M062X)= -2116.5172694AU

10 (CH_2Cl_2//PCM-M06-2X/6-31G*)

Standard orientation:

Center Number	Atomic Number	Atomic Type	Coordinates (Angstroms) X	Y	Z
1	6	0	-7.911516	2.102231	-0.147987
2	6	0	-8.003282	-0.332966	-0.512882
3	6	0	-5.806566	0.822153	-0.084075
4	8	0	-8.705699	-1.311484	-0.707727
5	8	0	-4.599230	0.851336	0.101242
6	16	0	-8.718399	3.556222	0.076614
7	7	0	-8.592015	0.942056	-0.441650
8	7	0	-6.540601	2.020875	-0.045234
9	6	0	-6.550372	-0.395289	-0.338801
10	6	0	-5.988232	-1.645511	-0.426002
11	1	0	-6.733984	-2.418240	-0.611327
12	6	0	-10.060302	0.955452	-0.607605
13	1	0	-10.287234	0.175965	-1.332977
14	1	0	-10.333288	1.921683	-1.024240
15	6	0	-5.737461	3.231899	0.223390
16	1	0	-4.776532	3.069414	-0.261552
17	1	0	-6.241304	4.068245	-0.254579
18	6	0	-10.771589	0.691153	0.711434
19	1	0	-11.853636	0.694061	0.554797
20	1	0	-10.482080	-0.284987	1.108975
21	1	0	-10.525603	1.464519	1.443900
22	6	0	-5.557278	3.463442	1.716473
23	1	0	-5.045084	2.613303	2.174417
24	1	0	-4.953094	4.359938	1.880451
25	1	0	-6.525257	3.604773	2.204027
26	6	0	-4.681913	-2.189089	-0.348694
27	6	0	-4.492177	-3.562938	-0.516249
28	16	0	-3.135775	-1.405458	-0.082685
29	6	0	-3.161095	-3.970382	-0.435794

30	1	0	-5.326008	-4.233315	-0.695816
31	6	0	-2.292244	-2.910385	-0.203753
32	1	0	-2.820818	-4.993853	-0.540903
33	6	0	-0.858810	-3.030282	-0.078257
34	6	0	-0.009865	-2.005773	0.154688
35	1	0	-0.482430	-4.044791	-0.188165
36	1	0	-0.426525	-1.003666	0.266940
37	6	0	1.436657	-2.081122	0.279393
38	6	0	2.167969	-0.914297	0.553035
39	6	0	2.170270	-3.269960	0.131348
40	6	0	3.545513	-0.919036	0.680030
41	1	0	1.637085	0.028219	0.664250
42	6	0	3.546078	-3.296311	0.254319
43	1	0	1.658682	-4.201965	-0.090630
44	6	0	4.279219	-2.119234	0.542257
45	1	0	4.050325	0.018965	0.876838
46	1	0	4.059812	-4.240869	0.126008
47	7	0	5.645781	-2.164505	0.690232
48	6	0	6.360358	-3.385681	0.359222
49	1	0	7.429607	-3.212294	0.485908
50	1	0	6.069788	-4.206014	1.024622
51	1	0	6.180803	-3.699923	-0.676963
52	6	0	6.422150	-0.948680	0.848247
53	1	0	7.384291	-1.219944	1.296435
54	1	0	5.934396	-0.271038	1.555701
55	6	0	6.654705	-0.225054	-0.480486
56	1	0	7.219490	-0.882741	-1.157422
57	1	0	5.689779	-0.016049	-0.955895
58	8	0	7.319758	1.003775	-0.290154
59	14	0	8.948753	1.155002	0.094835
60	6	0	9.894931	-0.318341	-0.587076
61	1	0	9.540589	-1.261633	-0.155851
62	1	0	9.808059	-0.394320	-1.676085
63	1	0	10.958083	-0.228593	-0.339139
64	6	0	9.156767	1.242393	1.961000
65	1	0	8.467741	1.972837	2.397392
66	1	0	8.963190	0.274070	2.434695
67	1	0	10.176923	1.540466	2.227560
68	6	0	9.497376	2.772442	-0.714497
69	6	0	9.178528	2.731265	-2.215217
70	1	0	8.105715	2.600738	-2.391971
71	1	0	9.489781	3.670175	-2.693670
72	1	0	9.707193	1.913689	-2.719699
73	6	0	11.007945	2.970147	-0.524016
74	1	0	11.323831	3.920320	-0.976193
75	1	0	11.288401	3.002213	0.535633
76	1	0	11.584628	2.170158	-1.003025
77	6	0	8.745624	3.946051	-0.070515
78	1	0	8.983364	4.042209	0.995363
79	1	0	9.026236	4.889436	-0.559090
80	1	0	7.660219	3.828808	-0.167178

E (M062X)= -2643.0054769AU

11 **AT** (CH_2Cl_2//PCM-M06-2X/6-31G*)

Standard orientation:

Center Number	Atomic Number	Atomic Type	Coordinates (Angstroms) X	Y	Z
1	6	0	3.324160	-3.824876	0.346469
2	1	0	4.013715	-4.645804	0.533699
3	6	0	1.943533	-4.221765	0.253604
4	6	0	1.451748	-5.501830	0.386153
5	16	0	0.647759	-3.095653	-0.058837
6	6	0	0.048060	-5.581799	0.240144
7	1	0	2.095049	-6.352346	0.584376
8	6	0	-0.546263	-4.362162	-0.001957
9	1	0	-0.522484	-6.501046	0.309988
10	6	0	-1.960077	-4.117619	-0.194461
11	6	0	-2.522415	-2.904763	-0.361368
12	1	0	-2.573953	-5.016215	-0.189053
13	1	0	-1.874767	-2.026828	-0.333670
14	6	0	-3.935167	-2.609826	-0.571943
15	6	0	-4.361350	-1.273795	-0.595864
16	6	0	-4.921437	-3.592006	-0.753407
17	6	0	-5.687547	-0.923270	-0.782472
18	1	0	-3.627986	-0.483642	-0.453032
19	6	0	-6.251460	-3.262468	-0.945466
20	1	0	-4.648186	-4.643591	-0.752614
21	6	0	-6.675748	-1.913447	-0.975995
22	1	0	-5.950795	0.127594	-0.771616
23	1	0	-6.969010	-4.061968	-1.082484
24	7	0	-7.997725	-1.596352	-1.209299
25	6	0	-8.992966	-2.654285	-1.215260
26	1	0	-9.977899	-2.209011	-1.362208
27	1	0	-8.814750	-3.358141	-2.035616
28	1	0	-9.005331	-3.218743	-0.273425
29	6	0	-8.468457	-0.230731	-1.079935
30	1	0	-9.413805	-0.146059	-1.627309
31	1	0	-7.771450	0.462183	-1.561444
32	6	0	-8.677431	0.180340	0.379678
33	1	0	-9.441166	-0.469636	0.831394
34	1	0	-7.745926	0.029075	0.936928
35	8	0	-9.032890	1.540674	0.492314
36	6	0	-11.833898	0.812353	0.204259
37	1	0	-11.679575	0.030004	-0.547360
38	1	0	-11.834346	0.336296	1.190410
39	1	0	-12.831837	1.232212	0.035603
40	6	0	-10.485798	2.850064	-1.667808
41	1	0	-9.745642	3.651261	-1.763376
42	1	0	-10.224729	2.068172	-2.388930
43	1	0	-11.461513	3.255443	-1.957483
44	6	0	-10.852940	3.548919	1.334554
45	6	0	-11.051725	2.935997	2.727396
46	1	0	-10.186080	2.334533	3.027844
47	1	0	-11.185701	3.728474	3.476377

48	1	0	-11.939733	2.294335	2.761584
49	6	0	-12.106001	4.345160	0.944523
50	1	0	-12.301383	5.128872	1.689201
51	1	0	-11.987504	4.836356	-0.028128
52	1	0	-12.997932	3.708598	0.896535
53	6	0	-9.642258	4.492400	1.365872
54	1	0	-9.468776	4.961790	0.390212
55	1	0	-9.808979	5.297398	2.094970
56	1	0	-8.729705	3.959800	1.653176
57	14	0	-10.536771	2.168262	0.081804
58	6	0	3.793178	-2.562641	0.208559
59	1	0	3.090417	-1.755116	0.004517
60	6	0	5.186991	-2.182607	0.272967
61	6	0	5.511726	-0.879279	0.016467
62	6	0	6.242741	-3.209091	0.577112
63	6	0	6.868043	-0.400952	-0.056461
64	1	0	4.711945	-0.186437	-0.198816
65	6	0	7.521194	-2.574201	1.130448
66	1	0	5.861925	-3.946571	1.292903
67	6	0	7.951836	-1.422635	0.212450
68	1	0	8.274325	-1.824905	-0.759417
69	6	0	7.179025	0.920161	-0.357805
70	6	0	8.568049	1.338806	-0.570779
71	6	0	6.152689	1.964468	-0.481325
72	6	0	7.900415	3.692327	-0.268199
73	8	0	4.967282	1.779912	-0.698366
74	8	0	9.493139	0.575505	-0.797848
75	7	0	8.837665	2.723828	-0.529899
76	7	0	6.587882	3.290858	-0.259719
77	16	0	8.338572	5.292837	-0.003646
78	6	0	10.257114	3.085992	-0.716250
79	1	0	10.655094	2.383500	-1.446152
80	1	0	10.283601	4.089463	-1.134354
81	6	0	5.505513	4.288236	-0.133677
82	1	0	4.665290	3.770818	0.325629
83	1	0	5.858947	5.063522	0.541949
84	6	0	11.033380	3.005195	0.589946
85	1	0	10.621844	3.700879	1.325617
86	1	0	10.993704	1.990083	0.993648
87	1	0	12.080742	3.265284	0.413649
88	6	0	5.113203	4.862095	-1.487308
89	1	0	5.966573	5.357669	-1.958034
90	1	0	4.751862	4.068244	-2.145620
91	1	0	4.315023	5.598510	-1.359499
92	6	0	7.288209	-2.054611	2.554921
93	1	0	7.010432	-2.878544	3.221201
94	1	0	8.204382	-1.598486	2.945442
95	1	0	6.492354	-1.304564	2.592462
96	6	0	8.636519	-3.620299	1.161432
97	1	0	9.563847	-3.185877	1.550383
98	1	0	8.358423	-4.459836	1.808291
99	1	0	8.838114	-4.014028	0.159152
100	1	0	8.834881	-0.940335	0.633593
101	1	0	6.470639	-3.759639	-0.348289

E (M062X)= -2993.0273955 AU

5. NLO measurements

Electric field induced second harmonic generation (EFISH) measurements have been performed using as the fundamental radiation the 1.9 μm output of a H_2 Ramen shifter pumped by a Q-switched Nd: YAG laser. This laser operates at 1064 nm, with a repetition rate of 10 Hz and pulse width of 8 ns. A computer controlled NLO spectrometer completes the SHG experimental set-up. The 1.9 μm incident light is split in two beams. The less intense one is directed to a *N*-(4-nitrophenyl)-(L)-prolinol (NPP) powder sample whose SH signal is used as a reference in order to reduce the effects of laser fluctuations. The other beam is passed through a linear polarizer and focused into the EFISH wedge shaped liquid cell. Voltage pulses of 5 kV and 3 μs are applied across the cell (2 mm gap between the electrodes) synchronously with the laser pulses. The harmonic signals from both the EFISH cell and the NPP reference are measured with two photomultipliers. Interference filters are used to remove the residual excitation light beyond the sample and the reference. The molecular μβ values have been determined in dichloromethane for all compounds. As a rule, three solutions of concentration in the range ($4x10^{-4}$M - $3x10^{-3}$M) were measured. $\mu\beta_0$ values were extrapolated using a two-level dispersion model.[6] Under the same experimental conditions $\mu\beta_0$ deduced for *DR1* was $480x10^{-48}$ esu, quite close to the value reported in the same solvent by Dirk et al.[7]

Film preparation and characterization.
Dye/polymer solutions in chloroform were filtered and spin coated on indium tin oxide (ITO) coated glass plates. Good quality films with chromophore content up to 20 wt% were prepared. The thickness of the films was measured by using a contact profilometer. Refractive indices were determined using a guided mode prism coupling method at 1306 nm. Optical absorption measurements of thin films were performed in a double beam UV-Vis-NIR spectrophotometer. Second harmonic generation (SHG) measurements were performed using the same excitation light source and harmonic signal detection system as described above.
In order to orient the NLO chromophores dispersed in the polymeric matrix, each film was submitted to a corona poling process. Firstly, films were held on a thermo-regulated fixed stage for in situ SHG measurements during the poling process. The angle of incidence of the 1.9 mm fundamental beam on the film was about 45 degrees. A positive electric discharge was applied across the film using a standard corona poling set-up. A DC voltage of +5 kV was applied to a needle perpendicular to the film. The distance between the needle and the film surface was about 1 cm. The sample was initially set at 25 ºC and the high voltage was switched on whereas the second harmonic signal was detected. After two minutes, the film was heated up at a rate of 10 ºC min^{-1}, with the electric field on. On reaching 135ºC, the films were maintained at this temperature for 20 min. Then, the films were cooled down to RT with the poling field still applied and finally the electric field was switch off. In order to obtain the d_{ij} non-linear coefficients the poled films were held on a rotating stage around the vertical axis. The fundamental light was either p or s-polarised and the p-polarised SH signal was detected as a function of the angle. The experimental data were analysed following the Jerphagnon and Kurtz method [8] using an X-cut quartz crystal (d_{11} = 0.4 pm V^{-1}) as a reference.

[6] Oudar, J.L.; Chemla, D.S. *J. Chem. Phys.* **1977**, 66, 2664-2668
[7] Dirk, C.W.; Katz, H.E. ; Schilling, M.L.; King, L.A. *Chem. Mater*., **1990**, 2, 700-705
[8] Jerphagnon J. and Kurtz S.K., J. Appl. Phys. **1970**, 41, 1667-1681

Graphical Abstract (for review)

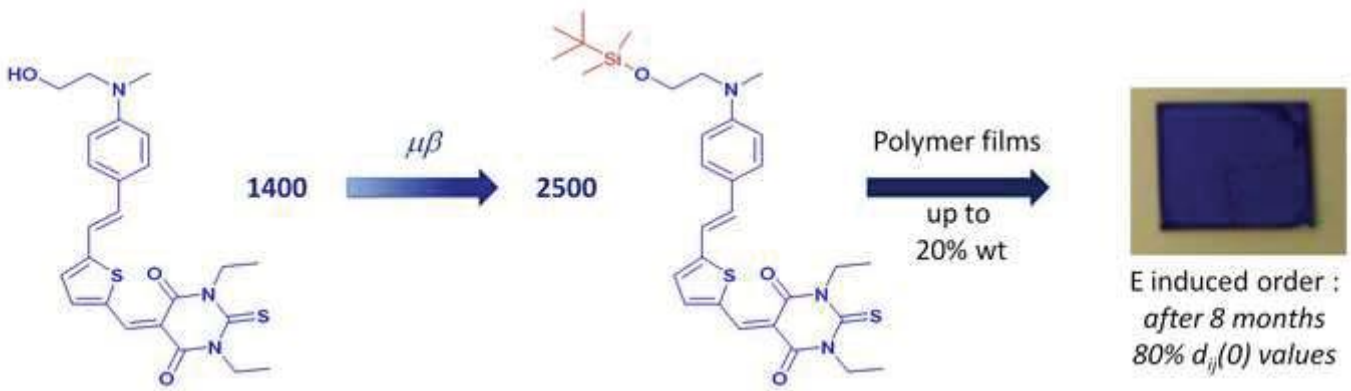

Figure
Click here to download high resolution image

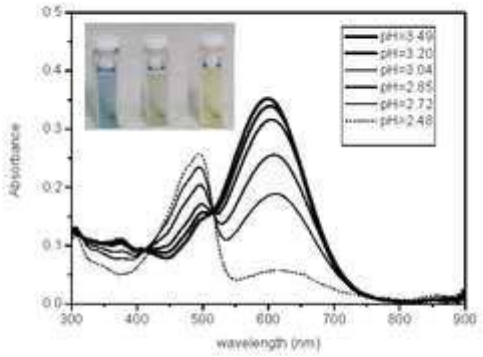

Figure
Click here to download high resolution image